UILU-ENG-81-2001

CIVIL ENGINEERING STUDIES

STRUCTURAL RESEARCH SERIES NO. 488

A STRUCTURAL SAFETY ANALYSIS OF BUILDINGS DURING CONSTRUCTION

By
S. KARSHENAS
and
A. H-S. ANG

Technical Report of Research
Supported by the
NATIONAL SCIENCE FOUNDATION
under Grants ENG 77-02007, ENV 77-09090, PFR 80-02584

DEPARTMENT OF CIVIL ENGINEERING
UNIVERSITY OF ILLINOIS
at URBANA-CHAMPAIGN
URBANA, ILLINOIS
FEBRUARY 1981

Errata: The figures given in Tables 6.6 and 6.7 should be corrected as shown below.

Table 6.6 Failure Probabilities-Flexible Connections

Number of Floors	3-Day Duration	10-Day Duration
2	6.2×10^{-6}	1.5×10^{-5}
4	6.5×10^{-5}	1.81×10^{-4}
6	4.01×10^{-4}	1.11×10^{-3}
8	1.08×10^{-2}	2.91×10^{-2}
10	2.01×10^{-2}	5.41×10^{-2}

Table 6.7 Probability of Floor Beam Buckling

Number of Floors	3-Day Duration	10-Day Duration
4	*	*
6	*	*
8	0.21×10^{-6}	0.61×10^{-6}
10**	4.61×10^{-6}	1.31×10^{-5}

*Probability 10^{-7}

**10-story Bare Frame with Completed Connections

A STRUCTURAL SAFETY ANALYSIS OF BUILDINGS DURING CONSTRUCTION

by

S. Karshenas

and

A.H-S. Ang

A Technical Report of

Research Supported Partially by the

NATIONAL SCIENCE FOUNDATION

under

Grants ENG 77-02007

ENV 77-09090

PFR 80-02584

Urbana, Illinois
February, 1981

50272-101

REPORT DOCUMENTATION PAGE	1. REPORT NO. UILU-ENG-81-2001	2.	3. Recipient's Accession No.

4. Title and Subtitle
A STRUCTURAL SAFETY ANALYSIS OF BUILDINGS DURING CONSTRUCTION

5. Report Date
February 1981

6.

7. Author(s)
S. Karshenas and A.H-S. Ang

8. Performing Organization Rept. No.
SRS No. 488

9. Performing Organization Name and Address
Department of Civil Engineering
University of Illinois
208 N. Romine
Urbana, Illinois 61801

10. Project/Task/Work Unit No.

11. Contract(C) or Grant(G) No.
(C) ENG 77-02007
ENV 77-09090
(G) PFR 80-02584

12. Sponsoring Organization Name and Address
National Science Foundation
Washington, D.C.

13. Type of Report & Period Covered

14.

15. Supplementary Notes
The safety of steel buildings, constructed by the tier method,

16. Abstract (Limit: 200 words)

The safety of steel buildings, constructed by the tier method, is evaluated. The probability of failure of steel frames supported on temporary connections is examined during the different stages of completion. The principal loading of concern is the maximum wind load over the critical stages of construction.

17. Document Analysis a. Descriptors
Structural safety
Construction safety
Building
Temporary structure

b. Identifiers/Open-Ended Terms

c. COSATI Field/Group

18. Availability Statement	19. Security Class (This Report) UNCLASSIFIED	21. No. of Pages 158
	20. Security Class (This Page) UNCLASSIFIED	22. Price

(See ANSI-Z39.18) *See Instructions on Reverse*

OPTIONAL FORM 272 (4-77)
(Formerly NTIS-35)
Department of Commerce

ACKNOWLEDGEMENTS

This report is based on the doctoral thesis of Dr. S. Karshenas, submitted in partial fulfillment of the requirements for the Ph.D. at the University of Illinois.

The study was conducted as part of a research program on the safety and reliability of structures, and was supported in part by grants from the National Science Foundation, specifically grants No. ENG 77-02007, ENV 77-09090, and PFR 80-02584. These supports are gratefully acknowledged.

TABLE OF CONTENTS

CHAPTER 1

INTRODUCTION AND BACKGROUND

1.1-General Remarks

One of the high risk industries is the construction industry. Accident statistics reveal that the chance of accidental death in construction is four times greater than the overall occupational hazard (Lew, 1971). In many countries, the losses in lives and dollars from the failure of buildings during construction greatly exceed those from collapse of buildings in service. For example, the annual risk of fatality for construction workers from the hazards of structural collapse in Ontario, Canada is approximately 30×10^{-6}, compared to 0.2×10^{-6} for users of completed structures (Allen, 1975). The most important reason for these unfavorable statistics is human error. Since there is little standardization in the construction process, human judgement and decision play an important role at all stages of construction. High uncertainty in loads and strength of structures during construction results in situations that require an experienced and competent person to make sound decisions.

In order to minimize the frequency of failures during construction , a consistent philosophy for the construction phase of a building is required. The development of such a philosophy must include a method for assessing the safety of a structure during the different stages of completion. This requires the identification of the uncertainties in the load and strength associated with a particular method of construction. Currently, this task is hampered by the lack of information for different types of structures during construction. Present knowledge of construction loads leaves much to be desired; so is the present state of knowledge for the strength of incomplete structures.

In this study, the reliability of steel buildings during construction under wind forces is examined. This is accomplished for a fairly common method of construction;

namely, the tier method of erection. Wind load is the major loading during the construction of this type of structures.

Table 1.1

RELATIVE FREQUENCY OF FAILURE OF STRUCTURES (I.C.E., 1969)

TYPE OF FAILURE	PERCENTAGE OF TOTAL FAILURE
Concrete structures	12
Steel structures	10
Temporary works	10
Foundations, piling and cofferdams	11
Excavation and earthworks	10
Trenching for pipelines and sewers	5
Plant and equipment	12
Methods of work	20
Miscellaneous	10

In a study by the Institution of Civil Engineers of England, over 2000 cases of construction failures occurring before 1966 were reported, as summarised in Table 1.1. These statistics show that failures of steel frames constitute about 10% of all failures during construction. Although the study did not single out failures caused by wind load, a review of the failure cases shows that most failures of steel structures during construction and some of the failures of temporary supports, are caused by inadequate resistance against wind loading.

1.2-Related Previous Studies

Structural failures are, in general, caused by excessive loading on or inadequate strength of the structure. This is true during the construction, or the service life, of a

structure. However, during construction, overloading or inadequate strength is more likely to occur because decisions are made or actions are taken by people who may not be technically qualified to assess the adequacy of the partially completed structure.

Pugsley (1969) was the first to point out the significance of human factors on the safety of a structure. He believes that proneness of a structure to failure can be predicted on the basis of pressures on designers and contractors. These pressures, in general, are classified as financial, political, scientific, professional, and industrial.

Blockley (1975,1977) using the concept of fuzzy sets (Zadeh 1965, 1973) attempted to predict the likelihood of a structure failing due to causes other than uncertainties in loading and structural strength. With this method, the factors that may result in failure are isolated, defined, and measured subjectively using fuzzy linguistic variables. The various operations and manipulations of these variables constituting the method, results in a solution which has also to be interpreted subjectively.

Silby and Walker (1977) attempted to find patterns in bridge failures. After examining several detailed bridge failure case histories, the authors concluded that one reason for failure of structures is the complacency and extrapolation from past experience without sufficient and careful thought. They explained that some factors which are of secondary importance in the early stage of development of a structural form, may become of primary importance and thus could lead to failure if not adequately considered. As time passes the basis of the design methods are forgotten and so are their limits of validity. Following a period of successful construction, a designer may unwittingly introduce a new type of behavior or simply extend the design beyond its allowable limits. Therefore, it is suggested that a committee of experts should observe design trends and predict incipient accidents.

Melchers (1977) by reviewing a few available bridge failure case histories shows the importance of the organization of a project on the safety of the project.

Durkee and Thomides (1977) performed a comprehensive review of steel bridge failures, and current construction codes and practices. They blame the arbitrary nature of current bridge erection requirements and erection-stressing philosophy for most bridge failures during construction. For example, structural steelwork design specifications, or special provisions, commonly specify that stresses in steel structures under erection shall not exceed certain multiples of the design allowable stresses. Fundamentally, there is no unique relation between service loads and the loading during construction; moreover, the behavior of a structure during the different stages of construction is invariably quite different from that of the completed structure. Therefore, the loads and strength of a structure at all stages of construction must be carefully examined; in addition to assuring a structure for safety during its service life, it ought to be designed also for safety at all stages of construction.

1.3-Purpose and Scope of Present Study

Judgement and decision of key personel involved in a construction project affect the safety of the project. A structure passes through several stages before completion; namely, design, planning and scheduling, selection of construction method, and fabrication and construction. Errors at any of these stages contribute to the probability of failure of a structure during construction. As long as human beings are fallible, design errors cannot be totally prevented, and may be minimized through rigid inspection and supervision. Decisions about construction method, planning, and scheduling of the project, and the field superintendent's decisions and actions play an important role in safely completing a building. Therefore, one way to reduce the rate of failures during construction is to study the reliability of different methods of construction, and identify the risk factors involved in each method. Such studies are the first steps toward eventually formulating codes or standards for construction practices; regulations that will not limit productivity of construction,

but will help the contractor avoid risky situations, may eventually be developed.

In this study, the structural reliability associated with a common method of constructing steel buildings is studied. The reliability or safety at different stages of construction, in terms of the probability of failure, as well as the variation of this reliability with changes in planning, scheduling, and field practices are examined.

The principal loading during the construction of a steel building is wind load. In order to quantify the concept of "construction safety", both load and resistance models of the incomplete structure are required. The load model is a probabilistic description of the wind force, including its probability of occurrence and severity. To achieve the objectives of this study, an analysis of the uncertainties in the prediction of the loads (or load effects), resistance, and behavior of an incomplete structure must be performed.

The probability of failure at a given stage of construction is evaluated by treating the loads and resistance as random variables Freudenthal (1966,1968), Ang(1973,1974), Ellingwood(1972). The risk of failure is a function of the maximum wind speed during a stage of construction, whereas the maximum wind speed depends on the duration of the given construction stage. Conceptually, the required probability is,

$$P(\text{failure}) = \int_0^\infty P(R \leq S \,|\, V=v) \cdot f_{V(t)}(v)\,dv \qquad (1.1)$$

where, S is the applied load which is a function of V; R is the structural strength, and $f_{V(t)}(v)$ is the probability density function of the maximum wind velocity over a duration t.

All the variables in Eq. 1.1 are random variables. In addition to the basic variabilities of these random variables, there are also uncertainties associated with errors in modeling

and estimations. Moreover, during construction, erection tolerances and fabrication inaccuracies may increase the uncertainty of the strength of the structure over that of the completed structure.

In order to use Eq. 1.1, the statistics of R and S are required. Frequently these variables are functions of other variables. For example, the flexural strength of a steel beam is a function of the yield strength of steel, the dimensions and geometry of its cross section. Each is a random variable with its own probability distribution and related statistics.

Generally, only the first and second moments are available; the exact probability distribution is usually not known. Therefore, the required probability must be determined on the basis of convenient distributions or of distributions favored by available but limited data.

The mean and variance of a variable are estimated from whatever data are available. Since the true mean is not known, a prediction error is assigned to the predicted mean, to account for inaccuracies in its estimation. If information is available to evaluate the accuracy of the estimated mean, a rough estimate of the prediction error may be obtained from this information. In those cases in which, due to inadequate data, uncertainty may not be evaluated objectively, probabilistic assumptions may be used to assess the errors in the predicted mean values. For example, if only the range of the mean is known, an estimate of the prediction error may be obtained by assuming some appropriate distribution for the mean over this range (Ang,1972). When no data is available, professional judgement would be the only basis for the estimation of the prediction error.

In the case of light or flexible structures (e.g., bare steel frames) the dynamic effect of wind becomes of great importance. The dynamic effect of wind on an incomplete frame is included in this study using elements of random vibration.

1.4-Organization

In Chapter 2, several methods of construction of steel buildings are reviewed, with an emphasis on the tier method which is the most common method of construction of steel buildings. The conditions of a steel frame at each stage of construction, and the potential modes of failure at each stage are identified. Finally, several failure cases for each mode of failure are discussed.

Chapter 3 contains the procedures for evaluating the failure probability of each mode of failure. The methods for calculating the probabilities of collapse of a frame caused by the instability of its members or by yielding of the connections are examined.

In Chapter 4, the statistics of the dynamic properties of a frame at each stage of construction are evaluated. A method is discussed for assessing the mean and coefficient of variation (c.o.v.) of the maximum response of a frame under wind loads based on random vibration theory. A method is also presented for determining the maximum wind velocity over short periods of time corresponding to the duration of each stage of construction.

Chapter 5 contains an analysis of the uncertainties in the resistance and dynamic properties of an incomplete frame at various stages of construction.

In Chapter 6, the risk levels associated with different practices of the tier method of construction are evaluated. The variation of the failure probability with changes in planning and scheduling of a job or field operations are discussed.

Chapter 7 contains the summary and conclusions of the study.

CHAPTER 2

CONSTRUCTION OF STEEL FRAMES

2.1-Introduction

There is no standard method for the construction of a steel frame. Even two identical structures are rarely built exactly alike. This is because of the many factors affecting the choice of an erection method, such as (1)conditions on and around the site of the project; (2) the size and design of the frame; (3)available equipment; (4)the hazards of one method over another; and (5)performance and preferences of the construction foreman.

The construction of steel frames consists of two major phases: fabrication and field erection. There is no clear-cut line separating these two phases. Sometimes large sections of a frame are shop-fabricated and shipped to the site, whereas if the job conditions do not allow this, the members of a frame are individually shop-fabricated and assembled on the site.

Several methods have been used for the construction of steel frames, see e.g. Cunningham (1975), and Reference 68 . Some of these methods are fast and economical, but their use is limited because of the requirement of special equipment, site condition, or experience for their application.

One method that is widely used in the construction of steel building frames is the "tier method." Each tier of a building frame represents a height of two or three stories. In erecting multistory buildings with this method, a common practice is to hoist (element by element) all columns and beams of a tier and install them in their place by temporary connections. After all the elements of a tier are in place, it is plumbed and fastened temporarily with cable guys, and the process is repeated for the next tier. The connections may be completed as soon as a tier is plumbed. But, because of the slower speed of the bolting crew, the raising crew are usually several tiers ahead of the permanent bolting operation.

Clearly, the safety or reliability of a building during

different stages of its erection will vary, and will be quite different from that of the completed structure. Safety during erection(field assembling) is studied herein. Since the method of tiers is a very common method for building frame construction, the safety associated with this construction method during the various stages of construction is examined.

2.2-Tier Method of Construction

In the tier method of construction the columns of the first tier are installed on the footings. Normally, it is difficult to build a footing to the exact elevation when pouring the concrete; consequently, footings are usually poured a few inches below their final elevation. Because of inaccuracies in the elevation of the footings, base plates are placed on shim packs to bring the plates to the correct elevation (Fig 2.1). A shim pack consists of a few square plates, usually 3 to 4 inches wide and range from 1/16 to 1/2 inch thick. After the erection has progressed a few tiers, the space under the base plate is grouted; however, grouting may be postponed until the construction of the frame is completed. The number and place of shim packs under the base plate depends on the configuration of the column anchorage and on the builder's subjective preference.

After the columns of the first tier are in place, beams are connected to the columns. Because of fabrication and erection tolerances and inaccuracies, the condition of the tier at this stage is usually out of plumb. Therefore, steel frames are erected first with temporary connections to facilitate subsequent plumbing operations. Some temporary beam-to-column connections for bolted frames are shown in Fig.2.2. These connections are framed (Fig.2.2a,b) or are seated (Fig.2.2c,d). Seated connections are usually used for beam-to-column webs. As shown in Fig.2.2, there are two types of temporary framed connections. In Fig.2.2a, angles are shop bolted to the beam web and field bolted to the column flange. Most fabricators and erectors prefer (AISC, 1971) the framing angles to be shop-bolted to the column (Fig.2.2b). This gives more

flexibility for plumbing the steel framework in the field. In this procedure, one connection angle is usually shop-bolted to the column and the other is loosely bolted for shipment. The angle bolted for shipment is removed in the field, and after erecting the beam, the angle is attached to the column and the beam. The number of bolts placed in a connection is arbitrarily selected by the ironworker. It is usually 1 or 2 bolts as shown in Fig.2.2. Occasionally, more bolts may be used in large joints. Bolts used in welded frames are always common bolts; they will not be of any use after the connection is completed. In the case of bolted connections, one or two high strength bolts are placed in the connection and hand-tightened during a temporary stage. When completing the connection, the remaining bolts are placed in the connection and all bolts are adequately tightened.

There is an established sequence for erection. The raising crew connects the members together with temporary fitting-up bolts. The number of bolts is kept to a minimum, just enough - in the builder's judgement- to draw the joint up tight and take care of the stresses caused by dead weight, wind, and construction forces. After alignment and plumbing, to within the tolerance limits, the raising crew begins to erect the next tier. Permanent connections may be installed as soon as a tier is plumbed. However, the permanent bolting or welding crew is usually one or two tiers behind the raising crew, because the raising crew moves faster to get rid of the heavy equipment as soon as possible. Sometimes when the erection equipment is mounted on top of the frame, the bolting crew skips every other floor, thus obtaining permanent connections as close as possible to the erecting equipment (Meritt,1975).

Successive tiers are connected to each other by column splices. A column splice during a temporary stage is shown in Fig. 2.3. Column splices are usually placed near mid-height of a column in order to avoid the region of heavy bending moment. The result is a connection sufficient to hold the column in place. However, column splices may have to withstand cosiderable stress during erection and before floor framing is

placed. Columns are first placed and secured by one or two bolts in each splice. After the erection and plumbing of the whole tier, the column splices are completed by additional bolting or welding.

2.3-Critical Stages of Construction

Certain stages of construction may be particularly susceptible to failure. In general, the critical stages of a project depend on a number of factors, such as frame design, construction method, and the contractor's experience. The person responsible for planning the construction, and the ironworkers' foreman supervising the job play important roles in safely erecting the frame. As there is usually no code or regulation governing the process of construction, the planning and scheduling of the job operations as well as decisions during construction, including the need for or amount of temporary bracing and the minimum required strengh for the temporary joints, etc., are based on subjective judgements of the field individuals, some of whom may not have the technical background to make the proper judgements.

Two identical structures built by two different contractors may pass through completely different stages and have different risk of failure at any stage. A review of available failures during construction reveal certain critical stages that might occur during construction, indicating also common failure modes.

The Engineering News Record (ENR) is the main source of information on failure of structures. Feld (1968), McKaig(1962), Merchant (1967), and Short (1967) have also reported failures of steel frames during consruction. The cases mentioned in these references do not include all the failures that have occurred; usually, only the most important and dramatic ones are reported.

Among the reported cases of failure, there are partial or complete collapse at all stages of construction. Invariably, the most critical stage of construction is when the frame is temporarily connected or supported. Among the

failures that have occurred at this stage is the failure of a steel frame in Pittsburgh on 9 June 1966 (ENR). One hundred and eighty tons of structural steel collapsed like "a house of cards" when winds gusting up to 50 MPH hit the area. The damage extended to four stories of partially erected structures. The collapse occurred when the columns were just plumbed. There were bolts in all connections, but the connections were not completed. Guy cables had been installed to brace the structure. A similar collapse happened in Hamilton Ontario (Feld, 1968) when a 3-story 600 x 225-ft framework was partially completed.

Prior to the installation of the permanent lateral supports, frames with flexible design also are susceptible to collapse under wind loading. One failure of this type occured in New York City on 17 February 1972 (ENR). An eight story steel frame under construction collapsed before its permanent bracing along the weak axis was in place. A similar accident occured in the Louisiana Civic Auditorium Project (ENR, 5 November 1970); before adequate cross members were in place, wind gusts whipped a 90-ft high network of structural steel and collapsed virtually all of the 207 tons of steelwork.

Lateral instability of the members is another reason for failure of a frame during construction. Before the concrete slabs of a floor have been placed, the steel floor beams of a frame may have a low lateral buckling capacity. Also, before the permanent lateral supports of a frame is in place, if the stiffness of the beams framing into a column is much less than that of the columns, the buckling length of a column will be several times the actual length of a one-story column. This reduces the strength of the column considerably. An eleven-story steel frame with its permanent connections in place, but before its permanent lateral supports were installed, collapsed in Toronto in 1958 (Feld, 1968). Subsequent investigations revealed that only one of the several hundred welds failed after the collapse.

Partial failure during construction may occur because of inadequate strength of the column splices. The AISC specification requires columns which are finished to bear at

splices, and those that bear on bearing plates must have enough fasteners to " hold all parts securely in place". Furthermore, the splice connection must also be proportioned to resist the tension, if any, that results from moments due to lateral forces acting together with 75% of the calculated dead load and no other gravity load (AISC, 1969). During construction, before the floors and walls are built, axial dead loads in the columns are negligible but the bending moment due to wind load at the column splices could be high. Therefore, the splice plates during construction may be under a high tension, even though there may be none when the building is completed. An example of this kind of failure is the partial collapse of the 270 x 100-ft Federal building in Jacksonville, Florida on 9 June 1966 (ENR). In this accident 300 tons of steel in the upper sections collapsed, separating from some of the lower portions of the structure that remained standing up and undamaged (Feld, 1968).

CHAPTER 3

PROBABILISTIC ANALYSIS OF FAILURE

3.1-Basic Concepts and Methods

The methods for evaluating the reliability of completed structures may be adopted for the evaluation of the failure probabilities of structures during construction. The principal elements of these methods are summarized below. The modes of failure that will be considered are the collapse of an entire frame or sections of the frame due to yielding of its members and connections, and frame failure due to instability of the members.

The probability of failure caused by yielding of the connections or members are evaluated with the assumption that failure will occur when enough plastic hinges have developed in the frame to result in the collapse of the entire frame or part of it. The second mode of failure will occur as a result of the instability of the beams or columns because of the lack of adequate lateral supports.

The general assumptions underlying the formulation of the failure probabilities are as follows:

(1) The applied loads and the member capacities are statistically independent.

(2) The capacities of all similar members (e.g., all beams or all connections) are perfectly and positively correlated. This assumption is reasonable because of common workmanship and properties of the members.

(3) The load effects among different members are also perfectly and positively correlated. The forces in the members are induced almost entirely by wind loading.

3.1.1 Analysis of Reliability of Structures

In the classical theory of structural reliability, the loads and resistance of a structure are assumed to be random variables and the respective probability laws are assumed to be known.

The performance function may be represented by a mathematical model, $Z=g(x_1,x_2,....,x_n)$, where x_i are the resistance and load variables. The limit state of interest may then be defined as $Z=\emptyset$. In general, the limit-state may be considered to contain just two variables; a resistance R and a load effect S expressed in term of a common unit. The failure event in this case is $Z=R-S \leq \emptyset$ and the probability of failure becomes

$$P_f = \int_0^\infty F_R(s)\ f_S(s)ds \qquad (3.1)$$

in which F_R is the probability distribution function of R and f_S is the probability density function of S. By specifying distribution functions for R and S, Eq. 3.1 may be evaluated numerically.

Due to the scarcity of data, the probability distribution functions of the resistance and load are seldom known precisely. In some cases, only the first two moments, i.e. the mean and variance, may be known with any confidence. Moreover, the performance function may be nonlinear in the design variables. Even if enough statistical information is available for the different variables, the numerical evaluation of Eq. 3.1, in general, is impractical.

First-Order Approximation -- The above-mentioned difficulties have resulted in the development of an approximate method called first-order second-moment reliability method. The random variables are characterized by their first and second moments and the function g(...) is linearized at the mean-values of the variables. The resulting first-order mean and variance of Z are:

$$\bar{Z} = g(\bar{x}_1, \bar{x}_2, \ldots, \bar{x}_n) \tag{3.2}$$

$$\sigma_Z^2 = \left[\sum_{i=1}^{n} \sum_{j=1}^{n} \left(\frac{\partial g}{\partial x_i}\right)\left(\frac{\partial g}{\partial x_j}\right) \mathrm{Cov}\,(x_i, x_j) \right] \tag{3.3}$$

This method gives correct results when the design variables are normally distributed and the performance function is linear. When $g(x_1, x_2, \ldots, x_n)$ is nonlinear, the first-order approximation should be evaluated at a point on the failure surface, i.e. on $g(\ldots)=0$, instead of at the mean-values. Such a point $(x_1^*, x_2^*, \ldots, x_n^*)$ is determined by solving the following system of equations (Rackwitz, 1976):

$$\alpha_i = \frac{(\partial g/\partial x_i)\,\sigma_{x_i}}{\left[\sum_{i=1}^{n} (\partial g/\partial x_i)^2 \sigma_{x_i}^2\right]^{1/2}} \tag{3.4}$$

$$x_i^* = \bar{x}_i - \alpha_i \beta \sigma_{x_i} \tag{3.5}$$

$$g(x_1^*, x_2^*, \ldots, x_n^*) = 0. \tag{3.6}$$

where the derivatives $\partial g/\partial x_i$ are evaluated at $(x_1^*, x_2^*, \ldots, x_n^*)$. The solution of Eqs. 3.4 through 3.6 yields the safety index β, from which the failure probabilities for normal $(x_1, x_2, \ldots, x_n)$ is

$$P_f = 1 - \Phi(\beta) \tag{3.7}$$

It will be shown later that many structural problems involve design variables that may not be normally distributed. Non-normal probability distributions may be incorporated in the above reliability analysis by transforming the non-normal variables into equivalent normal random variables. The statistics of the equivalent normal random variables are obtained such that the cumulative probability and the probability density functions of the actual and approximating normal variables are equal at the failure surface $g(x_1^*, x_2^*, \ldots, x_n^*)=0$. Thus, the mean and standard deviation of the equivalent normal distribution are,

$$\bar{x}_i^N = x_i^* - \Phi^{-1}[F_i(x_i^*)]\ \sigma_i^N \tag{3.8}$$

$$\sigma_{x_i}^N = \frac{\phi\{\Phi^{-1}[F_i(x_i^*)]\}}{f_i(x_i^*)} \tag{3.9}$$

where $F_i(..)$ and $f_i(..)$ are the non-normal distribution and density functions of X_i $\phi(...)$ and $\Phi(...)$ are the density and distribution functions of the standard normal distribution.

3.2-Failure of a Frame With Flexible Connections

A tier of a frame at a temporary stage, or a frame (with flexible design) before its permanent lateral support is in place may be modeled as shown in Fig. 3.1 (a two-story tier). Diagonal members in this figure are cable guys usually used as temporary lateral suport. Beam-to-column connections and column anchorages of the frame are modeled by rotational springs. The resistance to lateral loads is provided by the connections and the temporary bracings , if used. An unbraced frame collapses by yielding when the total load effect in the connections exceeds the resistance of the connections. Hence, for a frame with n connections the failure probability when subjected to wind velocity V=v is,

$$P(\text{failure}\,|\,V=v) = P\left(\sum_{i=1}^{n} M_{R_i} \leq \sum_{i=1}^{n} M_{S_i}\right) \tag{3.10}$$

where M_{R_i} is the resisting moment of connection i, M_{S_i} is the load effect at the connection i induced by the wind velocity v. The statistics of M_{R_i} and M_{S_i} are subsequently discussed in Chapters 4 and 5.

Let $R_t = \sum_{i=1}^{n} M_{R_i}$ and $S_t = \sum_{i=1}^{n} M_{S_i}$; then the conditional probability of failure becomes,

$$P_{f|v} = P(Z_y = R_t - S_t \leq 0) \tag{3.11}$$

Evaluation of the above relation requires knowledge of the density functions of S_t and R_t.

The maximum wind load effect , S_t , is composed of two components; namely, the mean, $\bar{S}_{mt}$, and the fluctuating component, S_{dt}. In Chapter 4, the fluctuating component of the

wind on a linear structure is modeled by a stationary Gaussian random process. Davenport (1964) has shown, relying in part on earlier work by Cartwright and Longquet-Higgins (1956), that the distribution function of the maximum of a zero-mean Gaussian random process is,

$$F_{S_{dt}}(s) = \exp\left[-\nu T \exp\left(-\frac{1}{2}s^2\right)\right] \tag{3.12}$$

The mean and standard deviation of the above distribution is presented in Chapter 4 (Eqs. 4.22 and 4.23). The first two moments of the equivalent normal distribution of the above distribution function may be calculated from Eqs. 3.8 and 3.9.

The uncertainties in the mean wind load effect, for given wind velocity, are due to uncertainties in the wind environment parameters (see Chapter 4). Since the distribution functions of these parameters are not known, a normal density function will be assumed for the mean wind load effect.

Because of inadequate statistical information on the strength of connections (incomplete or completed connections) the density function of R cannot be objectively evaluated. In this study, a lognormal distribution is prescribed for R_t. The statistics of Z_y are then as follows (M_{R_i} and M_{S_i} are statistically independent):

$$\bar{Z}_y = \bar{R}_t^N - S_{mt} - \bar{S}_{dt}^N \tag{3.13}$$

$$\mathrm{var}(Z_y) = \mathrm{var}(R_t^N) + \mathrm{var}(S_{dt}^N) + \mathrm{var}(S_{mt}) \tag{3.14}$$

M_{S_i} and M_{S_j} may be assumed to be completely correlated, as they

are induced only by wind loading. M_{R_i} are also highly correlated due to identical workmanship and material used in the connections. Thus,

$$\text{var}(R_t) = \left(\delta_{M_{R_i}} \sum_{i=1}^{n} M_{R_i}\right)^2 \tag{3.15}$$

$$\text{var}(S_t) = \left(\delta_{M_{S_i}} \sum_{i=1}^{n} \bar{M}_{S_i}\right)^2 \tag{3.16}$$

In a temporarily braced frame, collapse will be caused by the sequential failures of the cable bracings and connections. The failure of a cable guy is brittle; therefore, the sequence of failure is important in determining the collapse probability of the frame. If events B and C denote the failures of the bracing and the connections, respectively, a frame may fail in two ways: (1) bracing fails after the failure of the connections, and (2) bracing fails before the failure of the connections. Therefore, the failure probability may be calculated by:

$$P(F) = P(F|C) \cdot P(C) + P(F|B)P(B) \tag{3.17}$$

where, $P(F|B)$ is the conditional probability of failure of the frame after the bracings have failed. Since a frame may be assumed to have failed after the failure of the connections, $P(F|C) = 1.0$.

In the case of a frame with two tiers that are temporarily fastened and braced, the connections may yield: (1)before the failure of the bracings; (2)after the failure of the bracing in one tier; and (3)after the bracings in both

tiers have failed. If B_1 and B_2 denote the events of failure of the bracings in tier 1 and tier 2, respectively, the probability of collapse of the entire frame may be calculated as follows:

$$P(F) = P(F|C)\cdot P(C) + P(F|B_1B_2)\cdot P(B_1|B_2)\cdot P(B_2) +$$

$$P(F|B_1B_2)\cdot P(B_2|B_1)\cdot P(B_1)+P(F|CB_1)P(C|B_1)P(B_1) +$$

$$P(F|CB_2) \cdot P(C|B_2) \cdot P(B_2) \qquad (3.18)$$

The different ways that a two-tier frame can fail as reflected in Eq. 3.18, may be illustrated schematically as follows:

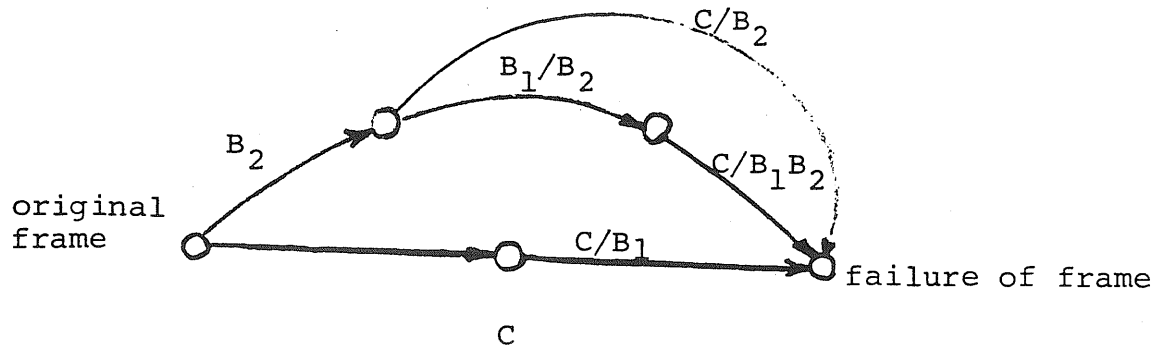

3.3-Failure Due to Instability of Members

Beams or columns of a frame during construction may become unstable because of inadequate lateral supports. The critical load for a column depends on its stiffness relative to that of the beams framing to it and on the presence or absence of a restraint against the lateral displacement of its ends. For frames that are erected several tiers with temporary connections, the equivalent unsupported length of the columns may be several times the story length, unless sufficient

lateral supports are provided. This reduces the buckling load of a column so much so that the weight of the upper stories plus a slight wind load could render the frame unstable. This may also occur to a bare frame with completed connections when the ratio of the stiffness of the beams to the stiffness of the connected column is not close to unity. This is usually the case for the weak axis of the columns in a frame with wide spans.

Before placing the floors of a frame, there is the possibility of buckling of the individual beams if the beams are entirely free from lateral restraint. However, in those cases in which cross beams provide lateral support at regular intervals, the lateral stability of the entire floor system may become critical (Fig. 3.2).

3.3.1-Failure of Columns

A column bending about its weak axis may fail by yielding (short columns), or instability (buckling as a beam-column). Let Z_p and Z_s denote the performance functions for these two modes of failure for a given wind velocity; Z_s represents an interaction curve, and Z_p is defined as follows:

$$Z_p = F_c - F_y \tag{3.19}$$

where, F_y is the yield strength of the column material and F_c is the maximum stress in the column for a given wind velocity.

The conditional failure probability of a column may be expressed by

$$P(\text{Failure}|V=v) = 1-p(Z_s \leq 1 \cap Z_p \leq 0) \tag{3.20}$$

The distribution function for Z_s may be determined on the assumption that all points on the interaction curve have the same probabilistic properties. The results of beam-column tests reported by Massonnet (1959) and Mason, et al, (1958) are used for this purpose. The histogram of these results is shown in Fig. 3.3. The same data are plotted in Fig. 3.4 on lognormal probability paper. It can be seen that a lognormal density function closely fits the available data for Z_s. Therefore, Z_s in Eq. 3.20 will be modeled by a lognormal density function.

Since the yield strength of steel may be modeled by a lognormal probability density function (Freudenthal, 1956), the statistics of Z_p may be obtained by

$$\bar{Z}_p = \bar{F}_y^N - F_{mc} - \bar{F}_{dc}^N \tag{3.21}$$

and

$$\sigma_{Z_p}^N = [\mathrm{var}(F_y^N) + \mathrm{var}(\bar{F}_{mc}) + \mathrm{var}(\bar{F}_{dc}^N)]^{1/2}$$

The probability distributions of F_{mc} and F_{dc} are as defined in Sect. 3.3 for the mean wind and fluctuating wind effects.

The collapse or partial collapse of a frame may be defined as the failure of one of its columns, in which case Eq. 3.20 gives the conditional failure probability of the frame. This assumption is probably reasonable in view of the fact that after a column buckles it does not support any load; its share of the load is redistributed to the remaining columns of the same floor. Resulting in overloading of the other columns and thus causing successive failure of the columns of the floor.

3.3.2-Failure by Lateral Instability of Beams

Beams in a bare frame under lateral wind load are subject to pure bending. The conditional probability of lateral buckling of an individual beam in a floor may be calculated by:

$$P(\text{Beam failure}|V=v) = P(M_{RB_i} - M_{SB_i} \leq 0) \qquad (3.23)$$

where M_{RB_i} is the lateral buckling resistance of beam i. The applied moment due to a wind velocity v is represented by M_{SB_i}.

In those cases where the floor beams are supported by cross beams at regular intervals, the stability of the entire floor system may become critical (Fig. 3.2). In such cases, the failure probability of the floor under a given wind velocity V=v, may be defined as

$$P(\text{floor failure}|V=v) = P(Z_{B_1} \leq 0 \cap Z_{B_2} \leq 0 \cap \ldots \cap Z_{BN} \leq 0) \qquad (3.24)$$

where, $Z_{Bi} = M_{RBi} - M_{SBi}$, and n is the number of beams in the floor in the direction of the wind. The load effects on the different beams would be highly correlated as they are all the result of the same wind loading. By virtue of a common material and workmanship, the strength of the different beams in a floor may also be assumed to be highly and positively correlated. Therefore, the correlation coefficient between Z_{Bi} and Z_{Bj} $(i \neq j)$ will all be close to 1; hence , Eq. 3.24 reduces to:

$$P(\text{floor failure} \mid V=v) = P(\text{Min. } Z_{B_i} \leq 0) \tag{3.25}$$

Evaluation of the probability of failure from Eq. 3.25 requires knowledge of the density functions of M_{RB} and M_{SB}. The distribution function of the maximum load effect is as given in Sect. 3.3. The lognormal distribution is a reasonable assumption for the distribution function of M_{RB}. In order to show this, let N_B denote the ratio of the test to the predicted lateral-torsional buckling strength of a beam, i.e.

$$N_B = \frac{(M_{RB})\ \text{Test}}{(M_{RB})\ \text{Pred.}} \tag{3.26}$$

A histogram of the ratios of the test strength to the predicted strength is shown in Fig. 3.5 (Yura, 1978). The same data are plotted on lognormal probability paper in Fig. 3.6. It can be seen that the data on N_B closely fit the lognormal distribution function. Since the distribution function of the ratio of two lognormal random variables is a lognormal distribution, it may be assumed that $(M_{RB})_{Test}$ and $(M_{RB})_{Pred.}$ are also individually lognormally distributed.

3.4-Calculation of Failure Probabilities

The failure probabilities discussed above were evaluated for a given wind velocity and thus are conditional failure probabilities. The probability of failure of a building frame at a given stage of construction depends on the maximum wind

velocity that occurs during the construction period of that stage; i.e. the maximum wind velocity is a function of the duration of the construction stage. If $f_{V(t)}(v)$ denotes the density function of the maximum wind velocity in a duration of t days, the failure probability of the frame in a t-day period may therefore be expressed as follows:

$$P(\text{failure}) = \int_0^\infty P_{f|V} \cdot f_{V(t)}(v)\, dv \qquad (3.27)$$

where $P_{f|V}$ is the conditional failure probability discussed earlier in Sects. 3.2 and 3.3. A method is presented in Chapter 4 for the evaluation of $f_{V(t)}(v)$.

CHAPTER 4

WIND AND WIND LOAD EFFECTS

4.1-Modeling an Incomplete Structure for Dynamic Analysis

As mentioned earlier, the major load on an incomplete frame is wind load. In a flexible structure, such as a steel frame during construction, the dynamic effect of wind could sometimes be several times greater than that of a static load. To evaluate the dynamic effect of wind on a structure, the dynamic properties of the structure must first be estimated. During the construction process, as the structure is being completed, its dynamic properties change. Therefore, the different stages of construction may require different analysis models with their respective dynamic structural properties.

In this chapter, the modeling of incomplete frames for dynamic response analysis and the key parameters for such analysis are discussed. The structural properties are treated as random variables, and the frame is assumed to have elastic properties with a dominant fundamental mode of response. Because of uncertainties in the properties of the frame components, the frame's dynamic properties are also random variables, where parameters may be evaluated from the statistcs of the member and connection properties.

In addition to the static and dynamic properties of a structure, the effect of wind also depends on the maximum wind speed that might occur during a given stage of construction. In order to evaluate the response in any given stage, the maximum wind speeds for short periods of time are predicted from available data for daily maximum wind speeds.

4.2-Dynamic Properties of an Incomplete Frame

4.2.1-Mass of the Frame

It is assumed that a steel frame is being built by equipment, such as a crawler crane, that works on the ground.

Therefore, members are usually stored on the ground and transferred to the erectors piece by piece, and there is no steel piled on the frame. When the wind starts blowing, workers usually stop working and leave the site for reasons of safety and difficulty of work. Thus, the mass of the frame is essentially that associated with the weight of the members, and may be idealised as being lumped at the floor levels. In this model the inertial moments at the joints due to joint rotation are neglected. Because of small variabilities in the length and dimensions of the members, the uncertainty in the estimation of the frame mass would be negligible.

4.2.2-Frame Stiffness

The stiffness of a frame is determined by the stiffness of its elements (members and connections). Both the beams and the columns of a frame can be modeled by the typical member shown in Fig 4.1, where the connections are represented by rotational springs having stiffnesses R_J and R_K. Rotational constants , R_i, can vary from zero (hinge connection) to infinity (rigid connection). Neglecting the joint size, and using the following notations, the stiffness matrix of a member would be as follows (Gere, 1963).

$$[S_M]=\frac{EI}{r^*}\begin{bmatrix} \frac{4\,r_{3J}}{\ell} & & & \\ \frac{6\,r_{2J}}{\ell^2} & \frac{12 r_o}{\ell^3} & & \\ \frac{2}{\ell} & \frac{6\,r_{2J}}{\ell^2} & \frac{4\,r_{3J}}{\ell} & \\ \frac{-6\,r_{2J}}{\ell^2} & \frac{-12 r_o}{\ell^3} & \frac{-6\,r_{2J}}{\ell^2} & \frac{12 r_o}{\ell^3} \end{bmatrix} \qquad (4.1)$$

where:

$$r^* = 12r_J r_K + 4\ (r_J + r_K) + 1$$

$$r_o = r_J + r_K + 1$$

$$r_{2J} = 2\ r_J + 1$$

and,

$$r_{3J} = 3r_J + 1$$

$$r_J = EI/(\ell \cdot R_J)$$

$$r_K = EI/(\ell \cdot R_K)$$

Uncertainty in $[S_M]$ is a function of the uncertainties in the member and joint stiffnesses at different stages of construction. The behavior and uncertainties in the stiffness of the connections will be discussed in Chapter 5. In estimating the uncertainties, it is assumed that the behavior of all temporary connections is identical; i.e. they have the same number of bolts and are placed in the same location in the connection, and identical connection angles are used throughout. Also, the same rotational behavior (in one direction) is assumed for all completed connections.

4.2.3-Natural Frequency

The response of a lightly damped, flexible structure is sensitive to the natural frequency of the structure. Therefore, the natural frequencies of a bare frame at different stages of construction and their uncertainties must be evaluated in order to calculate the response of the structure and its corresponding uncertainty.

The natural frequency of a system can be obtained by

$$\omega_i^2 = \frac{[\phi_i]^T[K_S][\phi_i]}{[\phi_i]^T[M_S][\phi_i]} \qquad (4.2)$$

where M_S and K_S are, respectively, the mass and the stiffness matrices of the structure; whereas ω_i and ϕ_i are respectively the ith natural frequency and mode shape. Since the same workmanship and material are used in the construction of a frame, it is reasonable to assume that the stiffnesses between connections, as well as the stiffnesses between bracings and between members, are perfectly correlated. On the other hand, any correlation between the stiffnesses of the members, connections, and bracings may be assumed to be negligible. Therefore, the variance of ω_1 may be obtained as follows(Hasselman, 1972).

$$\mathrm{var}(\omega_1) = \sum_{i=1}^{4} \left(\frac{\partial \omega_1}{\partial x_i}\right)^2 \mathrm{var}(x_i) \qquad (4.3)$$

where X_i are the random variables in the stiffness matrix of the frame, which are the temporary connection stiffness, R_i, column anchorage stiffness, R_c, temporary bracing stiffness , K_b, and member stiffness, EI. The stiffness of a beam-to-column connection is assumed to be statistically independent of the stiffness of the column anchorages.

Since the mass matrix is deterministic, the partial derivatives of ω_1 may be calculated as (Fox, 1968),

$$\frac{\partial \omega_1}{\partial x_i} = \frac{[\phi_1]^T \left[\frac{\partial K_s}{\partial x_i}\right] [\phi_1]}{[\phi_1]^T [M_s] [\phi_1]} \qquad (4.4)$$

Evaluation of the partial derivatives of the stiffness matrix of the structure is discussed in Appendix A .

If, instead of treating the stiffness matrix of the frame as a random matrix, it is assumed that the frame's stiffness matrix is composed of a random variable k' multiplied by a deterministic matrix $[\bar{K}]$ (the mean stiffness matrix), where the mean value of k'_s is equal to 1 with a c.o.v. of $\delta K'_s$ (Portillo, 1976), Eq. 4.2, then yields $\delta K'_s = \delta \omega_1$. With this assumption, the stiffness matrix will also yield a deterministic mode-shape vector for the structure. Since the gust response factor is not sensitive to the mode shape of the structure (Vickery, 1969), this simplification will have a small error on the calculation of the dynamic response of the structure. A prediction error of 10 per cent (e.i., $\Delta\phi_1$=0.10) will be used subsequently to account for this effect.

4.2.5-Damping

The damping ratio of a steel frame during construction depends on the type of connections, the structural configuration, and the stage of construction. Damping of a bare frame is composed of two parts; mechanical and aerodynamic.

In a bare frame, the mechanical damping will consists of the internal damping of the steel and friction in the joints. It is believed (Raggett, 1975) that the highest material damping for steel alone is about 0.25 per cent. Several tests have been performed to study the damping of full scale steel structures. Hogan (1971) reports that for small-amplitude motions, the completed John Hancock Building has a damping ratio of 0.5%. Ragget(1975) believes that this damping is due to the steel frame itself because most of the lateral forces are transmitted directly to the foundation by the external frame without stressing other components of the building. Bradshaw (1964) measured the damping ratio of a welded bare steel arch; his results yielded 0.8 per cent. From these observations an average value of 0.5 per cent is suggested(Raggett, 1975) for the mechanical damping ratio, β_M , of a bare frame with completed connections.

There is not sufficient data to investigate the uncertainty of the damping ratio of incomplete frames. The uncertainty in the damping of bare frames may be estimated from information for completed structures. Portillo and Ang (1976) examined the damping in completed reinforced concrete structures. The results of 135 tests on full scale structures, for a variety of test procedures, were analysed. The mean value and the c.o.v. of the damping ratio were estimated to be 4% and 0.5, repectively. The study showed that damping and natural frequencies may be assumed to be statistically independent.

A study of test results on completed steel structures (Rojiani, 1978) also confirms the statistical independence of the natural frequencies and damping in a structure. The mean and c.o.v. of the damping ratio in completed steel frames were 2% and 0.70, respectively.

In a completed structure a sizeable fraction of the energy-absorbing capacity of the structure is contributed by the architectural elements. For this reason, the damping in a completed structure may depend on the age of the structure. This may be the main reason for the high c.o.v. in the damping

ratio of completed structures. Since the mechanical damping in an incomplete steel frame is largely due to the internal damping of the steel and friction in the connections, uncertainty in the damping ratio of an incomplete frame should be lower than the corresponding uncertainty in damping of a completed structure. In this study a c.o.v. equal to 0.30 will be used for the damping ratio of an incomplete bare frame.

In an experimental study, damping of a steel frame at various stages of construction was measured as reported by Watanabe (1965). The average value of the equivalent damping ratio for the frame, with its temporary connections, varied from 2 to 3 per cent. Due to lack of sufficient data on mechanical damping of frames with temporary connections, uncertainty can only be estimated subjectively.

For the purpose of the present study, a mean damping ratio of 0.5 per cent will be used for bare frames with cmopleted connections. For the case of frames with temporary connections, the mean value of the mechanical damping ratio will be assumed to be 2 per cent. A c.o.v. of 0.30 will be used for both cases.

The aerodynamic damping in structures with low mass and large exposed area may become much higher than the mechanical damping. The aerodynamic damping coefficient, β_a, is given by(Davenport, 1964),

$$\beta_a = \frac{[f_\omega][\phi_1]}{2\omega_1 M_s^*} \qquad (4.5)$$

where: $\{f_\omega\} = \{f_{\omega_1}, f_{\omega_2}, \ldots, f_{\omega_n}\}$

$$f_{\omega_i} = \rho . v(z_i) . (A_{Bi} C_{dB} + A_{ci} C_{dc})$$

M_s^*=the generalized mass of the structure
$V(Z)$= wind speed at floor level i
A_{Bi} and A_{ci} are the total exposed area of the beams and columns at floor level i, arespectively, and
C_{dB} and C_{dc} are the drag coefficients of the beams and columns.

Using first-order approximation, the mean value and c.o.v. of the aerodynamic damping for a given wind speed may be calculated as follows:

$$\bar{\beta}_a = [\bar{f}_\omega][\phi] \;/\; 2\bar{\omega}_i \; M_s^* \tag{4.6}$$

$$\delta^2_{\beta_a} = \delta^2_{c_d} + \left\{ \frac{\alpha\,[\bar{f}_\omega \ln z/_{30}][\phi_1]}{[\bar{f}_\omega\,[\phi_1]} \right\}^2 \delta^2_\alpha + \delta^2_{\omega_1} + \Delta^2_{\phi_1} \tag{4.7}$$

4.3-Wind Load Effect

The stochastic wind force acting on a structure is usually broken down into two components: a mean force resulting from the mean wind velocity, and a time-varying force resulting from the wind gust. Calculation of the wind load effect will be based on the assumption that the wind speed fluctuations constitute a stationary Gaussian random process.

Since the frame is assumed to be a linear system, the induced maximum load effect can also be broken down into a mean response which is the static response of the frame under the mean wind force , and a maximum dynamic response due to the fluctuating component of the wind force. The assesment of the uncertainties underlying the determination of the response is discussed below.

4.3.1-Mean Wind Load Effect

In the case of frameworks, Ower (1948) claims that for a single frame with solidity ratio*, $\phi_s < 0.5$, (solidity ratios of bare building frames is usually less than 0.50), the summation of the forces on individual members yields results for the total wind load effect with satisfactory accuracy. Accordingly, the mean wind load at floor level i for a given wind speed may be calculated by:

$$F_{\omega_i} = \frac{1}{2} \rho \, v^2(z_i) \, (C_{dB} \, A_{Bi} + C_{dc} \, A_{ci}) \qquad (4.8)$$

The variables in Eq. 4.8 were as defined in Section 4.2.5. The static response in the first mode is calculated as follows;

$$\bar{y}_1 = [\bar{F}_\omega][\phi_1] / [\phi_1]^T [\bar{K}_s][\phi_1] \qquad (4.9)$$

$$\delta^2_{y_1} = \delta^2_{cd} + \frac{\alpha \, [F_\omega \, \ell n \, z/30][\phi_1]}{[F_\omega][\phi_1]} \, \delta^2_\alpha + \delta^2_{K_s'} + \Delta^2 \phi_1 \qquad (4.10)$$

where $\{F_\omega\} = \{F_{\omega_1}, F_{\omega_2}, \ldots, F_{\omega_n}\}$, and n is the number of floors. The static wind load effect in a member, S_{mi}, may then be obtained as,

---

*Solidity ratio = The solid elevation area divided by the total enclosed elevation area.

$$[S_m] = [SM][C][\phi_1]\, y_1 \tag{4.11}$$

where [c] is the displacement transfer matrix of the structure (a deterministic matrix), and SM represents the member stiffness matrix. The mean value of S_m is obtained by substituting the mean value of each parameter in Eq. 4.11, whereas the c.o.v. of the elements of S_m are:

$$\delta^2_{S_{mi}} = \delta^2_{cd} + \left\{ \frac{\alpha\ [F_\omega\ \ell n\, z/30][\phi_1]}{[F_\omega][\phi_1]} \right\}^2 \delta^2_\alpha + \Delta^2 \phi_1 \tag{4.12}$$

4.3.2-Wind Gust Effect

Because of the linearity of the structure, its dynamic response to the gust component would also be a stationary zero-mean Gaussian random process. The fluctuating wind force at floor level i may be written as,

$$F_{\omega_i}(t) = f_{\omega_i} \cdot v(t) \tag{4.13}$$

where, $f_{\omega_i} = \rho \cdot v(z_i)\ (C_{dB}\ A_{Bi} + C_{dc}\ A_{ci})$

Initially, it is assume that the wind speed is well correlated around the structure. Therefore, the generalized time-varying wind force on the frame would be (based on first mode).

$$F^*_{\omega}(t) = [f_\omega][\phi_1]^* v(t) \tag{4.14}$$

The power spectral density of the time-varying wind force is obtained as a function of the spectrum of wind velocity from Eq. 4.14, as follows:

$$S_f(n) = f_\omega^{*2} \cdot S_v(n) \qquad (4.15)$$

where: $\{f_\omega^*\}$ $\{[f_\omega][\phi_1]\}$

In reality, the wind speeds at different parts of the frame are not completely correlated; to account for this effect, a correlation function $C^2(n)$ may be introduced in Eq. 4.15. Several such functions have been suggested for $C^2(n)$ for completed buildings by, Davenport (1967), Vickery (1969), and Vellozzi, et al (1968). In the case of a bare frame, the relation proposed by Vellozzi (1968) will be used, which is as follows:

$$C^2(n) = \left\{\frac{1}{\zeta} - \frac{1}{2\zeta^2}(1-e^{-\zeta})\right\} \quad \left\{\frac{1}{\gamma} - \frac{1}{2\gamma^2}(1-e^{-2\gamma})\right\}$$

$$\left\{\frac{1}{\mu} - \frac{1}{2\mu^2}(1-e^{-2\mu})\right\} \qquad (4.16)$$

in which,

$$\zeta = \frac{3.85n.D}{\bar{v}} \qquad \gamma = \frac{11.5n.B}{\bar{v}}$$

$$\mu = \frac{3.85n.H}{\bar{v}} \qquad \bar{v} = \frac{\bar{v}_{30}\ (H/30)^{\alpha}}{1 + \alpha}$$

D, B, and H are the alongwind and crosswind dimensions, and the height of the structure. The spectrum of the wind force then becomes,

$$S_f(n) = f_{\omega}^{*2} \cdot C^2(n) \cdot S_v(n) \tag{4.17}$$

The variance of the dynamic response in the first mode and of its derivative are given by;

$$\sigma_{y_1}^2 = f_{\omega}^{*2} \int_0^{\infty} C^2(n) \cdot S_v(n) \left|H(n)\right|^2 dn \tag{4.18}$$

and

$$\sigma_{\dot{y}_1}^2 = f_{\omega}^{*2} \int_0^{\infty} n^2 . C^2(n) \cdot S_v'(n) \left|H(n)\right|^2 dn \tag{4.19}$$

where $|H(n)|^2$ is the frequency transfer function of the system. The standard deviation of the dynamic wind load effect S_D and of its derivative $\dot{S}_D$, in a member may be calculated from σ_{y_1} and $\sigma_{\dot{y}_1}$ as follows:

$$\sigma_{SD} = C_1 \cdot \sigma_{Y_1} \tag{4.20}$$

$$\sigma_{\dot{SD}} = C_1 \, \sigma_{\dot{Y}_1} \tag{4.21}$$

where C_1 is the effect of the first mode shape deformation on the member.

4.3.3-Maximum Dynamic Wind Load

Let $Y_m(t)$ be the maximum response in a duration t. The mean and standard deviation of Y_m are found to be (Davenport, 1961,1964),

$$\bar{Y}_m = \left(\sqrt{2 \ln \nu t} + \frac{.577}{\sqrt{2 \ln \nu t}} \right) \cdot \sigma_{Y_1} \tag{4.22}$$

and

$$\sigma_{Y_m} = \frac{\pi}{6} \cdot \frac{Y_1}{\sqrt{2 \ln \nu t}} \tag{4.23}$$

where, $\nu = \sigma_{\dot{Y}_1} / 2\pi\sigma_{Y_1}$. Substituting σ_{SD} and $\sigma_{\dot{SD}}$ of Eqs. 4.20 and 4.21 in the above equations, the maximum dynamic wind load effects in each member may be calculated. Since σ_{Y_1} and $\sigma_{\dot{Y}_1}$ are functions of the structural properties and the wind environment parameters, which are random variables σ_{SD} and $\sigma_{\dot{SD}}$ are also random variables. Using first order approximation, the mean and standard deviation of the maximum dynamic load effect on a member may be calculated as (Rojiani, 1978),

$$\bar{S}_{D_m} = \left(\sqrt{2 \ln \bar{\nu}_s t} + \frac{.577}{\sqrt{2 \ln \bar{\nu}_s t}} \right) \bar{\sigma}_{SD} \tag{4.24}$$

$$\sigma_{SD_m} = \left[\frac{}{\bar{S}_{D_m}^2} \left\{ \frac{\pi}{36} \frac{\bar{\sigma}_{SD}^2}{\sqrt{2 \ln \nu_s t}} + \sum_{i=1}^{n} \sum_{j=1}^{n} \left(\frac{\partial SD}{\partial x_i}\right) \left(\frac{\partial SD}{\partial x_j}\right) * \right. \right.$$

$$\left. \left. * \text{Cov}\,(x_i, x_j) + 0.2^2 \right\} \right] \qquad (4.25)$$

where; $\nu_s = \frac{\dot{\sigma}_{SD}}{2\pi\sigma_{SD}}$, X_i are the random structural and wind parameters, and $\bar{\nu}_s$ and $\bar{\sigma}_{SD}$ are mean values of ν_s and σ_{SD} . The partial derivatives $\frac{\partial SD}{\partial x_i}$ are developed in Appendix B .

In order to include the errors underlying the effect of simplifications in the above equations as well as other prediction errors, an additional c.o.v. of 0.20 is introduced as shown in Eq. 4.27.

4.3.4-Estimation of Wind-Parameter Uncertainties

In order to evaluate the first two statistical moments of the maximum of the wind-induced response from Eqs. 4.24 and 4.25, the uncertainties associated with the random structural and wind parameters are required. The uncertainties underlying the wind parameters are evaluated in this section; those associated with random structural properties are assessed in Chapter 5.

The drag coefficient of structural shapes is usually a function of the Reynolds number, aspect ratio, and yaw angle of the member relative to the wind direction. The effect of these factors, as well as the effect of shielding, must be included in the determination of the overall drag coefficient of the structure.

In general, the effect of the Reynolds number may be ignored with regard to frameworks of steel structures, as they

are comprised of members having sharp edges. The aspect ratio correction is used for members with a free end. No correction is necessary for structural members connected to a gusset plate or to a cross member (Scrunton, 1963). The influence of the yaw angle must be obtained by tests. In this study, it is assumed that the wind direction is normal to a side of the structure and thus a yaw angle correction factor of 1 is appropriate.

In steel buildings, there are several parallel frames. The shielding effect of the windward frame reduces the drag coefficient of the frames downstream. For example, the drag coefficient of the second frame downstream may be given as

$$C_{D_2} = \eta \cdot C_{D_1} \tag{4.26}$$

where C_{D_1} is the drag coefficient of the first frame, and η is the shielding effect of the windward frame. The value of η depends on the solidity ratio (ϕ_s) of the first frame and spacing ratio of the frames, S_s, which is equal to the distance of the frames divided by the frame height.

To date, all tests conducted to determine the effect of the shielding coefficient, η, have been for trusses or towers: no data appear to be available for building frames. From an examination of the available test data for towers and bridge structures, the following empirical relationship between η, ϕ_s, and S_s is developed (Ower, 1948).

$$\eta = 1 - 1.17\ (\phi_s - \sqrt{S_s/100}) \tag{4.27}$$

Eq. 4.27 is valid for $\frac{S_s}{12} < \eta < 1$ and $0.5 < S_s < 1$. The above relation has been adopted by some building codes. Other empirical relations and tables for evaluating the shielding effect of open frameworks have been used; e.g.

France (regels, NV65)
Italy (CNR, UNI 10012

$$\left\{ \begin{array}{l} \eta = 1\text{-}1.2\ \phi_s \\ \text{for } \phi_s \leq 0.6,\ S_s < 2 \end{array} \right. \qquad (4.28)$$

Denmark (DS 410, 1966)

$$\left\{ \begin{array}{l} \eta = 1.15\text{-}1.67\ \phi_s\ \sqrt[4]{S_s} \\ \text{for } \phi_s \leq 0.6,\ 1 \leq S_s \leq 5 \end{array} \right. \qquad (4.29)$$

Eqs. 4.27 through 4.29 are shown graphically in Fig. 4.2 .

There is little information on the shielding effects of structures with more than two parallel frames. However, based on limited evidence showing that the shielding effect is not cummulative, it is believed (Ower, 1948) that equal loading may be used for each shielded frame. Therefore, the overall drag coefficient of a structural frame may be obtained as follows,

$$\bar{C}_{Dt} = \bar{C}_{D1}\ [1 + (n-1)\bar{\eta}\ ] \qquad (4.30)$$

$$\delta_{C_{Dt}}^2 = \delta_{CD}^2 + \delta_{\eta}^2\ \left[\frac{(n-1)\eta}{1+(n-1)\eta}\right]^2 \qquad (4.31)$$

where n is the number of frames in the structure normal to the wind direction. For this study, the mean value of η is obtained as the average of Eqs. 4.27, 4.28, and 4.29. Whereas, the variance of η is obtained by assuming a uniform distribution for η between the minimum and maximum values obtained from these equations. The c.o.v. of η for values of ϕ_s that are close to the solidity ratio of structural frames (ϕ_s <0.5) varies from 3 to 7 per cent.

The drag coefficient of structural sections is estimated

Table 4.1

PRESSURE COEFFICIENTS FOR STRUCTURAL MEMBERS (Davenport, 1966)

Pressure coefficients $C_{n\infty}$ and $C_{t\infty}$ for simple and multiple sections

Normal force $K_{n,l} = k_{l.p} C_{n\infty} qF$ and tangential force $K_{t,l} = k_{l,p} C_{t\infty} qF$

For h/l = ∞

Wind normal to long axis.

For $k_{l,p}$ see No. 30

ℓ= length of member

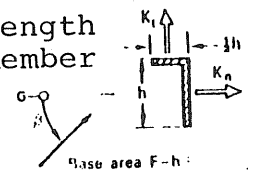

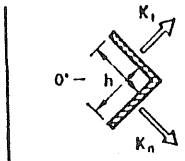

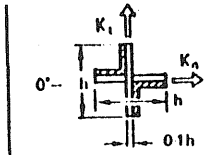

β	$C_{n\infty}$	$C_{t\infty}$	$C_{n\infty}$	$C_{t\infty}$	$C_{n\infty}$	$C_{t\infty}$
0°	+1·9	+0·95	+1·8	+1·8	+1·75	+0·1
45°	+1·8	+0·8	+2·1	+1·8	+0·85	+0·85
90°	+2·0	+1·7	−1·9	−1·0	+0·1	+1·75
135°	−1·8	−0·1	−2·0	+0·3	−0·75	+0·75
180°	−2·0	0·1	−1·4	−1·4	−1·75	−0·1

ℓ= length of member

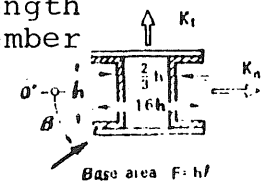

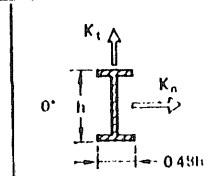

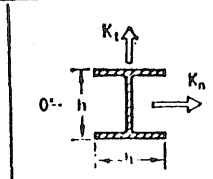

β	$C_{n\infty}$	$C_{t\infty}$	$C_{n\infty}$	$C_{t\infty}$	$C_{n\infty}$	$C_{t\infty}$
0°	+1·4	0	+2·05	0	+1·6	0
45°	+1·2	+1·6	+1·95	+0·6	+1·5	+1·5
90°	0	+2·2	−0·5	+0·9	0	+1·9

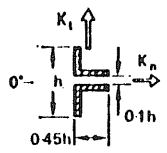

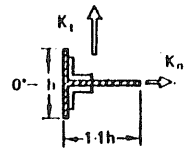

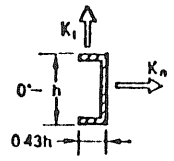

$C_{n\infty}$	$C_{t\infty}$	$C_{n\infty}$	$C_{t\infty}$	$C_{n\infty}$	$C_{t\infty}$
+1·6	0	+2·0	0	+2·05	0
+1·5	−0·1	+1·2	+0·9	+1·85	+0·6
−0·95	+0·7	−1·6	+2·15	0	+0·6
−0·5	+1·05	−1·1	+2·4	−1·6	+0·4
−1·5	0	−1·7	±2·1	−1·8	0

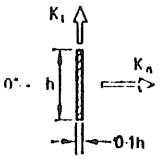

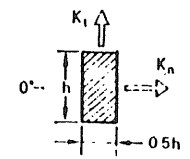

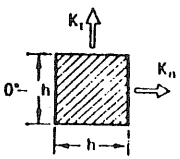

$C_{n\infty}$	$C_{t\infty}$	$C_{n\infty}$	$C_{t\infty}$	$C_{n\infty}$	$C_{t\infty}$
+2·0	0	+2·1	0	+2·0	0
+1·8	+0·1	+1·4	+0·7	+1·55	+1·55
0	+0·1	0	+0·75	0	+2·0

from wind tunnel tests. Since it is possible to run tests on full-scale structural shapes the error in the tabulated drag coefficient is small and would mostly be due to measurement inaccuracies. A c.o.v. equal to 0.05 will be used for the mean values of the drag coefficients given in Table 4.1.

Estimates of uncertainties in the prediction of α and surface drag coefficient, K_d, given by Vickery(1969) are $\delta_\alpha = 0.1$ and $\delta_{K_d} = 0.2$, respectively. There appears to be no experimental data for appraising the accuracy of the correlation function, $C^2(n)$, proposed by Cohen. A subjective c.o.v. of 0.20 will be used to account for the uncertainty in $C^2(n)$.

4.4-Determination of Extreme Wind Velocity During Construction

The probability of failure of a structure during a stage of construction depends not only on the strength of the structure at a particular stage, but also on the maximum wind velocity that may occur during the construction of that stage. The duration of the critical stages of construction of a building usually varies from a few days to a few weeks. Accordingly, the maximum wind velocity during the period of a critical construction stage is the velocity of concern; such a maximum velocity is also a random variable. Therefore, a probabilistic model is required to predict the maximum wind speed as a function of the duration of construction operation and the time of the year that construction is in progress.

One model for predicting the wind speed with return periods of less than a year, was proposed by Davenport (1967). The wind speed, V, is modeled as a continuous random process, whose first-order probability distribution is Rayleigh. A Rayleigh distribution is also used for the rate of change of velocity, $\dot{V}$. Then, using Rice's crossing rate expression and a Poisson process for streams of upcrossing, the distribution for the largest values of the process is obtained.

Gomes and Vickery (1977) used the above method with a Weibul distribution for the wind speed, V. Values for the statistics of $\dot{V}$ are estimated with a numerical method from five

years of hourly mean wind speeds. In the following, the required distribution of the maximum wind speed in a period of several days is determined on the basis of information for the daily maximum wind speeds.

4.4.1-Maximum Wind Prediction Model

Wind speed will be considered as a discrete time random process, V(t), t=0, 1, 2, ..., where V(t) is the daily maximum wind speed and t is time(in days). The problem is to determine the distribution of the maximum of this process over duration T (in days).

It is reasonable to assume that the statistical properties of the daily maximum wind speed do not change in short periods of time, such as one month. On this basis, the daily maximum wind speed, V(t), may be assumed to be stationary over a month. Observed daily maximum wind speed data are the only source of information for the selection of a mathematical form to represent the distribution of V(t). For annual maximum wind speed, the Type I Extreme Value distribution is often used. However, for the daily or monthly maximum wind speeds, the Type I Extreme Value distribution may not be appropriate. For example, modeling the monthly maximum wind speed with the Type I Extremal distribution could lead to monthly maximum wind speeds that are higher than the annual maximum speed for small exceedance probabilities.

The lognormal distribution appears to give the best fit with several years of observed daily and monthly maximum wind speeds; Figs. 4.4a and 4.5a show such fits for the daily maximum wind speeds for the months of March and July, respectively. This distribution fits other months' data equally as well. Thus, a Lognormal distribution will be prescribed for the first-order probability density function of the random sequence of daily maximum wind.

The following transformation changes this process to a normal random sequence;

$$x(t) = \ell n\ V(t) \tag{4.32}$$

That is, $x(t)$ is $N(\lambda, \zeta)$, where λ and ζ are the parameters of $V(t)$.

Van Marcke (1975) shows that the probability of a normal random process remaining below a level u in (0,t) can be obtained from the following relation:

$$F_{V(t)}(V < u) = \Phi(u_1) \cdot \exp[-\nu_u \cdot t/\Phi(u_1)] \tag{4.33}$$

where :

$$u_1 = \ell n \frac{\mu - \lambda}{\zeta}$$

$$\Phi(\mu_1) = \frac{1}{2\pi} \int_{-\infty}^{\infty} e^{(-\frac{1}{2} t^2)} dt \ ;$$

and, ν_u =the rate of exceedance of level u in a unit time, as determined below.

Consider the broken line (Fig. 4.3) joining the points $[t, X(t)]$, and the up and down crossing of this line with a given level u. The number of up-crossings in the interval $(t, t+1)$ is 1 if $[X(t) < U, X(t+1) > U]$, and is 0 otherwise. Then the mean number of up-crossings in this interval, ν_u, may be calculated as the following probability using the notation $n(t_i) = x_i$;

$$\nu_u = P(x_1 < \mu, x_2 > \mu)$$

$$= \int_{-\infty}^{\mu} \int_{\mu}^{-\infty} f_{X_1 X_2}(x_1, x_2) \, dx_1 \, dx_2 \tag{4.34}$$

in which the joint density function of X_1 and X_2 is bi-normal; i.e.

$$f_{X_1X_2}(x_1,x_2) = \frac{1}{2\pi\zeta^2\sqrt{1-\rho^2}} \exp\left\{\frac{-1}{2(1-\rho^2)}\left[\frac{(x_1-\lambda)^2}{\zeta^2} + \frac{(x_2-\lambda)^2}{\zeta^2} - 2\rho\left(\frac{x_1-\lambda}{\zeta}\right)\left(\frac{x_2-\lambda}{\zeta}\right)\right]\right\} \quad (4.35)$$

4.4.3-Verification of Above Results

Using the above method requires statistics of the first order probability density function of the sequence of maximum daily wind speeds and the autocovariance of the sequence $[K_{V_1V_2}(1)]$. The autocovariance can be calculated from a record of wind speed data as follows:

$$K_{V_1V_2}(1) = \frac{1}{n-1}\sum_{i=1}^{\ell}(v_i-\mu_v)(v_{i+1}-\mu_v) \quad (4.36)$$

$$\rho_v = K_{V_1V_2}(1)/\sigma_v^2 \quad (4.37)$$

To investigate how well the above method can predict the maximum expected wind speed in a given period, wind speed data recorded at Midway Airport, Chicago were used.

Using the daily maximum wind speeds for the month of March from 1971 to 1976, the distributions for the maximum wind speeds over durations of 5 days and 10 days were obtained. These distributions are plotted in Figs. 4.4b and 4.4c, and compared with the cumulative frequencies of the observed maximum wind speeds for the same durations in March. Figs. 4.5b and 4.5c show the same distributions for the month

of July. The data shown in Fig. 4.4 are for the month of July from 1965 through 1976.

CHAPTER 5

STRENGTH AND STIFFNESS OF INCOMPLETE STRUCTURES

5.1-Introduction

The resistance of an incomplete steel frame depends on the buckling strength of the beams and columns, as well as the strength and stiffness of its connecting elements including (1)column anchorages, (2)column splices, (3)temporary and permanent beam-to-column connections, and (4)the temporary bracing of the frame. In the development of the resistance models used herein, it is tacitly assumed that the strengths and section properties along a member are perfectly correlated, whereas those between different elements are uncorrelated.

5.2-Buckling Strength of Columns

The adequacy of a member to support an axial force and bending moment is usually determined by empirical interaction equations. The ultimate strength of such a member can be closely approximated by the following (low axial load).

$$\frac{f_a}{F_a} + \frac{c_m f_b}{F_b(1+f_a/F'_e)} \leq 1 \qquad (5.1)$$

$$f_b - F_y \leq 0 \qquad (5.2)$$

where f_a = axial compression stress.

F_a = allowable compression stress considering the member as loaded by axial compression only. F_a is obtained as follows;

$$F_{ae} = \frac{\pi^2 E}{S_y \cdot \lambda^2} \quad ; \quad Z_f = \lambda - C_c \geq 0 \tag{5.3}$$

$$F_{ai} = F_y \left[1 - \frac{F_y}{4\pi^2 E} \lambda^2\right]; \quad Z_f = \lambda - C_c \leq 0 \tag{5.4}$$

$\lambda = K\ell/r_y$ and $C_c = 2\pi^2 E/F_y$

K=effective length factor

F_y=yield stress of steel.

f_b= flexural stress based on bending moment.

F_b= allowable flexural stress considering the member loaded in bending only.

f'_e= Euler buckling stress

S_y, r_y=section modulus and governing radius of gyration

C_m=a reduction factor used for columns subjected to unequal end moments (Galambos, 1978).

The allowable compressive stress in a member, F_a, depends on the value of $Z_f = \lambda - C_c$ (as shown in Eqs. 5.3 and 5.4). Since λ and C_c are functions of the member properties and dimensions, Z_f is a random variable with the following statistics

$$\bar{Z}_f = \frac{\bar{K} \cdot \ell}{\bar{r}_y} - \frac{2\pi^2 \bar{E}}{\bar{F}_y} \tag{5.5}$$

and,

$$\delta^2_{Z_f} = \lambda^2 \delta^2_K + \lambda^2 \delta^2_{r_y} + C_c^2 \, \delta^2_E + C_c^2 \, \delta^2_{F_y} \tag{5.6}$$

Therefore, F_a is conditional on the value of Z_f, and thus,

$$P(F_a \leq f) = P(F_{ae} \leq f \mid Z_f \geq 0) \cdot P(Z_f \geq 0) + P(F_{ai} \leq f \mid Z_f \leq 0) \cdot P(Z_f \leq 0) \quad (5.7)$$

The corresponding statistics of F_a calculated with the above equations are;

$$\bar{F}_a = \bar{F}_{ae} \cdot P(Z_f \geq 0) + \bar{F}_{ai} \cdot P(Z_f \leq 0) \quad (5.8)$$

$$E(F_a^2) = E(F_{ae}^2) \cdot P(Z_f \geq 0) + E(F_{ai}^2) \cdot P(Z_f \leq 0) \quad (5.9)$$

Equation 5.1 represents the interaction between buckling and bending, and determines the strength of a member with low buckling strength. Equation 5.2 ensures that the plastic moment M_p is not exceeded by the end moments in a column. Since column translation in a floor is restricted to an equal amount for all columns of a floor, the weaker columns of a floor are assisted by the stronger ones. In view of this, Yura (1971) suggested an average value of the amplification factor, $(1+ f_a / F'_e)$, be used in the interaction formula for all columns in a story. When a story of a structure fails laterally, one floor translates relative to another as a unit. Thus the deflection, and hence the moment magnification, must be related among the compression members in the same story. The amplification factor in the column interaction formula, Eq. 5.1, therefore, becomes;

$$(1 + \sum_{i=1}^{n} f_{ai} / \sum_{i=1}^{n} F'_{ei}) \quad (5.10)$$

where n is the number of columns in a floor. A column fails when at least one of the inequalities (Eq. 5.1 or 5.2) does not hold. Representing the left hand side of Eqs. 5.1 and 5.2 by Z_s and Z_p, respectively, the event of failure may be represented as follows:

$$\{\text{failure}\} = (Z_p \leq 0 \cup Z_s \leq 1) \tag{5.11}$$

The parameters of Z_p and Z_s and the correlation coefficient correlation between them may be estimated by first order approximation from the following relations;

$$Z_s = \left[\frac{\bar{f}_a}{\bar{F}_a} + \frac{C_m \cdot \bar{f}_b}{\bar{F}_b\left(1 + \sum_i \bar{f}_{ai} / \sum_i \bar{F}'_{ei}\right)}\right] \cdot N_s \tag{5.12}$$

$$\bar{Z}_p = \bar{f}_b - \bar{F}_y \tag{5.13}$$

$$\delta^2_{Z_s} = D_1^2 \, \delta^2_{f_a} + D_2^2 \, \delta^2_{f_b} + D_3^2 \, \delta^2_{F_y} + D_4^2 \, \delta^2_{\lambda} + D_5^2 \, \delta^2_{E} + \delta^2_{N_S} \tag{5.14}$$

$$\delta^2_{Z_p} = \left(\frac{\bar{f}_b}{\bar{Z}_p}\right)^2 \delta^2_{f_b} + \left(\frac{\bar{F}_y}{\bar{Z}_p}\right)^2 \delta^2_{F_y} \tag{5.15}$$

$$\text{Cov}(Z_s, Z_p) = C_1^2 \, \text{var}(f_b) + C_2^2 \, \text{var}\,(F_y) \tag{5.16}$$

N_s is a random variable reflecting the discrepancy between the predicted and the experimental values of Z_s. The statistics of N_s will be evaluated subsequently. The coefficients D_i and C_i are given in Appendix C .

5.2.1-Evaluation of Individual Uncertainty Measures

Uncertainties in the load effects were discussed in Chapter 4. Other sources of uncetainty in the above formulations are the effective length factor k , the properties and dimensions of rolled sections, and inaccuracies of the prediction equations. Variabilities in rolled section dimensions are usually low. It was found (Ravindra, 1972) that the Handbook sectional properties of hot-rolled elements were equal to the mean values, with a c.o.v. of 0.05 . With the assumption of 0.02 variability for each of the section dimensions, the coefficients of variation shown in Table 5.1 were obtained for the sectional properties of hot-rolled structural elements by Rojiani (1978).

Table 5.1

UNCERTAINTIES IN SECTION PROPERTIES (Rojiani, 1978)

Section property	Coefficient of Variation
Area	.02-.03
Moment of Inertia, I	.05-.06
Moment of Inertia, I	.06-.07
Section modulus, S	.03-.04
Section modulus, S	.04-.05
Torsion constant, J	.04-.06
Warping constant, C	.07-.09

The buckling length of a column in a frame at a given stage of construction depends on the degree of fixity of its ends and the amount of lateral support provided for the incomplete frame at that stage. The stability of a column with elastic rotational restraints at the ends (Fig.) has been studied by Gurfinkel (1965), it is shown that the effective length factor, K , for such a column may be determined from the following relation;

$$\tan \frac{\pi}{K} = \frac{\pi/K(r_1+r_2)}{(\pi/K)^2-r_1r_2} \qquad (5.17)$$

where $r_1=\frac{R_1 \cdot \ell}{EI_c}$ and $r_2=\frac{R_2 \cdot \ell}{EI_c}$. R_1 and R_2 are the rotational stiffness at the ends of the column; i.e. the moment necessary to produce a unit rotation in the spring. For a column in the first floor of a frame, R_1 is the stiffness of the column anchorage, and R_2 is equivalent to the rotational stiffness of all the members. framing into the column in the plane of buckling. It can be shown (see Appendix D) that R may be evaluated as a function of the properties of the framing members as follows;

$$R_2 = \frac{6EI_c}{\ell_c} \sum_{i=1}^{2} \frac{EI_{bi}}{\ell_{bi}} \left[\frac{1}{1 + 6J_i}\right] / \sum_{i=1}^{2} \frac{EI_{ci}}{\ell_{ci}} \qquad (5.18)$$

where $J_i = \frac{EI_{bi}}{\ell_{bi} \cdot R_{bi}}$ is the beam to column joint factor (Gere, 1963); I_{bi} and I_{ci} are the moments of inertia of the beams and columns at the joint.

At different stages of construction, and depending on the structural design, the stiffness of the column anchorage or the beam-to-column connection could vary considerably. Therefore, the buckling length of a column in a frame at different stages of construction could also vary. Using Eq. 5.1 for a column in the first floor of a building shown in Fig. 6.1, the variation of the column length factor, K , as a function of the column anchorage stiffness and the effective stiffness of the beams framing into the column is shown in Fig. 5.1.

The statistics of K can be obtained from Eq. 5.17 by first-order approximation as follows;

$$\delta_K^2 = C_2'^2 \, \delta_{r_1}^2 + C_2'^2 \, \delta_{r_2}^2 \tag{5.19}$$

$$\delta_{r_1}^2 = \delta_E^2 + \delta_{I_c}^2 + \delta_{R_1}^2 \tag{5.20}$$

$$\delta_{r_2}^2 = \delta_E^2 + \delta_{I_b}^2 + \left(\frac{6J}{1+6J}\right)\left(\delta_E^2 + \delta_{I_b}^2 + \delta_{R_b}^2\right) \tag{5.21}$$

The coefficients C_i' are given in Appendix C . The c.o.v. of a beam-to-column connection stiffness, δ_{R_b} , and of a column anchorage stiffness, δ_{R_1} , are evaluated subsequently below.

An investigation on the variability of the yield stress of steel conducted by Ravindra (1972) shows that, for specimens obtained from the flange of I sections, the mean static yield stress is about 5 per cent higher than the nominal yield strength with a coefficient of variation of 0.10 . In the same study, the mean and coefficient of variation of the modulus of elasticity of steel have been evaluated as 29000 ksi and 0.06, respectively.

The statistics of N_s are calculated in two parts (Galambos, 1978) as follows:

$$N_s = B_{EX} \cdot B_{th} \tag{5.22}$$

where B_{EX} is the ratio of the test strength to the exact theoretical strength, and B_{th} is the ratio of the exact theoretical strength to the strength obtained with the interaction equation, Eq. 5.1, using mean material properties.

The statistics of B_{EX} have been determined on the basis of 83 beam-column tests as shown in Fig. 5.2. The mean and coefficient of variation are $\bar{B}_{EX}$=1.005 and δB_{EX}=.093.

The statistical properties of B_{th} were found to be $\bar{B}_{th}$=1.01 and δB_{th}=0.04 (Galambos, 1978).

A large series of buckling tests on mild steel columns of European rolled I-sections were conducted by Massonnet (1959). Fig. 3.3 shows the histogram of the accuracy of the interaction equation, Eq. 5.1, for predicting the failure of the columns. The mean and standard deviation are 1.05, and 0.10, respectively.

Based on these observations, a mean of 1.02 and a c.o.v. of 0.10 are obtained for N_s.

5.3-Buckling Strength of Floor Beams

There is usually no major transverse loading (i.e. vertical) on the beams of a bare frame during construction. The principal loading is the lateral loading due to wind, including bending moments in the members and connections. The theoretical expression for the critical elastic moment for lateral buckling of a beam (M_e) is as follows (Clark, 1960);

$$M_e = C_1 \pi \frac{\sqrt{EI_y GJ}}{K \cdot \ell_b} \sqrt{1 + \frac{\pi^2 E\, C_w}{(K\ell_b)^2 GJ}} \tag{5.23}$$

where C_w and J are warping and torsion constants of the cross section, respectively, ℓ_b is the length, and K is the effective-length coefficient of the beam.

The coefficients C_1 and k depend mainly on the conditions of the loading and supports for the beam. When the end moments produce double curvature in the beam (such as under lateral wind load), C_1 is in the range of 2.23-2.58 (Clark, 1960). Depending on whether the end conditions of the beam in the Y-Y direction is hinged or fixed, the value of k would be 1 or 0.5 . Eq. 5.23 is valid only in the elastic range. The European Convention for Construction Steelwork (ECCS) has recommended the following formula to account for inelastic behavior, including the effect of residual stresses (Fukumoto, 1977). Theoretical investigations and test results are the basis for the following formula:

$$M_u = M_p \left[\frac{1}{(1+\lambda_B^{2n})}\right]^{1/n} \tag{5.24}$$

$$\lambda_B = \sqrt{M_p/M_e} \tag{5.25}$$

where: M_u =the ultimate moment capacity.

M_p=the plastic moment capacity of the section.

M_e=the critical elastic moment calculated from Eq. 5.23.

Figure 5.3 shows a comparison of Eq. 5.24 with test results for 159 rolled beams with different loading and end conditions. It shows that for a value of n equal to 2.5, Eq. 5.24 closely corresponds to the mean-value of the test results. The coefficient of variation of the test results are also plotted in the lower part of Fig. 5.3, which shows that the

c.o.v. varies between 0.05 to 0.12 . Fig. 3.5 shows a histogram of the ratio of the test load to the predicted elastic load (Eq. 5.23) for 185 tests covering a variety of loading conditions and shapes (Yura, 1978). The mean is 1.03 and the c.o.v. is 0.09. In the present study, the mean value of M_u will be based on Eq. 5.24 (with n=2.5), and an average c.o.v. of 0.09 will be used.

5.4-Strength of Column Anchorages

5.4.1-Incomplete column anchorage

Because of the high cost of fabricating and constructing a moment-resisting footing anchorage, column anchorages are usually designed only for vertical loads. However, in view of the high ratio of lateral to gravity loads and the flexibility of the frame during construction, the column anchorages are often subjected to significant bending forces during construction.

As was mentioned earlier in Chapter 2, during the early stages of construction and sometimes even towards the end of the erection of a frame, base-plates are supported temporarily on shim packs to maintain proper elevation (Fig. 2.1a). Assuming that steel erection starts after the concrete of the footings is cured, the capacity of a column anchorage would be limited by (1)the tensile strength of the anchor bolts, and (2)the bending strength of the base-plates. If the strengths of the anchorage of a column, limited by the anchor bolt failure and base-plate failure, are designated as M_{R_1} and M_{R_2}, respectively , the strength of the incomplete anchorage, M_{R_i} would be,

$$M_{R_i} = \text{Min } (M_{R_1}, M_{R_2}) \qquad (5.26)$$

The disribution functions of M_{R_1} and M_{R_2}, in general, are not known. But, since M_{R_1} and M_{R_2} are products of several random variables, it may be reasonable to assume that they are lognormally distributed. M_{R_1} and M_{R_2} are also statistically independent since they do not have any variable in common. With these assumptions, it is shown in Appendix (E) that the statistics of M_{R_i} may be calculated by;

$$E(M_{R_i}) = E(M_{R_1}) \cdot C_1 + E(M_{R_2}) \cdot C_2 \tag{5.27}$$

$$E(M_{R_i}^2) = E(M_{R_1}^2) \cdot C_3 + E(M_{R_2}^2) \cdot C_4 \tag{5.28}$$

where:

M_{R_1} is $LN(\lambda_1, \zeta_1)$

M_{R_2} is $LN(\lambda_2, \zeta_2)$ and;

$$C_1 = \Phi\left|\frac{\lambda_2 - \lambda_1 - \zeta_1^2}{\sqrt{\zeta_2^2 + 2\zeta_1^2}}\right|$$

$$C_2 = \Phi\left|\frac{\lambda_1 - \lambda_2 - \zeta_2^2}{\sqrt{\zeta_1^2 + 2\zeta_2^2}}\right|$$

$$C_3 = \Phi\left[\frac{\lambda_2-\lambda_1 - 2\zeta_1^2}{\sqrt{\zeta_2^2 + 2\zeta_1^2}}\right]$$

$$C_4 = \Phi\left[\frac{\lambda_1-\lambda_2 - 2\zeta_2^2}{\sqrt{\zeta_1^2 + 2\zeta_2^2}}\right]$$

Statistics of M_{R_1} -- The strength of an anchorage limited by its anchor bolt strength, M_{R_1}, is defined as follows;

$$M_{R_1} = n \cdot R_y \cdot (d_1 + d_2) \qquad (5.29)$$

where n is the number of hold-down bolts; R_y is the yield strength of a hold-down bolt, and $d_1 + d_2$ is the distance between the hold-down bolts and the shim packs(Fig. 2.1a).

Column anchor bolts are usually threaded bars. The yield strength may be obtained by $R_y = \phi_B \cdot F_{y_B} \cdot A_B$, where F_{y_B} and A_B are the yield stress and cross sectional area of a bolt. The effect of embedment on the bolt strength is accounted for through ϕ_B.

Test results on column anchorages (LaFraugh, 1966) show that the yield strength of anchor bolts measured in connection tests, F_{y_C}, are slightly less than those obtained for bare (unembedded) bolts, F_{y_B}. Table 5.2 shows test results for embedded anchor bolts, and the ratio F_{y_C}/F_{y_B}, representing the ratio of the actual yield force to the yield force of a bare bolt. The mean and coefficient of variation of the ratio, ϕ_B were 0.92 and 0.065 , respectively. Assuming an additional c.o.v. of 0.05 the statistics of ϕ_B would be $\bar{\phi}_B$=0.92 and $\delta\phi_B$=0.08.

The actual yield strength of bare bolts, F_{y_B}, usually exceeds the nominal value, F_{N_B}. Tension tests on a few anchor bolts of hot-rolled plain bars having a yield stress of about 55 ksi show (LaFraugh, 1966) that the actual yield stress exceeds the nominal value by about 2.5% with a c.o.v. of 0.085 .

Table 5.2

TEST RESULTS ON EMBEDED BOLTS (LaFraugh, 1966)

3/4 inch Bolt		5/8 inch Bolt	
F_{Y_C} (ksi)	$\phi_B = F_{Y_C}/F_{Y_B}$	F_{Y_C} (ksi)	$\phi_B = F_{Y_d}/F_{Y_B}$
17.6	0.98	11.8	0.89
15.5	0.86	11.2	0.85
17.0	0.94	12.6	0.95
18.0	1.00	11.1	0.84
18.0	1.00		

Variation in $d_1 + d_2$ depends on the position of the shim packs under the base plate and the accuracy of placing the anchor bolts in concrete. There are always inaccuracies in setting the anchor bolts, which are placed in concrete when the footing concrete is poured. To allow for these inaccuracies, holes in the base plates are made larger than the bolt diameter(AISC, 1971) by $\pm$ e=1/2 to 1 inch. Thus, d_1 can vary +e/2 about its mean value. Assuming a uniform distribution for the variation of d_1 in this range, the c.o.v. of d_1 would be

$$\delta_{d_1} = \frac{e}{2\sqrt{3}\, d_1} .$$

Usually shim packs are placed imprecisely under the base plate beneath the column flange. A triangular distribution may be assumed for the location of a shim pack in the range shown in Fig. 2.1b. On this basis, the statistics of d_2 are:

$$\bar{d}_2 = \bar{d}_c + \frac{\bar{s}_s}{2} \tag{5.30}$$

and,

$$\delta_{d_2}^2 = 0.4 \left(\frac{\bar{b}_p}{\bar{b}_p + 2\,\bar{d}_c}\right)^2 \tag{5.31}$$

where d_c is the column depth, and S_s is the shim pack width. From Eq. 5.29, the c.o.v. of M_{R_1} may be calculated as follows:

$$\delta_{M_{R_1}}^2 = \delta_{R_{y_B}}^2 + \frac{\bar{d}_1^2}{(\bar{d}_1 + \bar{d}_2)^2}\,\delta_{d_1}^2 + \frac{\bar{d}_2^2}{(\bar{d}_1 + \bar{d}_2)^2}\,\delta_{d_2}^2 \tag{5.32}$$

The c.o.v. of the strength of an incomplete column anchorage for low to medium rise buildings, calculated from above relation, is about 0.22 to 0.24.

Statistics of M_{R_2} -- The flexural resistance of a base plate is given by

$$M_{R_2} = F_{y_p} \cdot b_p \cdot t_p^2/\sigma \tag{5.33}$$

in which t_p is the thickness and b_p is the width of the base plate.

Variation of the yield strength of plates depends primarily on the grade and thickness of the plate. Tests on a large number of samples show (Baker, 1977) that the average yield strength of the plates are about 9 to 21 per cent above the specified nominal values, with the lowest value corresponding to the higher strength material. The c.o.v. of the yield strength from these tests varies from 0.08 to 0.11 . A reasonable estimate for the variability of t_p is 0.02 . Uncertainty in b_p depends on the accuracy of the shop fabrication of the base plate. The dimensions of base plates in two jobs under construction were measured. The variability in b_p calculated from these measurements was about .055. The mean value of b will be assumed to be equal to the nominal value specified by the designer. With this information, the c.o.v. of M_{R_2}, calculated using Eq. 5.33 is 0.12.

5.4.2-Completed Column Anchorage

When the space under the base-plate is grouted, the connection is considered to be completed. Grouting changes the distance between the hold-down bolts and the center of gravity of the compressive forces under the base-plate. The exact location of the resultant compressive forces under the base-plate is not known. Experimental behavior of the anchorages of a few precast concrete columns indicate (LaFraugh, 1966) that assuming the centroid of the compression stresses under the column flange leads to theoretical results for column strength that are very close to the experimental values. This assumption is valid only for column anchorages of low to medium rise buildings and where the base-plate is about one inch thick.

The strength of a completed column anchorage, M_{R_C}, based on the above assumptions would be:

$$M_{R_C} = \text{Min.}\ (M_{R_1}, M_{R_2}) \qquad (5.34)$$

where M_{R_1} and M_{R_2} are as defined in the previous section, except that in Eq. 5.29, d_2 is replaced by the column depth, d_c. Thus,

$$M_{R_1} = n \cdot R_{y_B} \cdot (d_1 + d_c) \cdot N_{R_1} \tag{5.35}$$

where N_{R_1} represents the ratio of test to calculated results. Uncertainties in R_{y_B} and d_1 were discussed in the previous section. From this information, a c.o.v. of 0.15 was obtained for M_{R_c} for a completed column anchorage.

Table 5.3

THEORETICAL AND TEST STRENGTH OF COLUMN ANCHORAGES (LaFraugh,1966)

Column Load at Yielding in Bolt			Column Load at Yielding in Plate		
Test (kip)	Calc. (kip)	Test/Calc.	Test (kip)	Calc. (kip)	Test/Calc.
92	84	1.10	81	72	1.12
69	62	1.11	72	72	1.00
82	84	0.98	60	72	0.83
62	62	1.00	78	76	1.03
88	84	1.05	73	76	0.96
60	62	0.97	48	44	1.09
90	84	1.07	93	108	0.86
62	62	1.00	93	100	0.93
82	84	0.99			
93	84	1.10			

Theoretical results for the strength of completed column anchorages, obtained on the basis of the above-mentioned assumptions, and the real strength obtained from tests, are compared in Table 5.3. The thickness of base-plates in these tests varied from 7/8 to 1.25 inches. The statistics of N_{R_1} in Eq. 5.35 were estimated from the data in Table 5.3 yielding $\bar{N}_{R_1}$ =1.025 and δN_{R_1} =0.08. Therefore, the total c.o.v. in M_{R_C} is δM_{R_C} =0.17.

5.5-Strength of Temporary Beam-Column Connections

As discussed earlier, temporary beam-to-column connections are either framed or seated. Although they fall in the category of flexible connections, some of them are capable of resisting some moment. In the following, the behavior of these two common types of temporary connections are reviewed.

5.5.1-Seated Temporary Connections

Ordinarily, the end of a seated beam is stopped approximately 1/2 inch short of the face of the supporting column to which the seat angle is attached (erection clearance). Depending on the length and depth of the beam, the mill also allows itself a tolerance of about 3/8 to 1/2 inch (or more) on the nominal length of the beam. Because of these tolerances the supported beam is set back about 3/4 to 1 inch from the column face (Fig 2.2d). To meet these tolerances, usually slotted or oversized holes are used in this type of temporary connections. The beam set-back and the oversized holes make such a connection very flexible and thus may be assumed to behave like a hinge.

For deep beams, a top angle is installed when placing the beam to prevent overturning. In this case, the connection can resist some moment. Failure of this type of connection is due to excessive yielding of the top angle or tensile failure of the temporary bolts.

In order to calculate the resisting moment of the connection, the load-deformation behavior of the connection angle is required. A relationship developed by Lewitt, et al, (1969) for the load deformation behavior of angles is as follows;

$$P = C\ (\Delta)^N \tag{5.36}$$

where Δ represents the deformation of the angle (Fig. 5.4); C and N are constants whose values are tabulated by Lewitt (1969) for various combinations of gauge, fillet radius, yield point, fastener size, and angle thickness.

The resisting moment of a beam-to-column connection is obtained by(see Fig. 5.5),

$$M_{1R} = T_B \cdot (d_B + g) \tag{5.37}$$

where g is the gauge length and d_B is the depth of the beam. T_B is the tensile force applied to the top angle. Since Eq. 5.36 has been developed for two angles(see Fig. 5.4), the relationship between tensile force, T_B, and the deformation of the top angle using Eq. 5.36 would be,

$$T_B = \frac{1}{2}\, C \cdot (\Delta)^N \cdot \ell_a \tag{5.38}$$

where ℓ_a is the length of the connection angle. Substituting this in Eq. 5.37 and using $\Delta = \phi \cdot d_B$, Eq. 5.37 becomes,

$$M_{1R} = \frac{1}{2}\, C \cdot \ell_a\, (d_B+g) \cdot (\phi \cdot d_B)^N \tag{5.39}$$

Figure 5.6 shows the above relation for two common sizes of beam-to-column connections.

The accuracy of the moment obtained from Eq. 5.39 depends on the accuracy of Eq. 5.36, as well as on the variability of the angle properties and dimensions. The influence of workmanship on the behavior of a connection is also considerable. It is pointed out by Fisher (1974) that the behavior of a connection may vary by as much as 20/ to 50/ for identical specimens supplied by different fabricators. The theoretical load-deformation behavior obtained from Eq. 5.36 follows the experimental results closely (Lewitt, 1969). Therefore, the variability due to workmanship is the dominant factor and overshadows other sources of uncertainty. Since there are no experimental results on temporary beam-to-column connections, a triangular distribution will be assumed for the variation of M_{1R} between $.6M_{1R}$ and $1.4M_{1R}$. The c.o.v. calculated with this assumption would be 0.16 . The mean-value of M_{1R} will be calculated with Eq. 5.39 for a rotation equal to 0.03 radian.

Another mode of failure of temporary beam-to-column connections is due to failure of the temporary bolts. The moment capacity in this mode is;

$$M_{2_R} = F_{y_B} \cdot A_B \, (d_B+g) \tag{5.40}$$

where F_{y_B} is the yield stress of the temporary bolts. The resisting moment in this mode depends on the type and size of the bolts used. Test results show that the real tensile strength of bolts exceeds their required minimum (Fisher, 1974). Analysis of available data shows that the strength of A325 bolts, of sizes 1/2 to 1 inch diameter, exceeds the minimum by an average of 18%, with a standard deviation of

0.045. The statistics of the tensile strength of the same type of bolts, recommended by Fisher (1974) are $\bar{F}_{y_B} = 1.18F_{N_B}$ and $F_{Y_B} = 0.07$ (F_{N_B} is the minimum required tensile stress). These values will be used in this study.

5.5.2-Framed Temporary Connections

A common type of framed temporary beam-to-column connection is built with two framing angles shop-attached to the beam and field-connected to the column (Fig 2.2a). Two or more bolts are usually placed in the connection at a temporary stage. The resistance and moment-rotation ($M-\phi$) characteristics of the connection at this stage depends on several factors including,

a) number of bolts used in the connection,
b) location of bolts in the connection,
c) size and type of bolts, and
d) size and thickness of the connecting angles.

Failure of this type of connection may be caused by the failure of the temporary bolts or excessive yielding and tearing of the connection angles.

In order to determine the strength of a temporary connection, its $M-\phi$ relation may be examined first. It was suggested by Beaufoy (1948) that the $M-\phi$ relationship of framed beam-column connections can be derived from a consideration of the composite effect of short lengths of angles in tension and compression. It is shown in Fig. 5.7 how a connection angle is assumed to be subdivided into a number of short segments whose combined bending resistance is considered equivalent to that of a single angle of the same total length.

The method suggested above makes it possible to predict the $M-\phi$ characteristics of a flexible connection without dependence on tests of full size connections. What is required are the load-deformation characteristics of the angle segments and the location of the center of rotation.

The deformation of an angle in tension was discussed earlier in Eq. 5.36. The location of the center of rotation varies with the magnitude of the applied moment. During the

initial stages of loading, the location of the center of rotation is near the mid-length of the connection (Lewitt, 1969). The center of rotation moves toward the compression end of the angle as the applied moment increases. In the final stages, the center of rotation in completed connections was observed to be at 0.8 to 0.85 of the length of the connection angles from the tension end (Lewitt, 1969). Since the tension side of a temporary connection is more flexible than that of a completed connection (because of fewer bolts in a temporary connection), the center of rotation in temporary connections at the final stages of loading will be closer to the compression end. That is, it would be between 0.8 to the full length of the connection angles from the tension end. The mean distance of the center of rotation at the final stages of loading, therefore, may be assumed to be at 0.9 of the angle length.

Two relations will be obtained for the M-ϕ relation of this type of temporary connection. One is for the initial stage of loading and is based on the assumption that the center of rotation is in the middle of the framing angle. The other applies to the final stages of loading, and assumes that the center of rotation is at 0.9 of the length of the angle from the tension side. The complete M-ϕ curve of the connection is obtained by connecting these two portions with a smooth curve.

M-ϕ Relationship, Early Stage of Loading -- At the early stages of loading, the center of rotation is close to the middle of the connection. If the temporary connection has two bolts at the top of the connection (Fig. 2.2a), the connection may be modeled as shown in Fig. 5.8. The effect of the continuity of the connection angle will be included later. The resisting moment of the connection is $M_{lR}=T_B \cdot de$, where T_B is the tension in the bolts and d_e is the distance between the center of compressive and tensile stesses. Using Eq. 5.36 for T_B, the resisting moment of the connection becomes,

$$M_{lR} = C(\Delta)^N \cdot \ell_d \cdot d_e$$

where ℓ_d is the "tributory" length (see Figs. 5.7 and 5.8) for a bolt. The above relationship is valid for deformations less than or equal to about 0.02 inch in the connection angles; load deformation tests show (Lewitt, 1969) that angles remain elastic in this range of deformation. Therefore, the center of rotation is in the middle of the angle.

The above relationship was derived by loading individual segments of the connection angle. Lewitt (1969) shows that continuity increases the stiffness of the angle segments by about 7% for ℓ_d equal to 3 inches. Therefore, Eq. 5.36 would be revised to $P=1.07\ C(\Delta)^N$ and ;

$$M_{1R} = 1.07\ C(\Delta)^N \cdot \ell_d \cdot d_e \tag{5.42}$$

Substituting $\frac{\phi \cdot \ell_a}{2}$ for Δ , where ℓ_a is the connection length (see Fig. 5.8);

$$M_{1R} = 1.07\ C\ (\frac{\phi \cdot \ell_a}{2})^N \cdot \ell_d \cdot d_e \tag{5.43}$$

<u>M-ϕ Relationship, Final Stage of Loading</u> -- At the final stages of loading, plastic yielding would have occurred in the tension side of the conection angles. The resisting moment at this stage can be calculated as follows,

$$M_{2R} = 1.07\ C \cdot \ell_d(0.9\ \ell_a\phi)^N \cdot (0.95\ \ell_a - e_d) \tag{5.44}$$

in which e_d is the bolt edge distance. For two common types of framed connections, the above relations are plotted in Fig 5.9. Eq. 5.43 is valid in the elastic range, whereas Eq. 5.44 is for the stage in which complete plastic yielding have formed in the tension side of the connection. The part of the curve which represents the transition from elastic to complete

plastic behavior is shown by a smooth curve joining the elastic and plastic portions.

The uncertainties in this type of connection, as in the case of seated connections, are generally due to workmanship in fabrication and field assembly. Therefore, the uncertainty that was used for seated connections will be used also in this case; namely, a c.o.v. of 0.16.

5.6-Strength of Column Splices

AISC (1969) specification requires that a column splice be designed for wind-induced bending moment after being counteracted by 75% of the dead load. During construction, when the dead load is largely absent, the wind load effect may exceed the connection's strength. In the following discussion, the strength of column splices, in its completed and incomplete stages, and their respective uncertainties are examined.

5.6.1-Strength at Temporary Stage

At a temporary stage, there are only a few bolts in the splice connection. Therefore, a connection may fail by shearing of the temporary bolts. The resisting moment of a column splice at this stage may be calculated as follows (see Fig. 2.3),

$$M_{R_S} = n \cdot A_B \cdot \tau_B \cdot d_c \tag{5.45}$$

where τ_B is the shearing strength of a temporary bolt; A_B is the cross sectional area of a bolt; n is the number of bolts in one side of the column; and d_c is the column depth.

From tests of 142 high-strength bolts, it was observed (Fisher, 1974) that the shear strength of bolts may be represented as a function of the tensile strength, T_B, of the bolt; i.e. $\tau_B = N_B \cdot T_B$, where N =0.625 and $\delta\bar{N}_B$ =0.033. The statistics of the tensile strength of bolts, T_B , was discussed

in Sect. 5.6.1. From this information, the c.o.v. of M_{R_S} is evaluated to be 0.06.

In the case of a completed column splice, failure may occur through the yielding of a splice plate. Therefore, the resisting moment at this stage would be,

$$M_{R_{SC}} = F_{y_p} \cdot A_p \cdot d_c \tag{5.46}$$

Its corresponding c.o.v. may be given by,

$$\delta^2_{M_{R_{SC}}} = \delta^2_{F_{y_p}} + \delta^2_{A_p} + \delta^2_{d_c} \tag{5.47}$$

where A_p and F_{y_p} are the cross sectional area and yield strength of the splice plates. The c.o.v. in A_p and F_{y_p} were discussed earlier in Sect. 5.4.1 .

5.7-Strength of Temporary Bracing

Temporary bracing during construction is generally provided by wire ropes. During erection, the need for bracings, and the amount and type of bracing are usually determined by the ironworker foreman. The availability of wire ropes at the site is an important factor in the amount of bracing used. Wire ropes used for bracing are often crane boom lines that have been discarded for reason of inadequate or unsafe strength due to wear or broken wires.

Fulweiler (1936) tested 229 specimens taken from 79 worn wire ropes of different construction. From these tests nomographic charts were prepared. These charts give the strength of a rope on the basis of the length of wear on the outside wires, and the number of broken wires in the strands. However, it is impractical and uneconomical to evaluate the strength of temporary bracing with these charts.

A statistical analysis of available data is used to

determine an empirical value for the strength of ropes used. Since there is extensive data available on the strength of worn ropes, the result would be a representative value for the strength of ropes used as bracing.

Wire ropes come in different diameters and construction. Ropes used for bracing are usually 1/2 inch to 5/8 inch in diameter. Six-strand 19-wire construction made from plow steel will be considered here.

All test specimens were discarded wire ropes used in cranes, dredges, or elevators. The statistics of the strength of 5/8-inch diameter ropes obtained from tests on 80 specimens are

$$T_R = 20604 \text{ lb} \qquad \delta_{T_R} = .252$$

and for 1/2-inch specimens,

$$\bar{T}_R = 13220 \text{ lb} \qquad \delta_{T_R} = .297$$

The mean strengths are approximately 60% of the strength of new ropes. These data are for ropes that have just been discarded from use, and therefore are lubricated with no rust. After being reused in the field for a period of time they rust and the strength is reduced. To account for these effects, a reduction coefficient N_p will be used. The parameters of N_p can only be assigned subjectively based on the number of times a rope has been used in the field and the field condition. Here, $\bar{N}_p = .95$, $\delta_{N_p} = .05$ will be assumed. The total c.o.v. of the strength of a used wire rope then will be about 0.30.

5.7.1-Wire Rope Fittings

Since wire ropes cannot be tied into knots, or kinked, without damage, fastening accessories are required. Wire ropes are usually wrapped around beams or columns before being secured by clips. Bending reduces the wire rope strength considerably depending on the rope and the bend diameter. Skillman (1924) has studied the reduction of strength of wire ropes on sheaves. His tests show that the strength of 5/8-inch rope on a sheave with an 18-inch diameter is 95.3% of that of straight rope. The same rope on a 10-inch sheave has 87.4% of its straight strength. When a rope is wrapped around a beam or

column sections with sharp edges, the bend diameter would be much less than that of a 10 inch bend. To account for this effect on rope strength, a reduction factor N_R will be used. Based on Skillman's test results, a mean value of 0.80 seems reasonable for N_R. A c.o.v. of 0.05 will also be assumed for N_R. Hence, the remaining strength of a rope, W , would be,

$$\overline{W} = 0.76\overline{T}_R \tag{5.48}$$

with a c.o.v. of 0.30.

5.8-Stiffness of Column Anchorages

5.8.1-Incomplete Column Anchorage

The moment-rotation characteristics of a column anchorage at a temporary stage of construction depends on its connection elements such as,

(a) base plate dimension and thickness,

(b) number ,place,size,diameter,and grade of anchor bolts,

(c) placement of shim packs under the plate.

Salmon, et al, (1957) have developed theoretical relationships to describe the characteristics of column anchorages. There are also experimental results for completed column anchorages. The results of these studies will be used to derive the stiffness and associated uncertainty of a column anchorage at each stage of construction.

The rotation of a column anchorage is due to the elongation, ϕ_B , of the tension bolts and the bending, ϕ_p , of the base plate between the column and the hold-down bolts.

Rotation Due to Anchor Bolt Elongation -- The elongation of an anchor bolt in a temporary column connection consists of two parts; the displacement of the embedded length and the elongation of the length between the base plate and the footing surface. Thus,

$$\Delta_B = (e_E + \frac{H}{EA_B}) \cdot R_B = e_t \cdot R_B \tag{5.49}$$

where, e_E is the slip of the embedded length per unit load, H is the height of the shim packs under the base plate, A_B is the bolt cross sectional area, and R_B is the tension in the bolt. The rotation and stiffness of the column anchorage associated with this deformation are,

$$\phi_B = \Delta_B/(d_1 + d_2) \tag{5.50}$$

$$K_B = n \cdot (d_1 + d_2)^2/e_t \tag{5.51}$$

where n is the number of hold-down bolts in column anchorage.

The uncertainty in K_B is primarily due to the uncetainties in H, d_1+d_2, and e_E. The space under the base plate usually varies between 1 and 2 inches. Assuming a uniform distribution for the value of H in this range, an estimate of the statistics of H would be H=1.5 inches and $\delta_H = 0.19$. The variations in d and d were calculated in Sect. 5.4.1, whereas, e_E must be estimated experimentally. A series of tests were run on 1/2-inch anchor bars embedded in concrete. The load and slip at the pull-out ends were observed for straight anchor bars and anchor bars with a bend at the embedded end (Fishburn, 1947). The variables in the investigation were the dimensions of the bend and the length of the embedment. The range of the loads on the bent-bar anchorage for slips up to 0.02 inch and the average loads are shown in Fig. 5.10. Each curve in the figure represents the mean load carried by bent bar anchorages, irrespective of the length of the embedment. The rectangles, drawn on the ordinates for the different values of slip, show the range of the loads. Curve 1 shows the load-slip variation for a deformed anchor bar, whereas Curve 2 represents the load deformatin relation for a plain bar. In the case of deformed anchor bars, the c.o.v. of the load at a slip of 0.005 inch was 9%. At the maximum load, the c.o.v. was 4%; whereas for

the plain anchor bars these values were 16% and 11%, respectively. In a building, the embedment length of column anchor bolts are usually the same. Therefore, the coefficient of variation of the load-slip relationship of an anchor bolt will be less than the above values. In this study, an average c.o.v. of 0.05 will be used for e_E .

Fig. 5.10 also shows the load-slip relationship for a headed anchor bolt with a smooth shank(Shoup, 1963). For the calculation of the mean value of e_E, the curves in Fig. 5.10 were linearized as shown in dash lines. The c.o.v. of K_B is then obtained by,

$$\delta^2_{K_B} = \delta^2_{d_1+d_2} + \left(\frac{e_E}{e_t}\right)^2 \delta^2_{e_E} + \left(\frac{H}{EA_B e_t}\right)^2 \delta^2_H \qquad (5.52)$$

Rotation Due to Base Plate Deformation -- Modeling the section of the base plate between the column and the hold-down bolt as a beam, the mean stiffness due to base-plate deformation would be,

$$K_p = \frac{3\bar{E}_p \bar{I}_p}{\bar{d}_1^3} (\bar{d}_1 + \bar{d}_2)^2 \qquad (5.53)$$

with c.o.v.,

$$\delta^2_{K_p} = \delta^2_{E_p} + \delta^2_{I_p} + \frac{4\bar{d}_2^2}{(\bar{d}_1+\bar{d}_2)^2} \delta^2_{d_2} + \frac{(d_1+3d_2)^2}{(d_1+d_2)^2} \delta^2_{d_2} \qquad (5.54)$$

where E_p and I_p are the modulus of elasticity and moment of inertia of the base-plate, respectively.

The mean and c.o.v. of the total stiffness of an incomplete column anchorage, therefore, are:

$$\frac{1}{\bar{K}_t} = \frac{1}{\bar{K}_B} + \frac{1}{\bar{K}_p} \tag{5.55}$$

and,

$$\delta^2_{K_t} = \frac{\delta^2_{K_B}}{K^2_B} + \frac{\delta^2_{K_p}}{K^2_p} \tag{5.56}$$

5.8.2-Completed Column Anchorage

Normally a column is welded to the base-plate. Therefore, the section of the base-plate under the column behaves like a rigid beam. In those cases where the base-plate is not very thick, it is reasonable to assume that the center of rotation of the column anchorage is under the compression flange of the column. Therefore, Eqs. 5.51 and 5.53 for a completed column anchorage would be as follows,

$$K_{BC} = n \quad (d_1 + d_2)^2/e_E \tag{5.57}$$

$$K_{pc} = \frac{2EI_p}{d_1^3} (d_1 + d_2)^2$$

In the above equations, d_1 is the same as for incomplete anchorages, $\bar{d}_2 = d_c$ and the c.o.v. of d_2 will be assumed to be to 0.10. The statistics of the total stiffness may then be calculated also with Eqs. 5.55 and 5.56.

5.9-Stiffness of Temporary Beam-Column Connections

The M-ϕ relationship of a temporary beam-to-column connection is nonlinear from the beginning of loading. Since wind produces a non zero-mean excitation in a system , using a nonlinear moment-rotation relationship would complicate the

vibration problem considerably. To avoid such complications, a linear approximation of the M-ϕ relation of the connection will be used.

Lewitt (1969) shows that for deformations that are less than about 0.02 inches in the connection angles, the behavior of a connection is essentially linearly elastic. Thus, an approximate linear stiffness may be obtained from the ratio $K_c = \frac{M_{.02}}{\phi_{.02}}$, where $M_{0.02}$ is the applied moment producing 0.02 inch displacement at the extreme tension end of the connection angles, and $_{0.02}$ is the corresponding rotation due to this moment. The mean stiffness of two connections calculated by this method is shown in Fig 5.9. The c.o.v. of K_C would be the same as that of M_R, which was discussed in the previous section.

5.10-Stiffness of Temporary Bracings

After a tier is temporarily erected, it is braced with wire rope and plumbed. The stiffness of the bracing system depends on the elongation of the wire ropes under a load. For a new wire rope, this elongation is the result of two components; the structural stretch, caused by the adjustment of the wires and strands to the load; and the elastic stretch caused by the elongation of the wires. Structural stretch occurs during the initial periods of the useful life of a rope. Structural stretch of worn wire ropes used as bracing is negligible, especially if the frame is plumbed by tightening the ropes. The elastic stretch is obtained as follows,

$$K_{BR} = \frac{n \cdot A_R \cdot E_R \cdot \cos^2\alpha \cdot \sin\alpha}{\ell_t} \qquad (5.59)$$

where: n=number of ropes in one direction,
A_R=cross sectional area of rope,
E_R=modulus of elasticity of rope, and
ℓ_t=tier height.

Variation in K is primarily due to uncertainties in the modulus of elasticity and the metalic area of the ropes. The modulus of elasticity of a wire rope varies throughout its life and is a function of rope construction and working conditions. Limited tests were performed on 5/8-inch worn rope of 6-strand 19-wire construction; the modulus of elasticity was obtained to be E_{BR}=13500 kips/inch (Skillman, 1924). There are vitually no test data on the modulus of elasticity of worn ropes; the mean value of E_{BR} for worn ropes will be assumed to be equal to 13500 kips/inch with a variability equal the variability of the rope strength, as calculated earlier in Sect. 5.7.

The area of a worn rope is less than new ropes because of broken wires in the strands and worn outside wires. The area of a number of 1/2 and 5/8-inch worn wire ropes have been measured (Fulweiler, 1936). The mean value and standard deviation were $A_{5/8}$=0.085 in with a c.o.v. of 0.30; $A_{5/8}$ =0.13. in with $A_{5/8}$=0.28 .

CHAPTER 6

FAILURE PROBABILITIES OF STEEL BUILDINGS DURING CONSTRUCTION

6.1-Introduction

The planning and scheduling of a construction project, as well as the decisions of the field superintendent made on the project site, are among the most important factors affecting the reliability or safety of a building during its construction. A major fraction of the total cost of a building is usually the cost of labor and equipment. For this reason, the dominant objective during the planning and scheduling of the construction of a building is to minimize these costs. After a project has been planned and scheduled, safety is generally determined subjectively. With the high degree of uncertainty in the construction loads and resistances of an incomplete structure, a subjective assessment of structural safety is invariably crude and unreliable. In reality, this unreliability may increase the expected cost of a project substantially. In other words, a rational or realistic way to minimize the the total cost of a project is to include the expected loss of failure during construction into the cost function in planning the project.

Information on the reliability of a building during construction as a function of the method of construction, and its sensitivity to various construction practices, should serve to determine the current level of construction safety and identify bad practices that ought to be avoided. The same information may also be useful for establishing codes and regulation for construction practices. The reliability at any stage of construction is a function of project planning, scheduling, field practice, and design of the structure. Accordingly, the reliability may vary with these parameters.

A multistory steel building constructed with different plans and schedules is examined. First the conditional failure probabilities, i.e., probability of failure or partial failure for a given mean wind velocity are calculated. The probability

of failure at a given stage of construction may then be evaluated by combining these conditional probabilities with the distribution of all possible maximum wind velocity during the construction of that stage.

The building used in the example calculation is a 10-story office building, with three bays in the short direction and five bays in the long direction. The elevation and dimensions of the structure are given in Fig. 6.1. Resistance to lateral loads in the short direction is provided by rigid connections. Two systems of lateral support will be assumed for the frame in the long direction; namely, (1) concrete shear wall or deep concrete spandrel beams resisting lateral loads, and (2) lateral strength provided by X-bracings. In the first case, the permanent lateral support is not built simultaneously with the steel frame. The steel frame must go up several tiers before the concreting crew can start their work. Sometimes the steel frame may be completed before the concrete subcontractor can start building the lateral supports. However, if steel X-bracings are used as the permanent lateral support, it can follow the erecting crew closely.

The Tier Method of construction will be considered for the erection of the frame. Each tier will be two-story high. The column anchorages are as shown in Fig. 6.2. Temporary bracings are 5/8-inch diameter cable guys.

6.2-Planning and Scheduling

Planning a project requires obtaining information on material, equipment, manpower, money, and time needed for the performance of the project. There are several types of equipment that can be used in the erection of a steel frame. In the planning stage, decisions are required regarding type, size, and number of equipment that will be used and the number of crew for each activity. One possible combination of equipment and manpower for the erection of steel frames is as follows (Means, 1977):

1 structural steel foreman
5 structural steel workers
1 equipment operator (heavy)

1 equipment operator (oiler)

1 60-ton crane

The average daily output of this crew is about 12 to 14 tons of steel erected with temporary connections. Temporary erection activity is followed by the bolting crew who will complete the connections. A basic bolting crew consists of two structural steel workers whose average daily output is about 160 bolts (Means, 1977).

If a building is built with the above combination of crew and equipment, and the permanent bolting activity starts as soon as the first tier is plumbed, the schedule for construction would be as shown in Fig. 6.3. In Fig. 6.3, each activity is represented by a line whose slope is the speed of performing that activity. With a productivity of 12 tons of steel per day, it takes about 8 days for the raising crew to build one tier of the building uunder consideration. The bolting crew can complete the connections of each story in about 6 days.

In this study, the reliability of the frame built with the schedule shown in Fig. 6.3 will be evaluated. Variations in reliability with changes in construction productivity or crew size will~^ also be examined.

6.3-Conditional Failure Probabilities During Construction

Variation of the strength of a structure during construction is also a function of the particular design of the structure. For the present study, the variation of the reliability during construction for three common types of steel building designs; namely, rigid design, flexible design with shear wall, and flexible design with X-bracings, will be examined.

6.3.1-Rigid Design

In the short direction the frame shown in Fig. 6.1 has a rigid design. The specific six stages shown in Fig. 6.4 are selected for reliability analysis. It is assumed that the temporary beam-column connections in this direction have four high strength bolts as shown in Fig. 2.2a, and the temporary column anchorages as shown in Figs. 2.1a and 6.2a. The column anchorages are assumed to be completed at stage 2. The effect of the stiffness of the column anchorages on the reliability are also examined.

The total damping ratio (mechanical and aerodynamic), natural frequency of the frame, and gust response factor calculated for each of the six stages of construction are summarized in Table6.1 . Aerodynamic damping is given for a wind speed of 20 mph, and a mechanical damping coefficient of 0.02 is assumed for all stages of construction (see Chapter 4).

TABLE 6.1

DYNAMIC PROPERTIES DURING CONSTRUCTION (RIGID DESIGN)

STAGE OF CONSTRUCTION	NATURAL FREQUENCY	DAMPING	GUST RESPONSE FACTOR
1	1.63	.022	3.77
2	1.56	.023	3.29
3	1.20	.026	3.00
4	0.78	.029	2.82
5	0.82	.032	2.62
6	1.03	.028	2.55

The gust responce factor for the structure in the short direction varies from 3.77 for the first stage of construction to 2.49 for the last or completed stage. The reduction in the gust factor for the latter stage is due to the increase in the height of the building which reduces the effect of surface roughness. Since the total damping of the structure is

relatively high, the gust response is not very sensitive to the natural frequency. The statistics of the dynamic response for given values of the wind velocity were evaluated according to the method discussed in Chapter 4.

The conditional probabilty of collapse, or partial collapse of the frame at the six stages shown in Fig. 6.4 and of the completed frame (stage 7) for given wind velocities are plotted in Figs. 6.5 through 6.1Ø. As expected, for given wind velocities, the failure probability of incomplete sections of the frame is much higher than the probability of total collapse. Moreover, the probability that the whole incomplete section of the frame separates from the completed section is higher than partial failure of the incomplete section. This can be seen in Figs. 6.7 and 6.8 where the two top tiers of the frame are incomplete, but the probability of failure of the top tier is much less than the probability of failure of the whole incomplete section. Fig. 6.1Ø shows that in a completed frame the probability of total collapse (i.e. T_5) is higher than those for partial failures (i.e. T_1 through T_4). One reason for this is the lower strength of the column anchorages compared with the column splices. In Figs 6.6 to 6.1Ø conditional failure probabilities of the beams in the first floor of the frame are also plotted. In this structure, failure by buckling of the floor beams becomes critical after stage 4 of construction. It can be seen that in stages 5 through 7, failure of the temporarily connected tiers and the instability of the floor beams are the critical modes of failure. However, when all the connections of the frame are completed, lateral buckling of the beams becomes the most critical mode of failure; see Fig. 6.1Ø.

6.3.2-Flexible Design

Case 1 -- In the longer direction, the frame has a flexible design. In this case it is assumed that the permanent lateral support will be provided by reinforced concrete elements, such as shear walls or deep concrete spandrel beams. If construction of the permanent lateral support does not start

until the steel erection is completed, which is not a rare case with the aforementioned planning and schedule, the seven stages of construction (prior to the construction of any lateral support) are as shown in Fig. 6.11. The details of the complete and incomplete connections in this direction are shown in Figs 6.12 and 2.2a. The natural frequency, damping ratio, and gust response factor of the frame at each of the seven stages of construction are shown in Table 6.2. The mechanical damping ratio was assumed to be Ø.Ø2 for each stage (see Chapter 4).

Conditional failure probabilities for different wind speeds are plotted in Figs. 6.13 through 6.18 It can be seen from these figures that when subjected to a given wind velocity, a frame with flexible connections (before its permanent lateral supports is in place), will have higher probability of complete collapse than corresponding probabilities of partial failures. This has been observed in actual failures of flexible frames without lateral supports.

TABLE 6.2

DYNAMIC PROPERTIES DURING CONSTRUCTION (Y-Y DIRECTION, CASE 1)

STAGE OF CONSTRUCTION	NATURAL FREQUENCY	DAMPING	GUST RESPONSE FACTOR
1	1.6Ø	.Ø23	3.9Ø
2	1.Ø2	.Ø26	3.54
3	Ø.81	.Ø31	3.Ø5
4	Ø.59	.Ø36	3.ØØ
5	Ø.57	.Ø37	2.58
6	Ø.6Ø	.Ø36	2.56
7	Ø.61	.Ø34	2.42

Failure due to instability of the columns may become the dominant failure mode during the construction of frames with flexible design. This is due to the high effective length of

the columns caused by small rotational stiffness of the beam-to-column connections. If the column anchorages are also rotationally flexible, the effective length of the columns of the first floor which have the highest axial load also becomes large.

The probability of a first-floor column becoming unstable at stage 5 was calculated for two cases; (1) when column anchorages are rotationally stiff (Fig. 6.2a), and (2) the case in which the column anchorages do not resist large moments (Fig. 6.2b). In the first case column instability is not very critical (curve C of Fig. 6.16), but in the case of flexible column anchorages, frame instability may become the most critical mode of failure (curve C , Fig. 6.16).

Case 2 -- In this case, it is assumed that the permanent lateral support in the long direction is provided by X-bracings. The earliest time that such permanent X-bracings of a tier can be built is as soon as the member connections of that tier are completed. Assuming that the permanent bracings of a tier is installed at the earliest possible stime, the six stages identified in Fig. 6.19 were examined for safety. The failure probabilities of the completed stories of the frame were negligible (of the order of $\leq 10^{-7}$), and are not shown. Conditional failure probabilities of the incomplete stories are shown in Figs. 6.20 and 6.21. Table 6.3 shows the corresponding natural frequencies, damping, and gust responce factors for the different stages of construction, which were part of the information used in developing Figs. 6.20 and 6.21.

6.4-Failure Probability During Period of Construction

The probability of total failure or partial failure at any stage of construction depends on the conditional failure probability and the duration of construction of that stage. The longer the duration of construction of a stage, the higher will be the maximum mean wind velocity; hence, the failure probability will accordingly be also higher. Therefore, if the number and size of the construction equipment and the crew performing the job are not properly selected, the failure

TABLE 6.3

DYNAMIC PROPERTIES DURING CONSTRUCTION (Y-Y DIRECTION, CASE 2)

STAGE OF CONSTRUCTION	NATURAL FREQUENCY	DAMPING	GUST RESPONSE FACTOR
1	1.60	.023	3.90
2	1.60	.024	3.12
3	1.16	.027	2.93
4	0.90	.031	2.77
5	0.84	.033	2.58
6	1.43	.030	2.50

probability of some critical stages of construction may become very high. The maximum wind velocity that may occur during a stage of construction depends also on the time of the year and location of the project. In this study, it is assumed that the structure is being built during the months of July and August in Chicago, when construction is most active.

If the combination of equipment and crew, as mentioned earlier is used for constructing the structure, each of the stages of construction shown in Fig. 6.4 is exposed to wind for about 3 days. At this speed of construction, the probability of collapse, or partial collapse, at the different stages of construction are shown in Figs. 6.22 and 6.23 for the rigid design. In these figures are also shown (in dashed lines) the failure probabilities for each stage if the exposure duration is increased to 10 days. The increase in the duration of construction for a stage may be due to several reasons, such as using different size of equipment and crew, lower productivity, bad weather, etc.

The corresponding failure probabilities for frames with flexible designs (case 1), are given in Figs. 6.24 and 6.25. The results are for an average duration for each stage of 3 days and for a project in Chicago during the months of July and August. Variations in the reliabilities for the same frame

with X-bracings are shown in Fig. 6.26. The total expected loss (probability of failure times cost of failure) during the construction of a composite structure (e.g., steel frame with shear wall) can be much higher than that of steel frames with flexible design having x-bracings for permanent lateral support. This is due to practical reasons; namely, the earliest possible start time for the construction of the permanent lateral support for the latter type of buildings is, in general, much earlier than for the composite structure.

6.5 Summary of Failure Probabilities

The gust response factor during several stages of construction of a steel frame (city exposure) were evaluated. In general, the gust respose factor decreased as the number of floors of the frame increased. For the ten-story example structure shown in Fig. 6.1 , the gust response factor decreased from about 3.9 for the two-story incomplete frame to about 2.5 for the structure at the final stage of construction.

Table 6.4 summarizes the failure probabilities during the construction of the example structure (rigid and flexible designs). In the case of the flexible design with shear wall as permanent lateral support, the failure probabilities were calculated assuming that the shear wall is constructed after the steel erection is completed; whereas, in the case of flexible design with x-bracings the permanent lateral supports are installed when completing the connections of a story. The probabilities for rigid design are for the short direction of the frame, whereas the design in the long direction is assumed to be flexible. The different construction stages considered herein are shown in Figs. 6.4, 6.11 and 6.19.

During its construction, the structural properties and behavior of the building change with the stage of completion. Moreover, the probability of failure of a given stage will depend on the duration of construction of that stage. For an

average duration of 3 days for each stage, the pertinent failure probabilities are shown in Table 6.4. Table 6.5 shows the corresponding probabilities for a 10-day duration for each stage. Wind data are from Chicago Midway Airport.

The probability of collapse of a frame with flexible connections increases rapidly with an increase in the number of stories erected without permanent lateral support. Table 6.6 shows the probabilities of the collapse of the entire frame if erected without its permanent bracings.

Table 6.7 shows the variation in the probability of lateral buckling of a beam in the first floor as the number of floors increases. These probabilities are calculated for the short direction of the structure. It appears that after the fourth stage of construction, the lateral buckling of the beams become the dominant mode of failure.

The effect of the stiffness of the column anchorages on the stability of the frame with flexible design (built without its permanent lateral supports) may be observed in Fig. 6.16, representing the failure probability for stage 5. For the case in which the column anchorages are stiff, the probability of column instability is 1.1×10^{-4}. This probability increased to 4.0×10^{-2} when the column anchorages are assumed to be flexible, (ten-story bare frame).

Table 6.4: Failure Probabilities for Different Stages (3-Day Duration)

Stage	Section Failing	Rigid Design	Flexible Design	
			Shear-Wall Type Frame**	X-Bracing Type Frame
1	Entire Frame	0.8×10^{-6}	6.2×10^{-6}	6.2×10^{-6}
2	Upper Tier	2.9×10^{-5}	2.9×10^{-5}	9.8×10^{-6}
	Entire Frame		6.5×10^{-5}	*
3	Upper Tier	5.4×10^{-6}	4.2×10^{-6}	7.7×10^{-6}
	Upper 2 Tiers	0.5×10^{-6}	2.5×10^{-5}	*
	Entire Frame		4.0×10^{-4}	*
4	Upper Tier	$2.cx10^{-6}$	7.5×10^{-6}	7.8×10^{-6}
	Upper 2 Tiers	8.9×10^{-3}	2.1×10^{-3}	1.7×10^{-3}
	Upper 3 Tiers	0.3×10^{-6}	2.8×10^{-3}	*
	Entire Frame	0.4×10^{-6}	1.08×10^{-2}	*
5	Upper Tier	4.9×10^{-6}	1.1×10^{-5}	3.1×10^{-5}
	Upper 2 Tiers	9.3×10^{-3}	2.3×10^{-3}	2.0×10^{-3}
	Upper 3 Tiers	1.5×10^{-6}	2.1×10^{-3}	*
	Upper 4 Tiers	0.6×10^{-6}	5.2×10^{-3}	*
	Entire Frame	1.0×10^{-6}	$2.0x.0^{-2}$	*
6	Upper Tier	5.2×10^{-5}	5.8×10^{-5}	2.0×10^{-4}
	Upper 2 Tiers	*	4.3×10^{-4}	*
	Upper 3 Tiers	*	2.5×10^{-3}	*
	Upper 4 Tiers	*	7.0×10^{-3}	*
	Entire Frame	0.4×10^{-6}	2.7×10^{-2}	*
7	Upper Tier	*	1.3×10^{-3}	*
	Upper 2 Tiers	*	1.4×10^{-4}	*
	Upper 3 Tiers	*	1.2×10^{-3}	*
	Upper 4 Tiers	*	4.0×10^{-3}	*
	Entire Frame	*	1.7×10^{-2}	*

* Probability of Failure $<10^{-7}$

** It is assumed that shear wall will be constructed after the completion of steel frame.

Table 6.5: Failure Probabilities for Different Stages (10-Day Duration)

Stage	Section Failing	Rigid Design	Flexible Design	
			Shear-Wall Type Frame**	X-Bracing Type Frame
1	Entire Frame	2.2×10^{-6}	1.5×10^{-5}	1.5×10^{-5}
2	Upper Tier	7.9×10^{-5}	8.0×10^{-5}	2.7×10^{-5}
	Entire Frame	*	1.8×10^{-4}	*
3	Upper Tier	1.5×10^{-5}	1.1×10^{-5}	2.1×10^{-5}
	Upper 2 Tiers	1.4×10^{-6}	7.0×10^{-5}	*
	Entire Frame	*	1.1×10^{-3}	*
4	Upper Tier	6.3×10^{-6}	2.0×10^{-5}	8.4×10^{-5}
	Upper 2 Tiers	2.4×10^{-2}	5.6×10^{-3}	5.4×10^{-3}
	Upper 3 Tiers	0.9×10^{-6}	7.7×10^{-3}	*
	Entire Frame	1.0×10^{-6}	2.9×10^{-2}	*
5	Upper Tier	1.3×10^{-5}	3.1×10^{-5}	8.4×10^{-5}
	Upper 2 Tiers	2.5×10^{-2}	6.2×10^{-3}	5.4×10^{-3}
	Upper 3 Tiers	4.3×10^{-6}	5.9×10^{-3}	*
	Upper 4 Tiers	1.6×10^{-6}	1.4×10^{-2}	*
	Entire Frame	2.8×10^{-6}	5.4×10^{-2}	*
6	Upper Tier	1.0×10^{-4}	1.6×10^{-4}	5.5×10^{-4}
	Upper 2 Tiers	*	1.2×10^{-3}	*
	Upper 3 Tiers	0.1×10^{-6}	6.8×10^{-3}	*
	Upper 4 Tiers	0.2×10^{-6}	1.9×10^{-2}	*
	Entire Frame	1.1×10^{-6}	6.9×10^{-2}	*
7	Upper Tier	*	3.7×10^{-7}	*
	Upper 2 Tiers	*	3.9×10^{-4}	*
	Upper 3 Tiers	*	3.3×10^{-3}	*
	Upper 4 Tiers	*	1.1×10^{-2}	*
	Entire Frame	0.2×10^{-6}	4.6×10^{-2}	*

* Probability $<10^{-7}$

** It is assumed that shear wall will be constructed after the completion of steel frame.

Table 6.6 Failure Probabilities-Flexible Connections

Number of Floors	3-Day Duration	10-Day Duration
2	0.810	2.210
4	6.510	1.810
6	4.010	1.110
8	1.0810	2.910
10	2.010	5.410

Table 6.7 Probability of Floor Beam Buckling

Number of Floors	3-Day Duration	10-Day Duration
4	*	*
6	*	*
8	0.210	0.610
10**	4.610	1.310

* Probability 10^{-7}

** 10-story Bare Frame with Completed Connections

CHAPTER 7

SUMMARY AND CONCLUSIONS

7.1-Summary of Study

The present study evaluates the reliability of steel frame buildings during the different stages of construction. The specific method of construction considered is the tier method, which is the most common method of erecting steel buildings. At each stage of construction, the potential modes of failure are identified and formulated for reliability analysis. The dominant load during construction of this type of buildings is wind loading. Uncertainties associated with the properties of the structure at each stage of construction and the wind environment parameters are included in the formulation in terms of the first two statistical moments of the variables.

Variations of reliability during construction for steel frames with rigid and flexible designs were examined. In the case of frames with flexible design, the variation of reliability also depends on the type of permanent lateral support of the structure; namely, lateral support provided by shear walls or X-bracings.

In addition to the construction procedure and type of structural design, reliability during construction is also a function of the planning and scheduling of the project. Variations in the planning of a project may affect the duration of each stage of construction, and thus change the maximum wind load on each construction stage. A method is presented for determining the maximum wind velocity over such durations. Changes in the scheduling of the activities of a project may also affect the criticality of the different stages of construction.

The reliability of a ten-story steel frame building, built by a common combination of crew and equipment, was examined in detail; the results for this example structure may have significance and implications for buildings in general.

7.2-Conclusions

On the basis of the numerical results discussed and summarized in Chapter 6, the following conclusions may be observed:

(1) The dynamic effect of wind on incomplete low-rise frames is higher than on medium and high-rise structures. In the example problem, the gust response factor for the stage with only two stories erected was 3.9, as compared to 2.5 for the final stage of erection. This may explain, in part, the high rate of failure of industrial framed buildings during construction.

(2) The strength and stiffness of column anchorages play an important role on the safety of a frame during construction. A small amount of column base restraint in an incomplete frame reduces the effective length of the columns considerably, resulting in significant reduction in the probability of column instability.

(3) The planning and scheduling, especially relative to the construction of the permanent lateral supports, could significantly affect the reliability of the entire structure during its construction. Two schedules were examined for the construction of the example structure: (1) the permanent lateral support is constructed after the steel frame erection is completed (the case with shear wall), and (2) the permanent lateral support is built as soon as possible (the case with x-bracings). In the first case, the probability of complete collapse of the erected bare frame could be as high as 2.70×10^{-3} for an average duration of three days for each stage; whereas, in the second case, the probability of the complete collapse is negligible (less than 10^{-7}).

(4) Reliability during construction depends also on the structural design. For example, composite structures generally have a lower reliability during construction because their permanent lateral support is provided by concrete elements, whose construction are usually started only after the steel erection is several tiers up.

(5) A frame that is temporarily connected and braced will have a very low reliability if built higher than one tier at a time. Increasing the amount of temporary guy wire bracings will have little effect on the safety of a temporarily connected frame built higher than two tiers in a given stage.

(6) In the case of frames with rigid design, buckling of the floor beams may be the dominant failure mode, i.e. prior to placing the floors and walls. In the case of the example structure, failure of the frame due to lateral buckling of the floor beams become the dominant mode of failure beyond stage 4 of the construction. Therefore, it would generally be good practice to start placing the floors of a frame as soon as possible.

REFERENCES

1. AISC, "Specification for the Design, Fabrication, and Erection of structural Steel for Buildings," New York, New York, 1969

2. AISC, "Structural Steel Detailing," Illinois Area Advisory Board, New York, New York, 1971

3. Allen, D.E. "Limit State Design- A Probabilistic Study," Canadian Journal of Civil Engineering, Vol. 2, No. 1, March 1975

4. Ang, A. H.-S., "Probability Considerations In Design and Formulation of Safety Factors", Symposium on Concepts of Safety of Structures and Methods of Design, I.A.B.S.E., London, 1969

5. Ang, A. H.-S., "Development of a Probabilistic Basis for Evaluating Structural Safety and Design of Deep Submersibles," Final Report of Contract N00014-69-C-0436, Naval Ship Research and Development Center, Washington, D.C., April 1972

6. Ang, A. H.-S., "Structural Risk Analysis and Reliability Based Design", Journal of the Structural Div., ASCE, Vol. 99, No. St9, September 1973

7. Ang, A.H.-S. and Cornell, G.A., "Reliability Basis of Structural Safety and Design," Journal of the Structural Div., ASCE, Vol. 100, No.st9, Paper 10777, Sept., 1974

8. Baker, M.J., "Variations in the Mechanical Properties of Structural Steel," Tall Building Criteria of Loadings, Vol. Ib, Proc., International Conference on Planning and Design of Tall Buildings, Lehigh University, Bethleham, Pa., August 21-26 1972

9. Beaufoy L.A. and Moharram, A., "Derived Moment-Angle Curves for Web-Cleat Connections," Preliminary publication, Third

10. Congress, International Association for Bridge and Structural Engineering, 1948

11. Blockley, D.I., "Predicting the Likelihood of Structural Accidents", Proceedings of the Institution of Civil Engineers, Part 2, 59, December 1975

12. Blockley, D.I., "Analysis of Structural Failures", Proceedings of the Institution of Civil Engineers, Part 1, 62, February 1977

13. Bradshaw, R.R., "Aeroelastic Vibration of a Steel Arch," Journal of Str. Div., ASCE, Vol. 90, No. St3, June 1964

14. Cartwright, D.E. and Longuet-Higgins, M.S., "Statistical Distribution of the Maxima of a random Function," Proc. Roy. Soc. A, Vol. 237, 1956

15. Clark, J.W. and Hill, H.N., "Lateral Buckling of Beeams," Proc., ASCE, Vol. 86, No. ST7, July 1960

16. Cloud, W. "Period Measurement of Structures in Chile," Bulletin of the Seismological Society of America, Vol. 53, No. 2, Febraury 1963

17. Cunningham, K.D., "Steel Construction," Planning and Design of Tall Buildings, Tall building Systems and Concepts, Vol. Ia

18. Davenport, A.G., "The Buffeting of Large Superficial Structures by Atmospheric Turbulence", Annals, New York Academy of Science, Vol. 116, June 1964

19. Davenport, A.G. "Wind Loads on Structures," Tech. Paper 88, Divn Build. Res., Nat. Res. Council, Canada, Ottawa, March 1966

20. Davenport, A.G. "Gust Loading Factor," Journal of Str. Div., Proc., ASCE, Vol. 93, No. St3, June 1967

21. Davenport, A.G., "Note on the Distribution of the Largest Value of a Random Function With Application to Gust Loading", Proceedings of the Institution of Civil Engineers, Vol. 28, June 1964

22. Davenport, A.G., "The Application of Statistical Concepts to the Wind Loading of Structures", Proceedings of the Institution of Civil Engineers, Australia, Vol. 19, August 1961, pp 449-472

23. Davenport, A.G., "The Dependence of Wind Loads on Metheorological parameters", Proceedings of the 1967 International Conference on Wind Effects on Buildings and Structures, Ottawa, Canada

24. Durkee, J.L. and Thomaides, S.S., "Erection Strength Adequacy of Long Truss Cantilevers", Journal of the Structural Div., ASCE, Vol. 103, No. St1, January 1977

25. Ellingwood, B. and Ang, A. H.-S., "A Probabilistic Study of Safety Criteria for Design", Structural Research Series No. 387, University of Illinois, Urbana, Illinois, June 1972

26. Ellingwood, Bruce, Galambos,T.V., MacGregor,J.G., and Cornell, A.C., " Development of a Probability Based Load Criterion for American National Standard A58," National Bureau of Standards Special Publication 577

27. ENR, December 11, 1958

28. Feld, Jacob "Construction Failures", John Wiley & Sons, Inc. 1968

29. Fishburn, C.C. "Strength and Slip Under Load of Bent-Bar Anchorages and Straight Embedments in Haydite Concrete," Journal of the American Concrete Institute, Proceedings, Vol. 44, No. 4, December 1947

30. Fisher, J.W., Galambos, T.V., Kulak,G.L., and Ravindra, M.K., "Load and Design Criteria for Connections," J. of Str. Div., ASCE, Vol. 104, No. ST9, Sept. 1978

31. Fisher, J.W. and Struik, J.H.A. "Guide to Design Criteria for Bolted and Revited Joints," John Wiley & Sons, Inc., 1974

32. Fox, R.L. and Kapoor, M.P., "Rates of Change of Eigenvalues and Eigenvectors," AIAA journal, Vol. 6, No. 12, December 1968

33. Freudenthal, A.M. "Safety and Probability of Structural Failure," Transaction of ASCE, Vol. 121, 1956

34. Freudenthal, A.M., Garrelts, J.M. and Shinozuka, M., " The Analysis of Structural Safety", Journal of the Structural Div., ASCE, Vol. 92, No. Stl, February 1966

35. Freudenthal, A.M., "Critical Appraisal of Safety Criteria and Their Basic Concepts", Preliminary Publication, Eighth Congress, I.A.B.S.E., September 1968

36. Fukumoto, Y. and Kubo, M., "An Experimental Review of Lateral Buckling of Beams and Girders," International Qolloquium on Stability of Structures under Static and Dynamic Loads," Washington D.C., May 1977

37. Fulweiler, W.H., Stang, A.H. and Sweetman, L.R., "Inspection and Tesile Tests of Some Worn Wire Ropes," Journal of Research of the National Bureau of Standards, Vol. 17, July to December 1936

38. Galambos, T.V., "Structural Members and Frames", Prantice Hall 1978

39. Gere, J.M., "Moment Distribution," Van Nostrand Company, Inc., Princeton, New Jersey, 1963

40. Gomes, L. and Vickery, B.J., "On the Prediction of Extreme Wind Speeds From the Parent Distribution", Journal of the Industrial Aerodynamics, No. 2 (1977)

41. Gurfinkel, G. and Robinson, A.R., "Buckling of Elastically Restrained Columns", Journal of the Structural Div., ASCE, Vol. 91, No. St6, December 1965

42. Hasselman, T.K. and Hart, G.C. "Modal Analysis of Random Structural Systems"," Journal of the Engineering Mechanics Div., ASCE, Vol. 98, No. EM3, June 1972

43. Hogan, M. "The Influence of Wind on Tall Building Design," BLWT-4-71, PH.D. Dissertation, University of Western Ontario, at London, Canada, March 1971

44. Institution of Civil Engineering, "Safety in Civil Engineering," Proc., Vol. 42, January 1969

45. LaFraugh, R.W. and Magura, D.D. "Connections in Precast Concrete Structures-Column Base Plates" Journal of the Prestressed Concrete Institute, Vol. 11, No. 6, December 1966

46. Lay, M.G. and Galambos, T.V., "Tests on Beam and Column Subassemblages", Welding research concil Bulletin, No. 110, November 1965

47. Lew, H.S., "Safety During Construction of Concrete Buildings - A Status Report", National Bureau of Standards, Series 80

48. Lewitt, C.W., Chesson, Jr., E. and Munse, W.H., "restraint Characteristics of Flexible Riveted and Bolted Beam-to-Column Connections," Engineering Experiment Station Bulletine 500, Unversity of Ill., 1969

49. Mason, R.E., Fisher, G.P., and Winter, G., "Tests and Analysis of Eccentrically Loaded Columns", Proceedings, ASCE, Vol. 84, No. EM4, October 1958

50. Massonnet, C., "Stability Considerations in the Design of Steel Columns," Journal of Structural Div., Vol. 85, No. St7, September 1959

51. Means Building Construction Cost Data 1974

52. McKaig, T.H., "Building Failures", McGraw-Hill Book Company Inc. 1962

53. Melcher, R.E., "Influence of Organization on Project Implementation", Journal of the Construction Div., ASCE, Vol. 103, No. Co4, December 1977

54. Merchant, W., "Three Structural Failures: Case Notes and General Comments," the Institution of Civil Engineers, Proceedings, Vol. 36, March 1967

55. Merritt, F. S., "Building Construction Handbook," Third Edition, McGraw-Hill Book Company, 1975

56. Ower, E., "Wind Resistance of Lattice girder Bridges," Inst. of Civil Engs. and Inst. of Structural Engs., London 1948

57. Portillo, G.M. and Ang, A. H.-S., "Evaluation of Safety of Reinforced concrete Buildings to Earthquakes", Structural Research Series No. 433, University of Illinois, Urbana, Illinois, October 1976

58. Pugsley, A.G., "The Engineering Climatology of structural Accidents", International Conference on Structural Safety and Reliability, Washington, 1969, pp335-340

59. Rackwitz, R., Fiessler, B., "Note on Discrete Safety Checking When using Non-Normal Stochastic Modes for Basic Variables," Loads Project Working Session, MIT, Cambridge, June 1976

60. Ragget, Jon D., "Estimating Damping of Real Structures,"

61. Journal of Structural Div., ASCE, Vol. 101, No. st9, September 1975

62. Ravindra, M. K. and Galambos, T.V., "Load Factor Design of Steel Beams", Proceedings Specialty Conference on Safety and Reliability of Metal Structures, ASCE, Pittsburg, PA, November 1972

63. Rojiani, K. B., "Evaluation of Reliability of Steel Buildings to Wind Loading", Ph.D. dissertation, University of Illinois, Urbana, Illinois, 1978

64. Salmon, C.G., Schenkner, L., and Johnson, B.G., "Moment Rotation Characteristics of Column Anchorages", Transactions of ASCE, Vol. 122, 1957

65. Scrunton, C. and Newberry, C.W., "On the Estimation of Wind Loads for Building and Structural Design," the Institution of Civil Engs., Vol. 25, June 1963

66. Short, W.D., "Structural Collapses During Erection and Demolition," the Institution of Civil Engs., Proc., Vol. 36, March 1967

67. Shoup, T.E. and Singleton, R.C., "Headed Concrete Anchors," Journal of the American Concrete Institute, Proc., Vol. 60, no. 9, September 1963

68. Silby, P.G. and Walker, A.C., "Structural Accidents and Their Causes" the Institution of Civil Engs. Part 1, 62, May 1977

69. Skillman, E., "Some tests of Steel-Wire Ropes on Sheaves," Technologic Papers of the Bureau of Standards, Department of Commerce, Vol. 17, pp227-243, 1924

70. "Steel Construction in Multi-Story Buildings", Acier, Stahl, Steel, No.7-8, July-August 1960

71. Steinberg, J. and Stempel, M., "Practices and Methods of Construction", Prentice-Hall, Inc. 1957

72. Van Kuren, R.C. and Galambos, T.V., "Beam-Column Experiments" Journal of the Structural Div., ASCE, Vol. 90, April 1964

73. Van Marcke, E.H., "On the Distribution of the First-Passage Time for normal stationary Random Process", Transactions of ASME, Vol. 42, Series E, No. 1, March 1975

74. Vellozzi, J. and Cohen, E., "Gust Response Factors", Journal of the Structural Div., ASCE, Vol. 92, No. St6, June 1968

75. Vickery, B.J., "On the Reliability of Gust Loading Factors", Proceedings, Technical Meeting Concerning Wind Loads on Building and Structures, National Bureau of Standards, Washington, D.C., January 1969, Building Sciece Series 30

76. Vickery, B.J., "On the Assessment of Wind Effects on Elastic Structures," C.E. Transactions, The Institution of Engs., Aust., Vol. CE8 , No. 2, October 1966

77. Watanabe, S., Kida, Y., and Higuchi, M., "The Vibrational Analysis of a steel Structure", Proceedings of the Third World Conference on Earthquake Engineering, New Zealand 1965

78. Yura, J.A., "The Effective Length of Columns in Unbraced Frames", AISC Engineering Journal, Vol. 8, No. 2, April 1971

79. Yura,J.A., Galambos, T.V., Ravindra, M.K., "The Bending Resistance of Steel Beams," J. of the Str. Div., ASCE, Vol. 104, NO. ST9, Proc., Sept., 1978

80. Zadeh, L.A., "Fuzzy Sets", Information and Control, 1965, 8,

81. Zadeh, L.A., "Outline of a New Approach to the Analysis of Complex Systems and Decision Processes", Transaction Systems, Man & Cybernetics, IEEE 1973, SMC-3

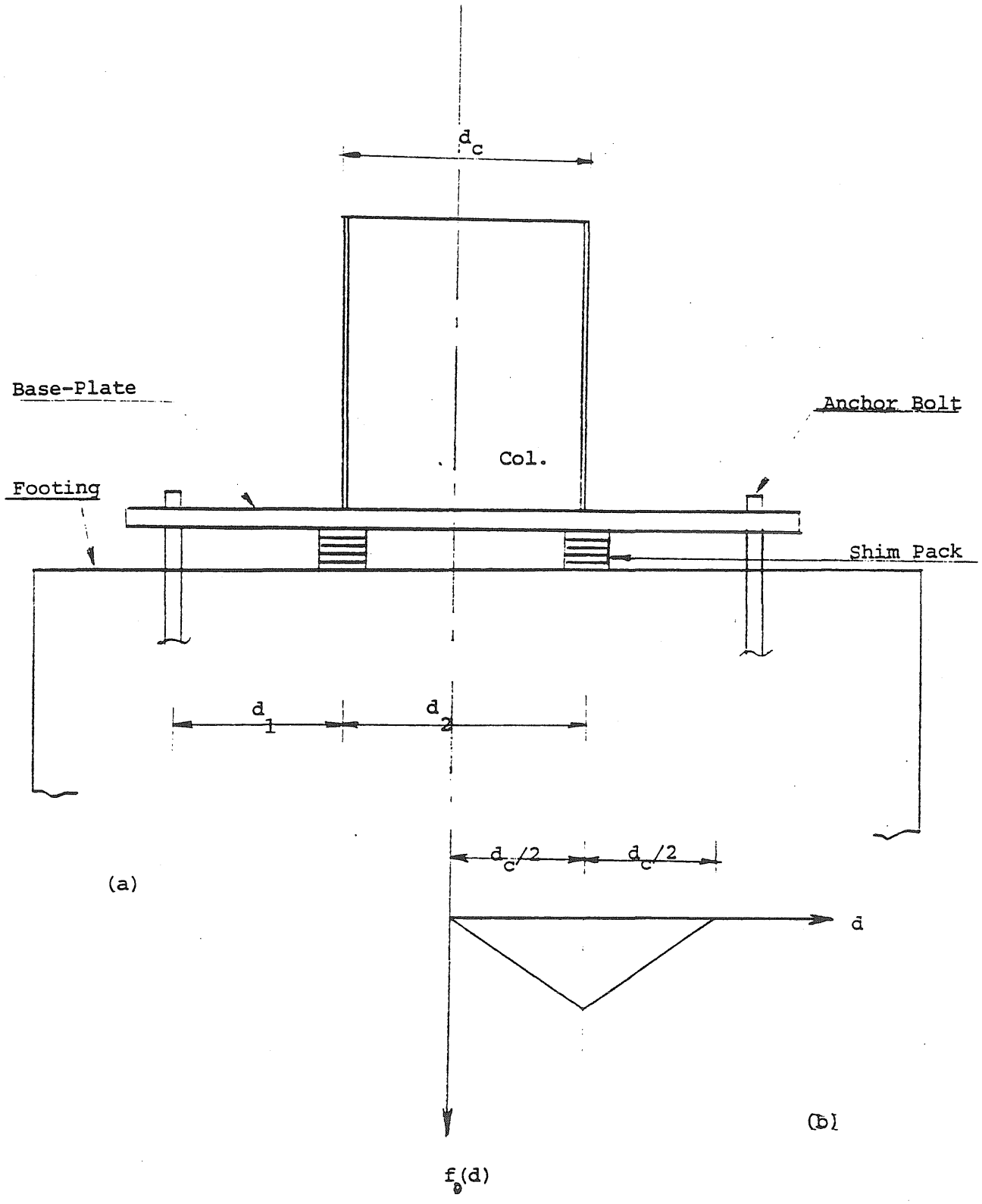

Fig. 2.1 a) An Incomplete Column Anchorage, b) Distribution of the Location of a Shim Pack Under a Column

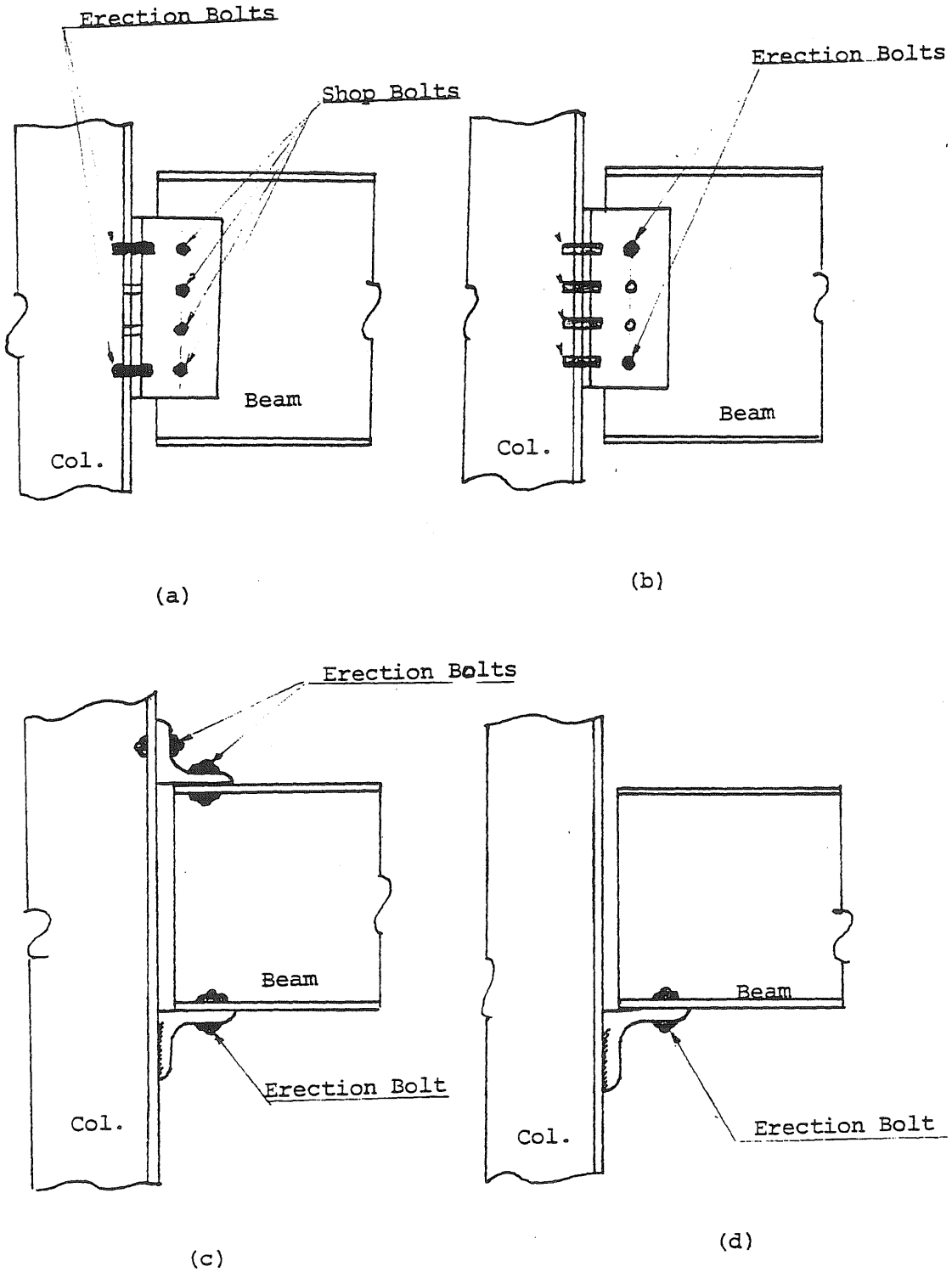

Fig. 2.2 a,b) Framed Temporary Beam-to-Column Connections
c,d) Seated Temporary Beam-to-Column Connections

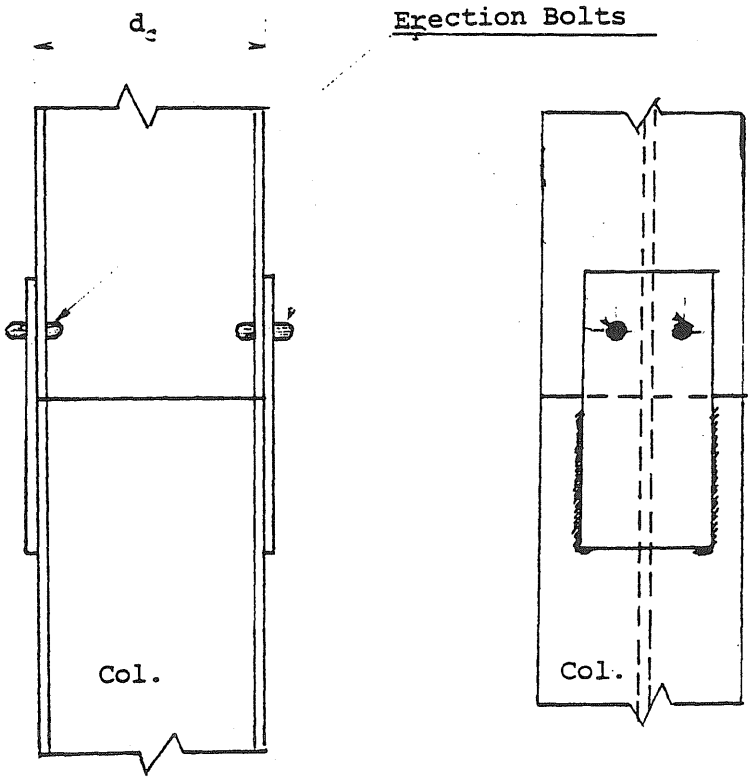

Fig. 2.3 A Welded Column Splice at Temporary Stage

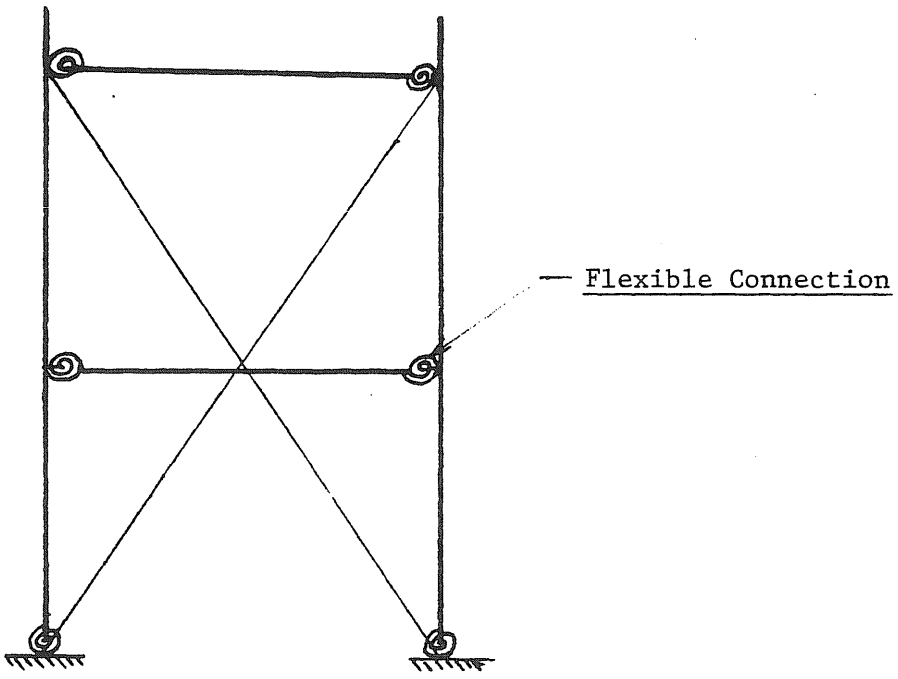

Fig. 3.1 A 2-Story Tier

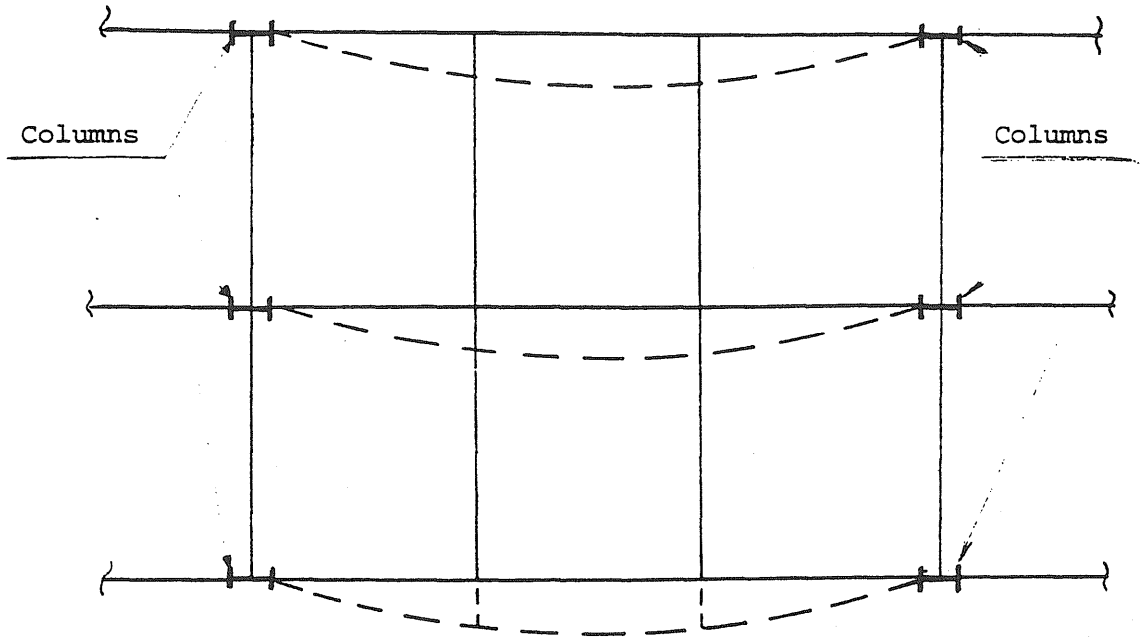

Fig. 3.2 Buckling of a Floor

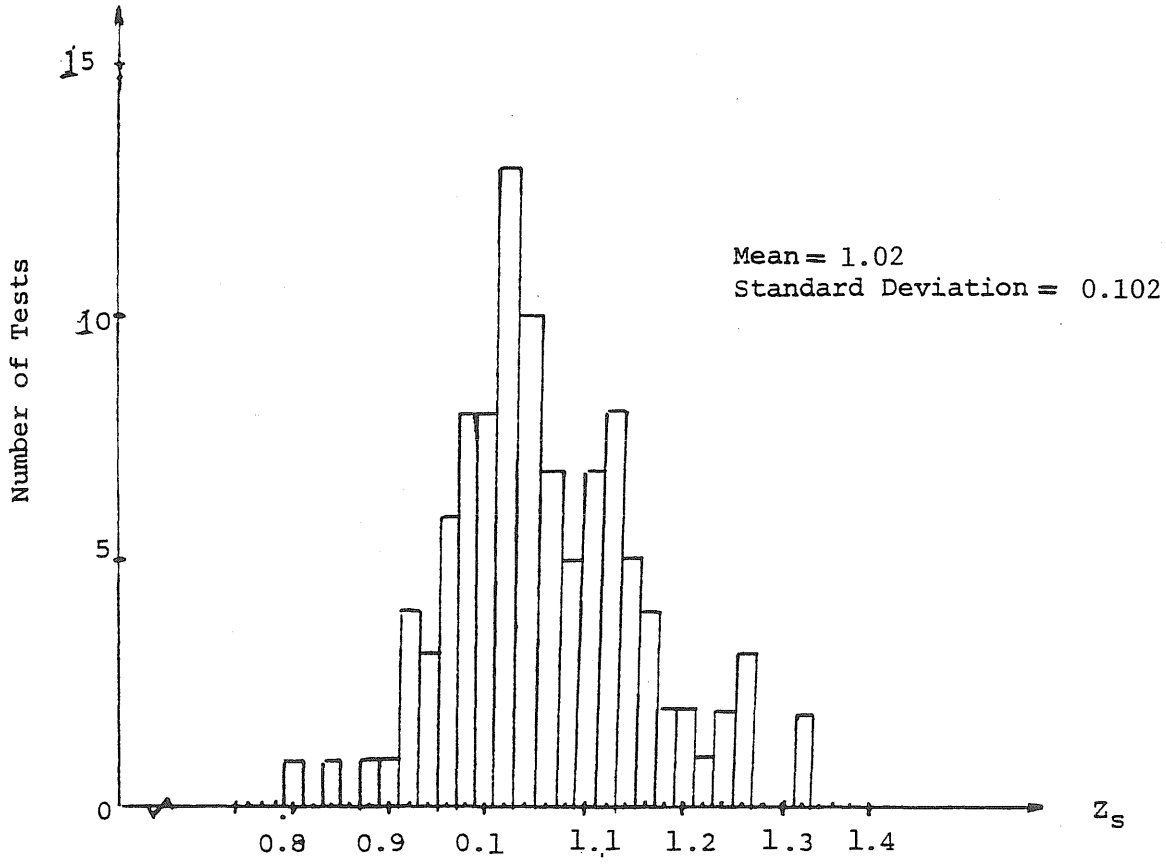

Fig. 3.3 Histogram of Beam-Column Tests Data from (Mason, 1958; Massonnet, 1959)

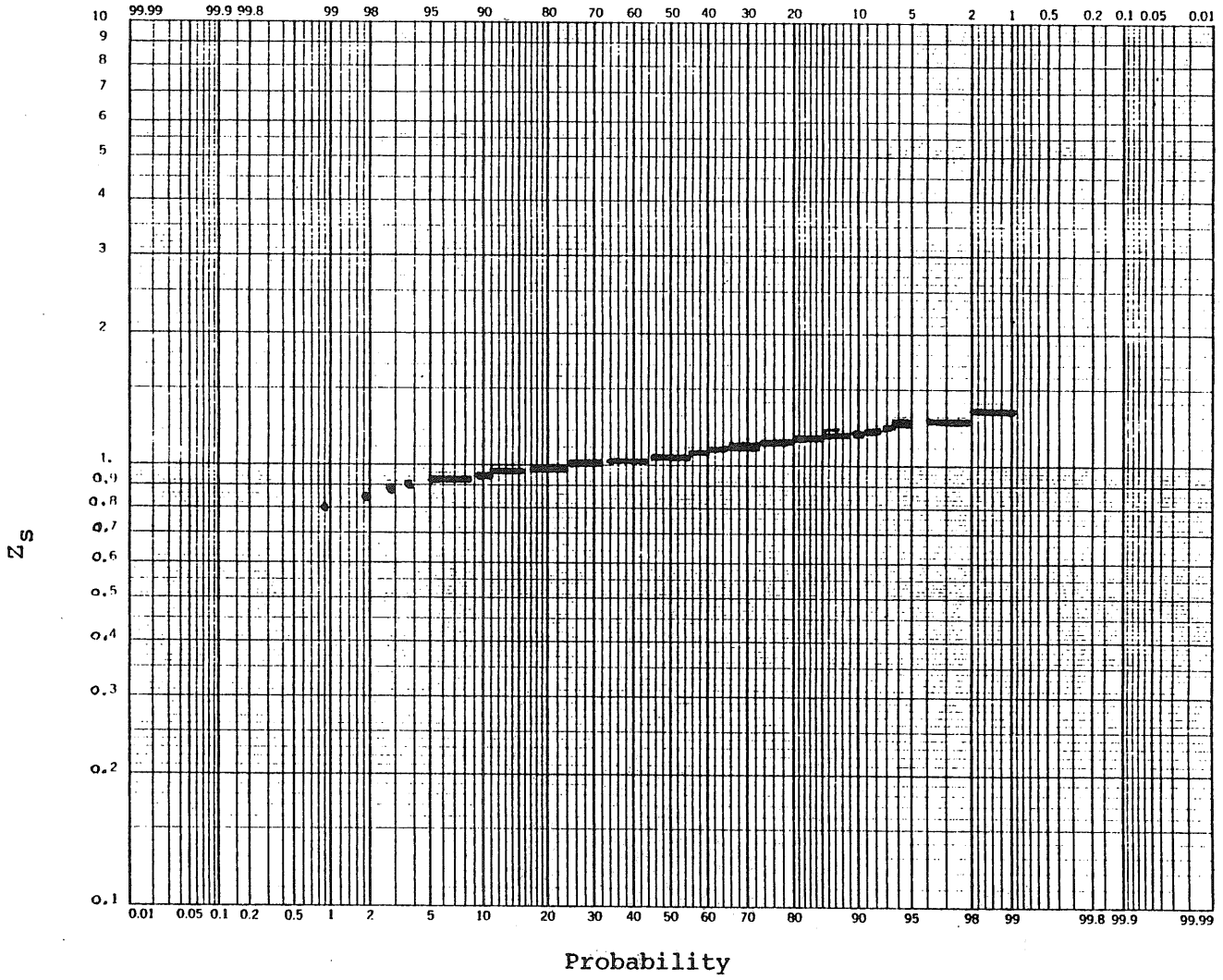

Fig. 3.4 Cumulative Distribution Function of 122 Beam-Column Tests

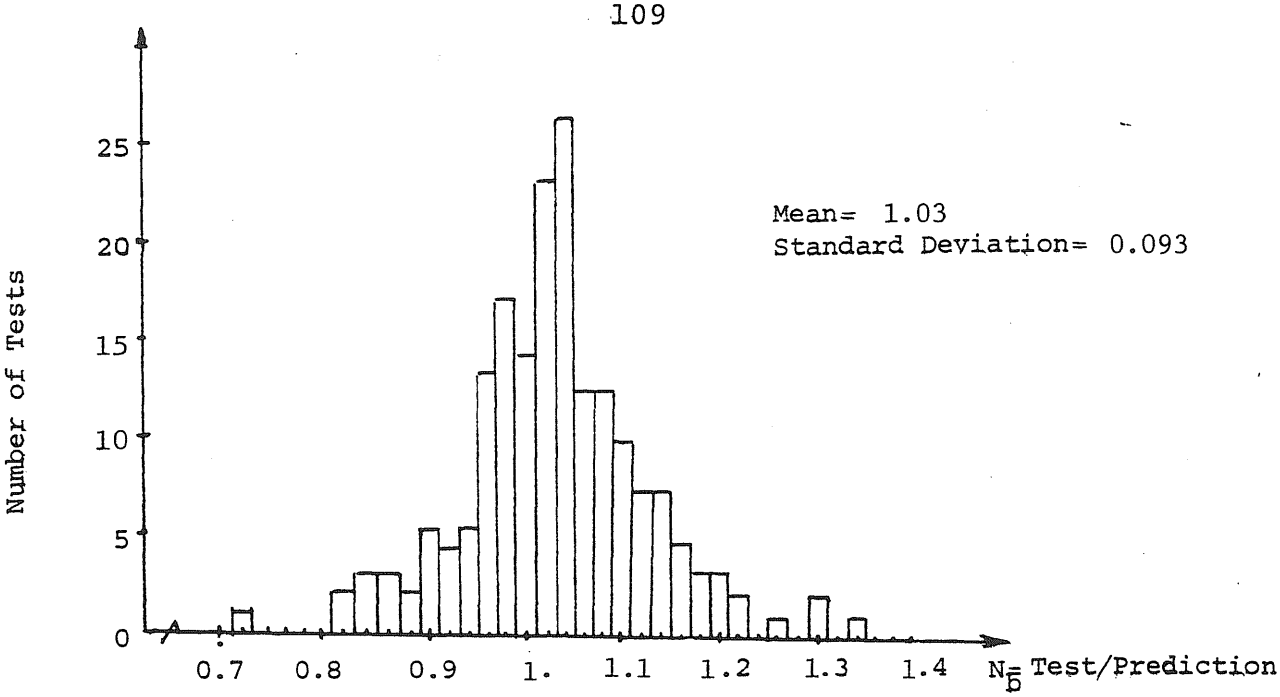

Fig. 3.5 Histogram of Elastic Lateral-Torsional Buckling Tests of Beams (Yura, 1978)

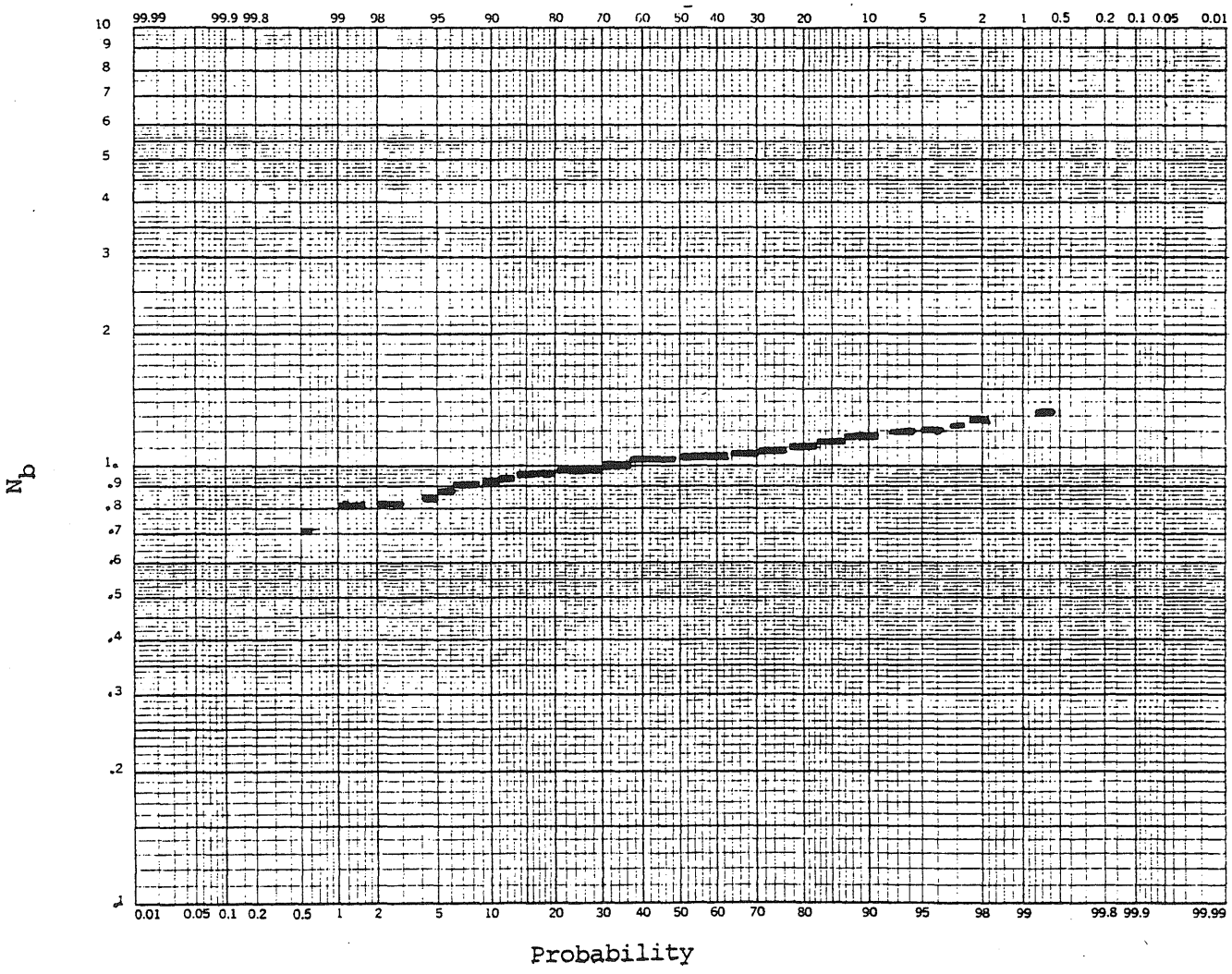

Fig. 3.6 Cumulative Distribution Function of N_b

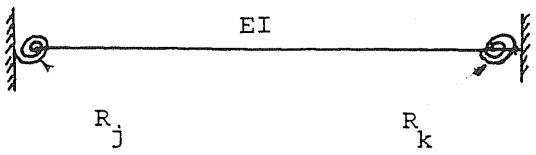

Fig. 4.1 A Typical Beam with Temporary Connections

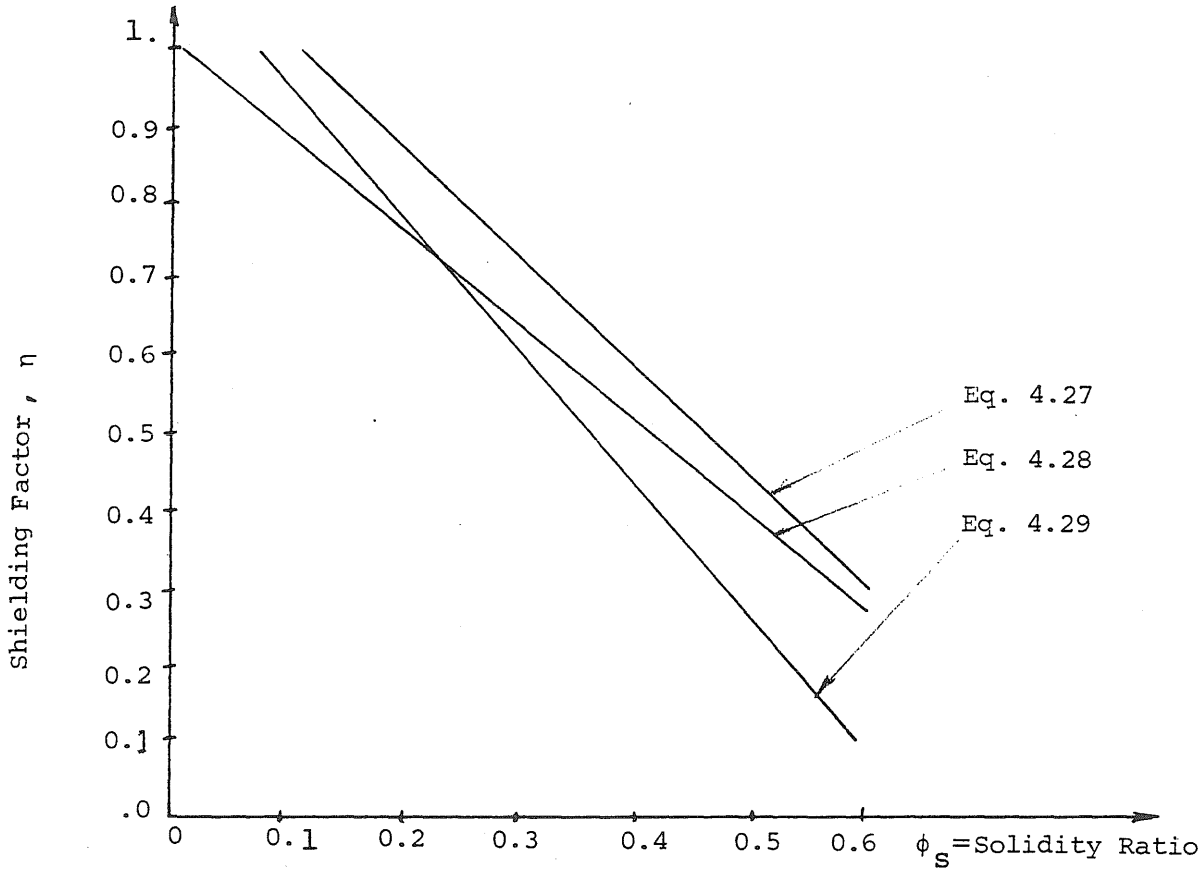

Fig. 4.2 Relations Between Shielding Factor and Solidity Ratio (S_s=1)

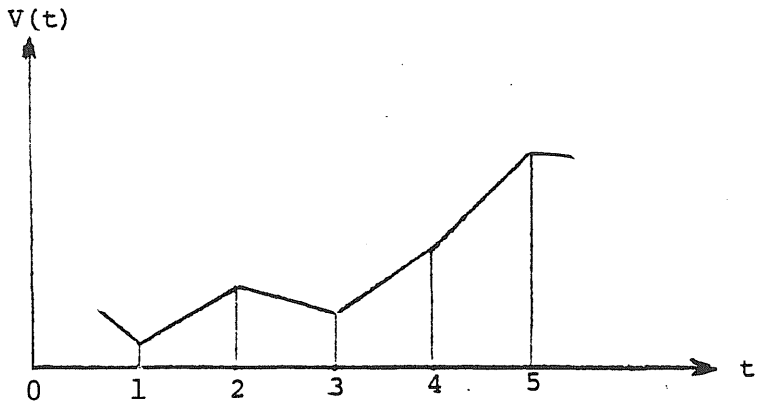

Fig. 4.3 Daily Maximum Wind Speed Process

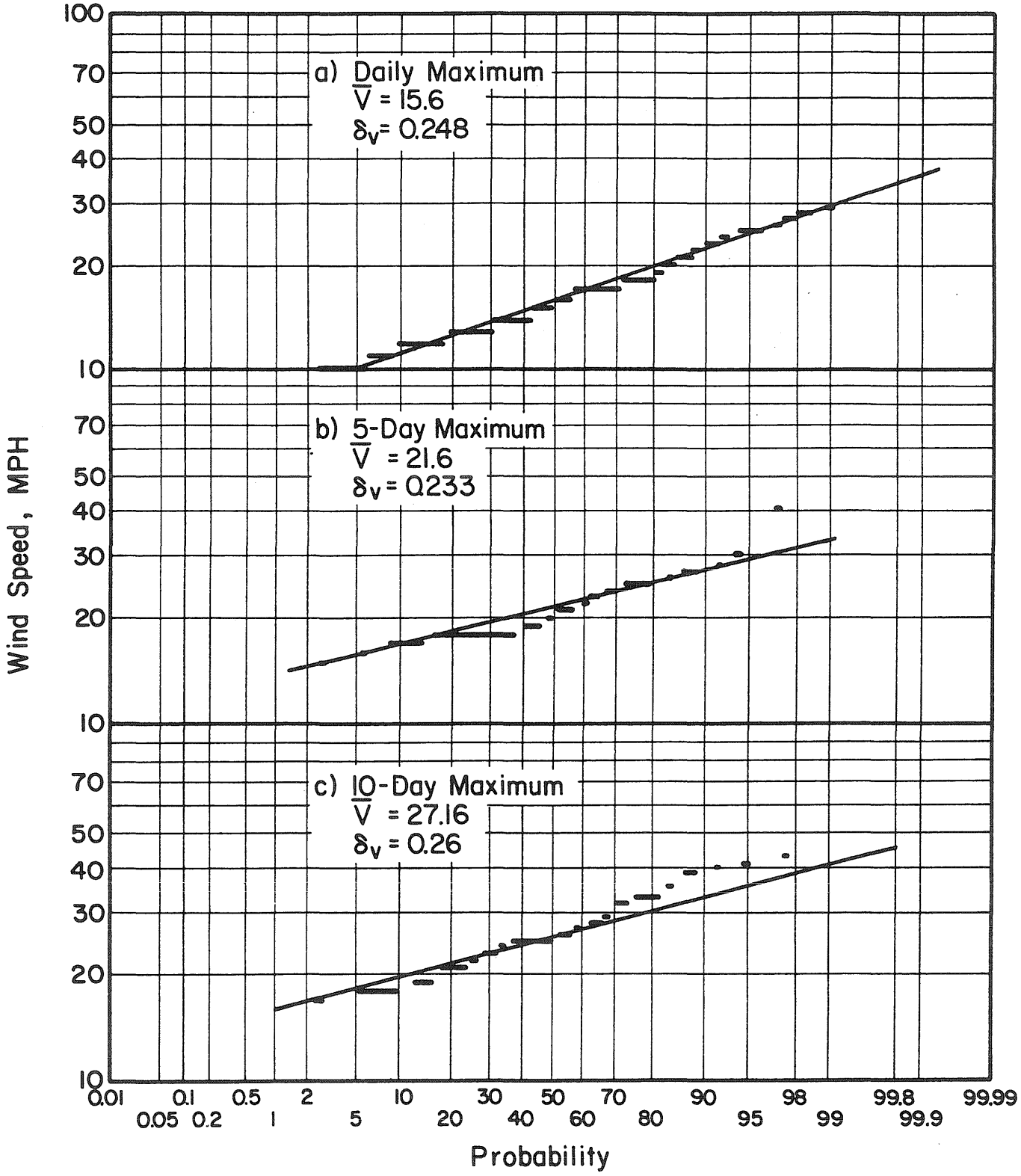

Fig. 4.4 Distributions of Maximum Wind Speeds in Chicago for July a) Daily Maximum, b) 5-Day Maximum, c) 10-Day Maximum

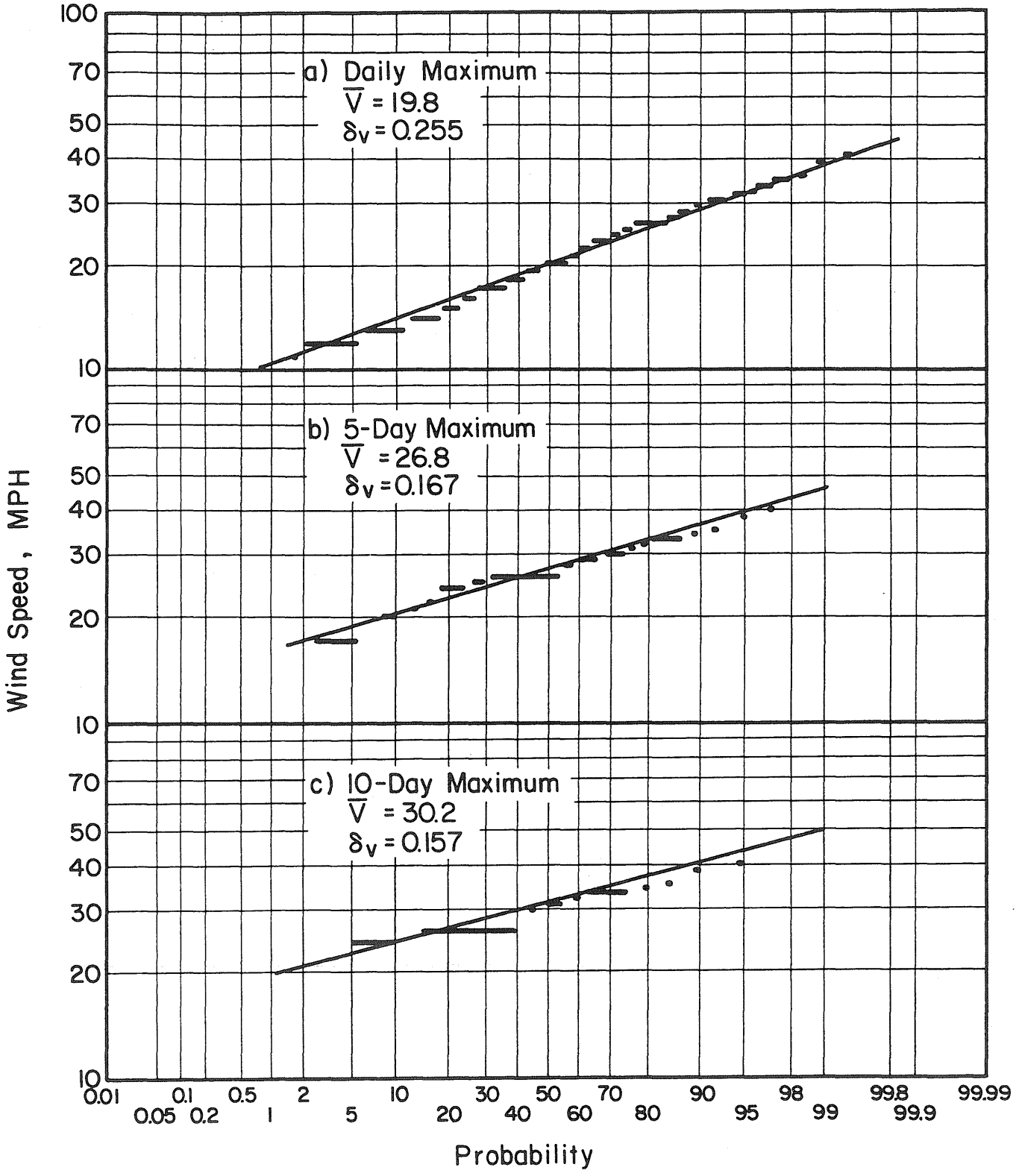

Fig. 4.5 Distributions of Maximum Wind Speeds in Chicago for March a) Daily Maximum, b) 5-Day Maximum, c) 10-Day Maximum

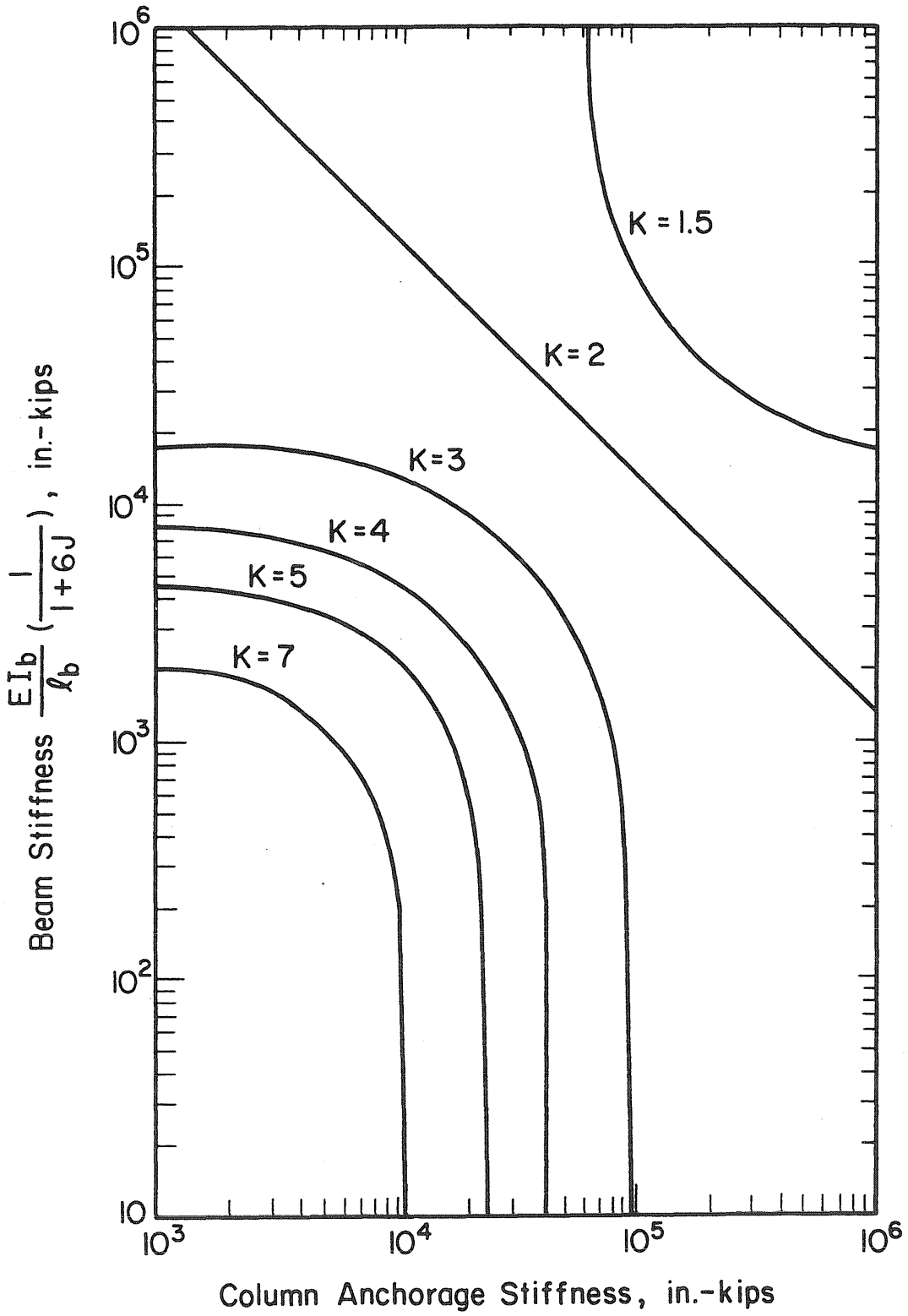

Fig. 5.1 Variation of Effective Length Factor

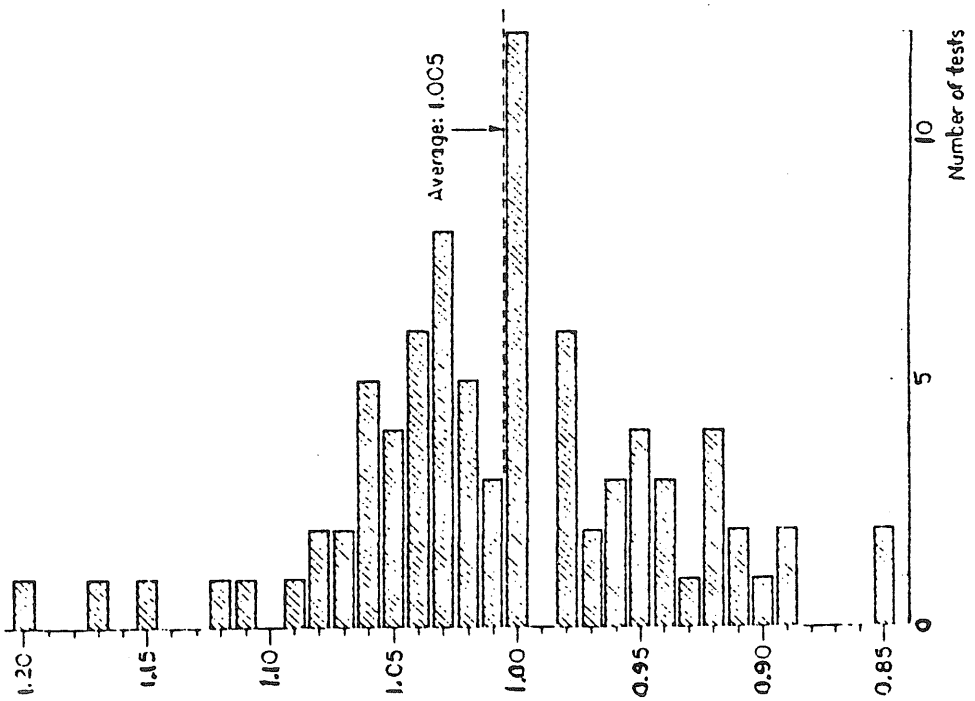

Fig. 5.2 Comparison of Experimental and Theoretical Exact Strength of Beam-Columns (Galambos, 1978)

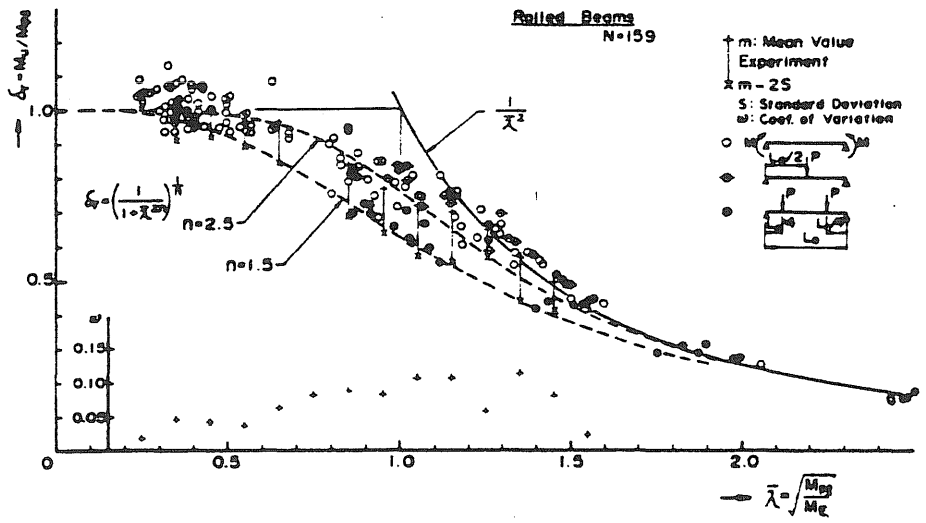

Fig. 5.3 Test Results of Lateral Buckling of Beams (Fukumoto, 1977)

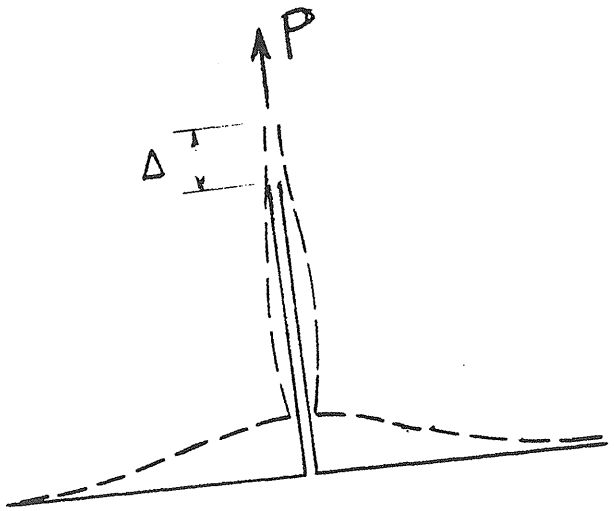

Fig. 5.4 Load-deformation of Connection Angles

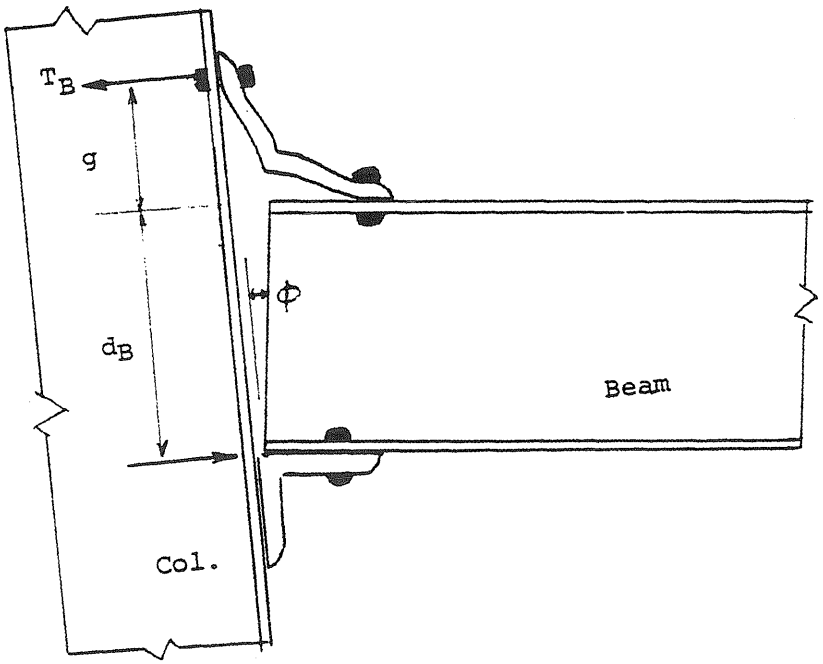

Fig. 5.5 Deformation of a Seated Temporary Connection

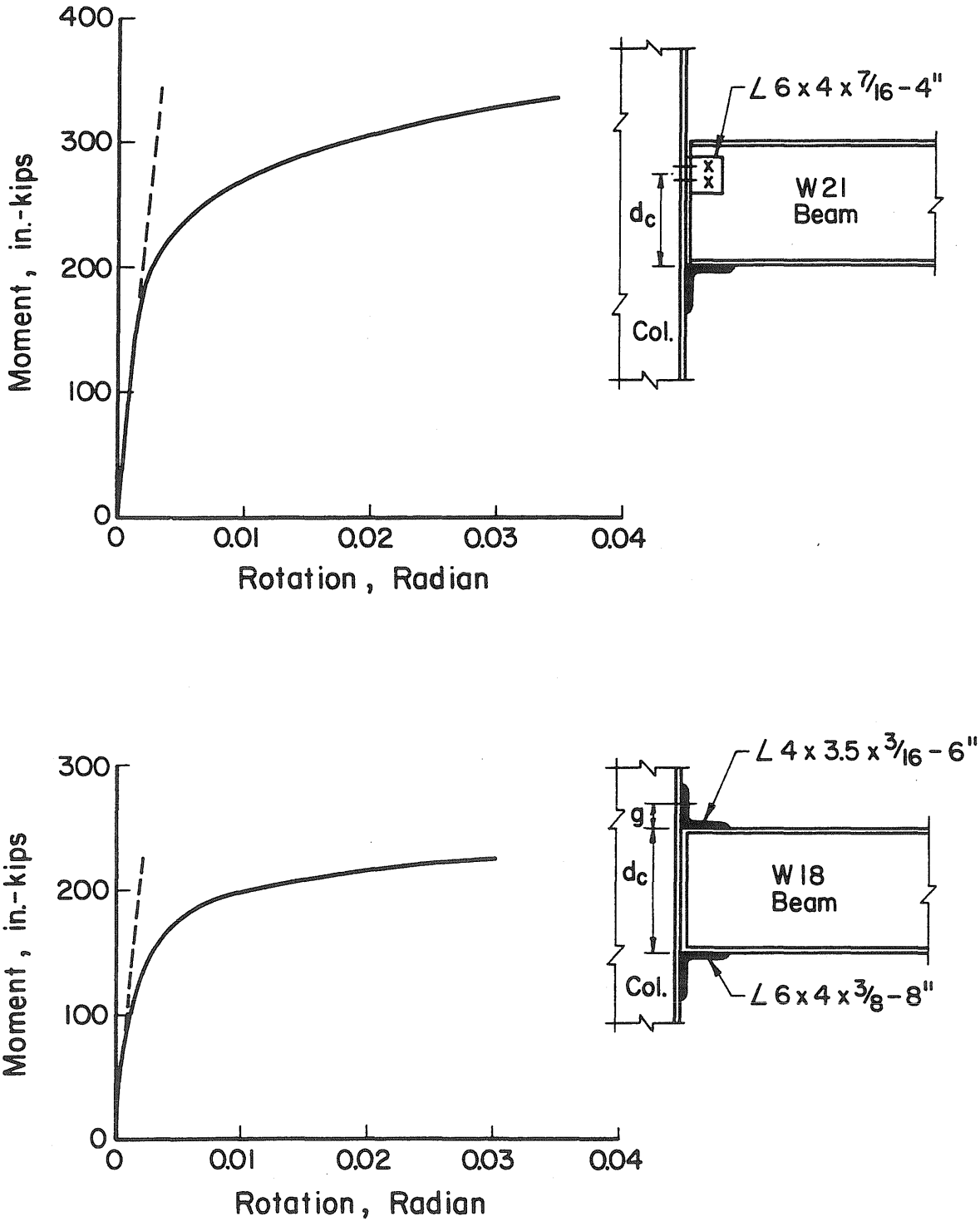

Fig. 5.6 Moment-Rotation Curves of Imcomplete Seated Connections

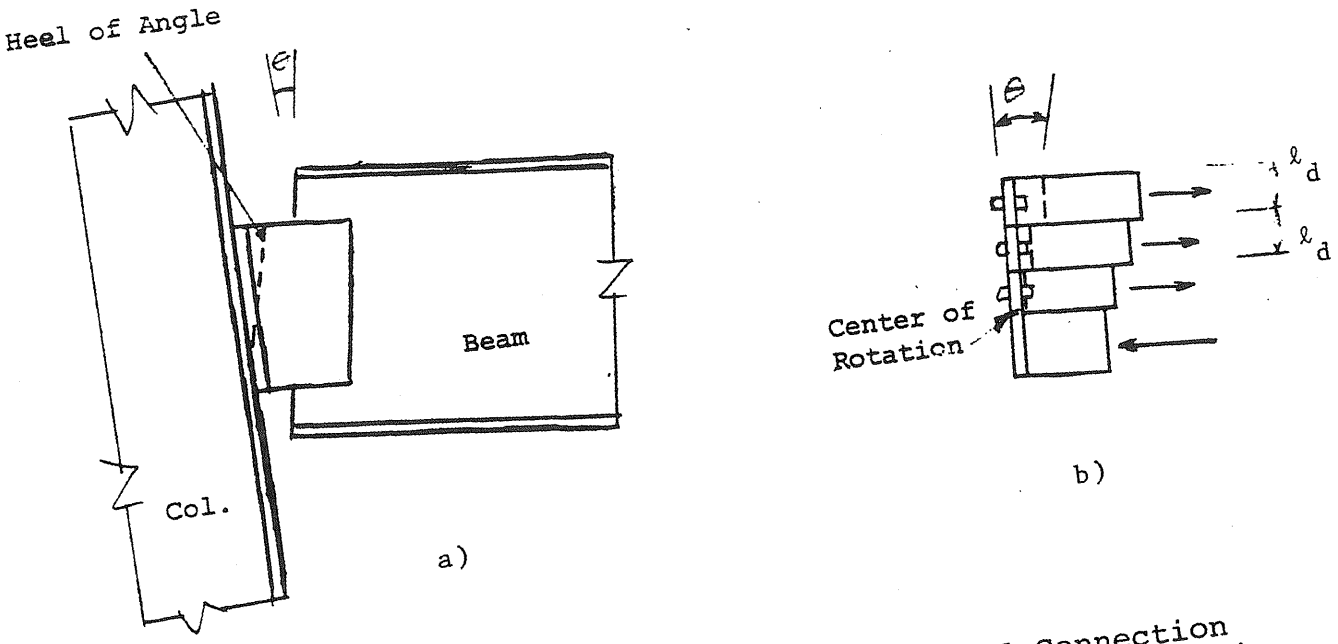

Fig. 5.7 a) Deformation of a Framed Connection
b) Model Used for Mathematical Analysis
(Beaufoy, 1948)

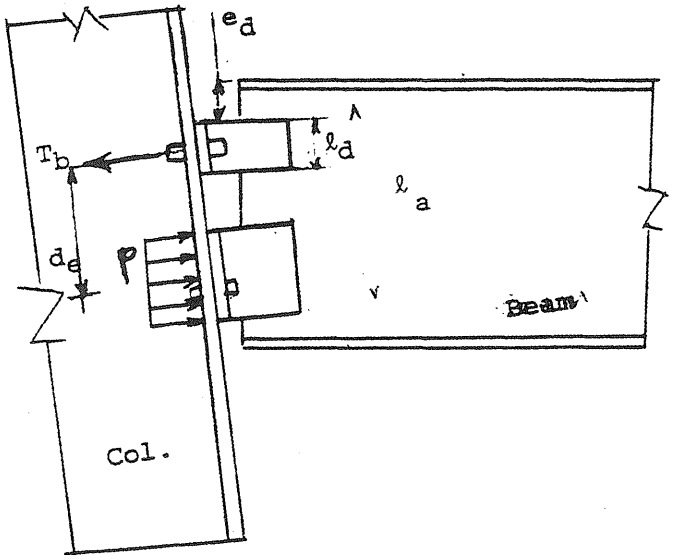

Fig. 5.8 Model Used for Analysis of Framed Temporary Connections

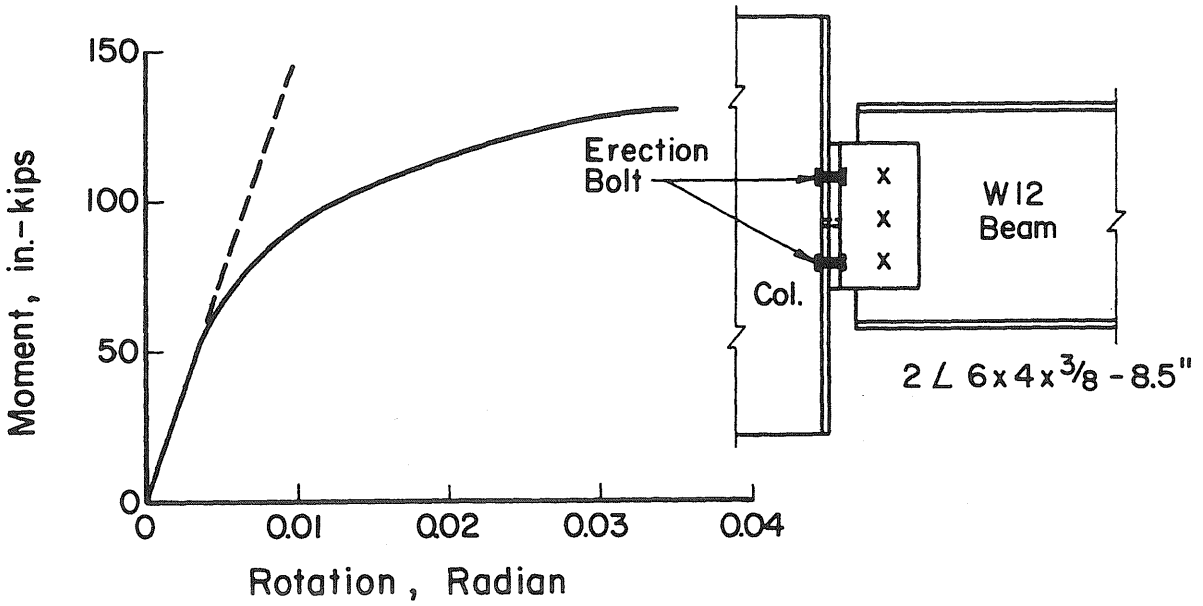

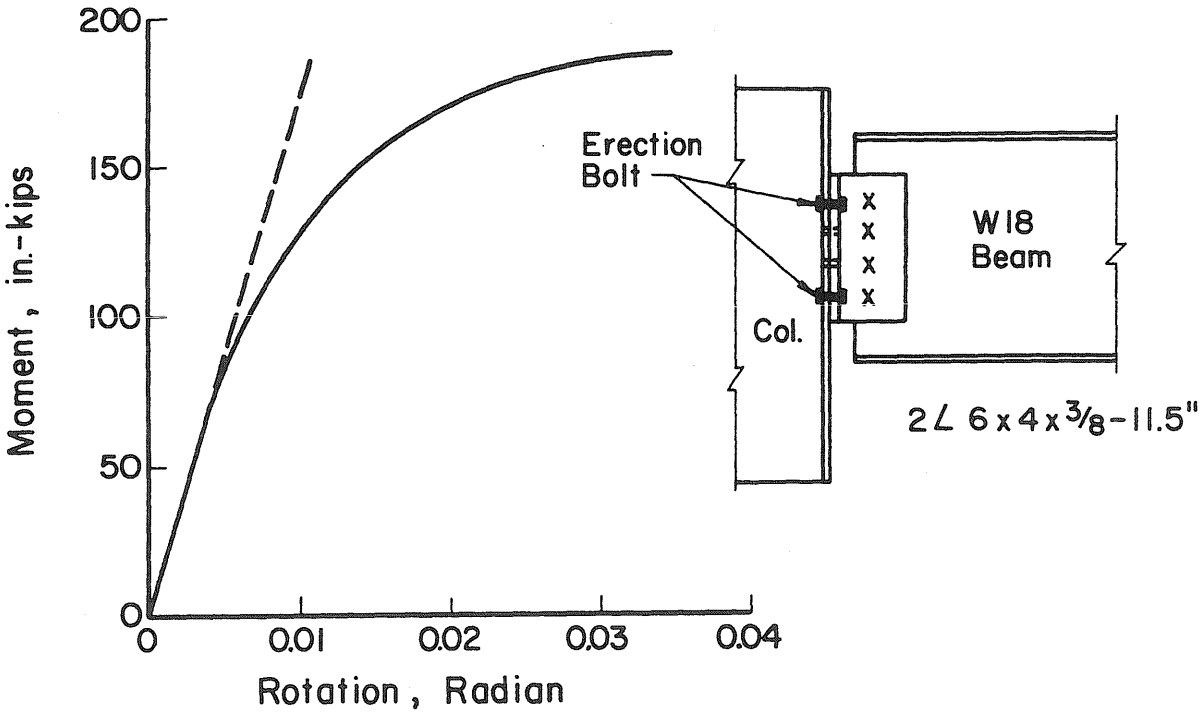

Fig. 5.9 Moment-Rotation Curves of Incomplete Framed Connections

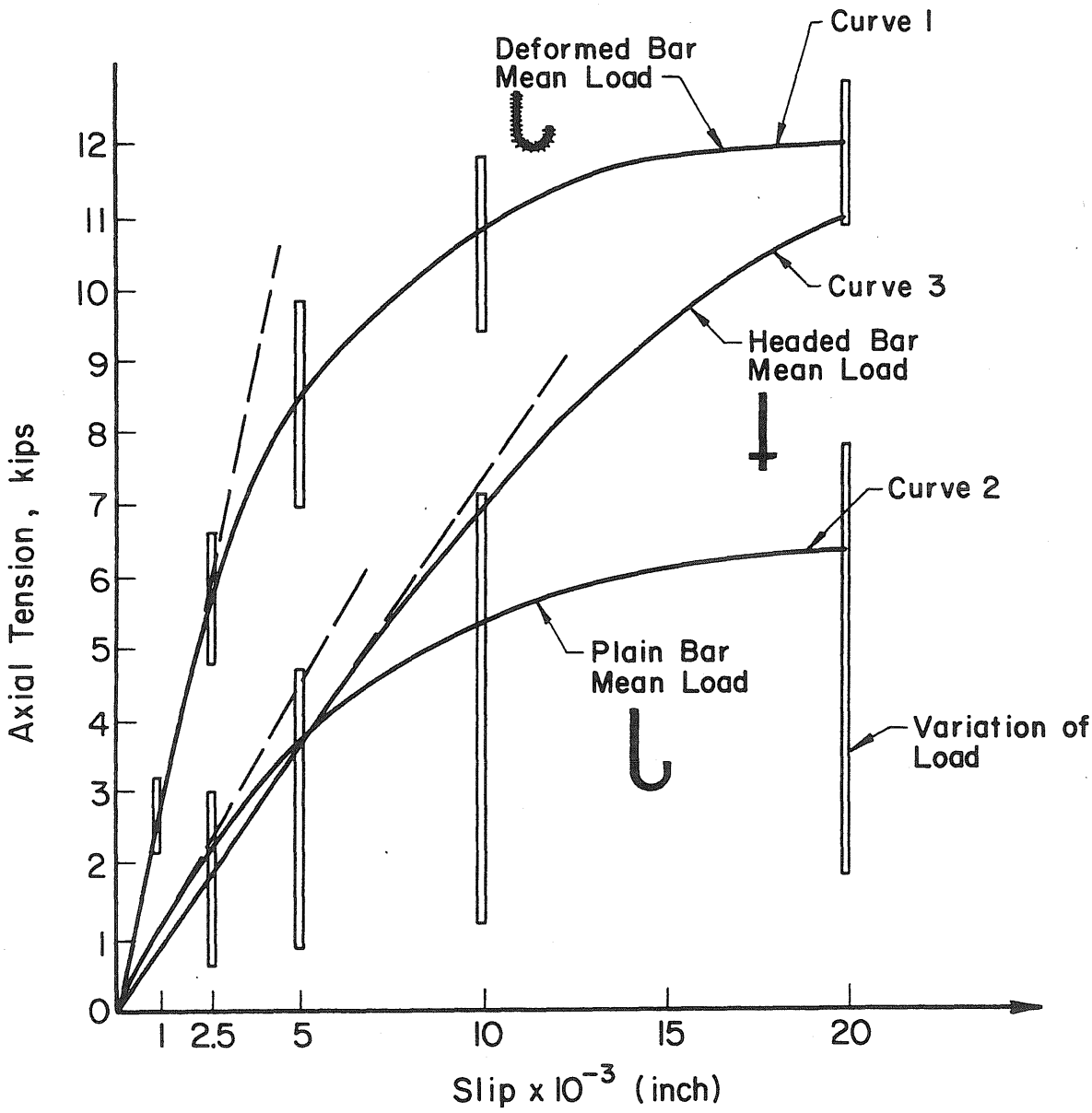

Fig. 5.10 Load Carried by Different Bar Anchorages at Different Loads (Fishburn, 1947; Shoup, 1963)

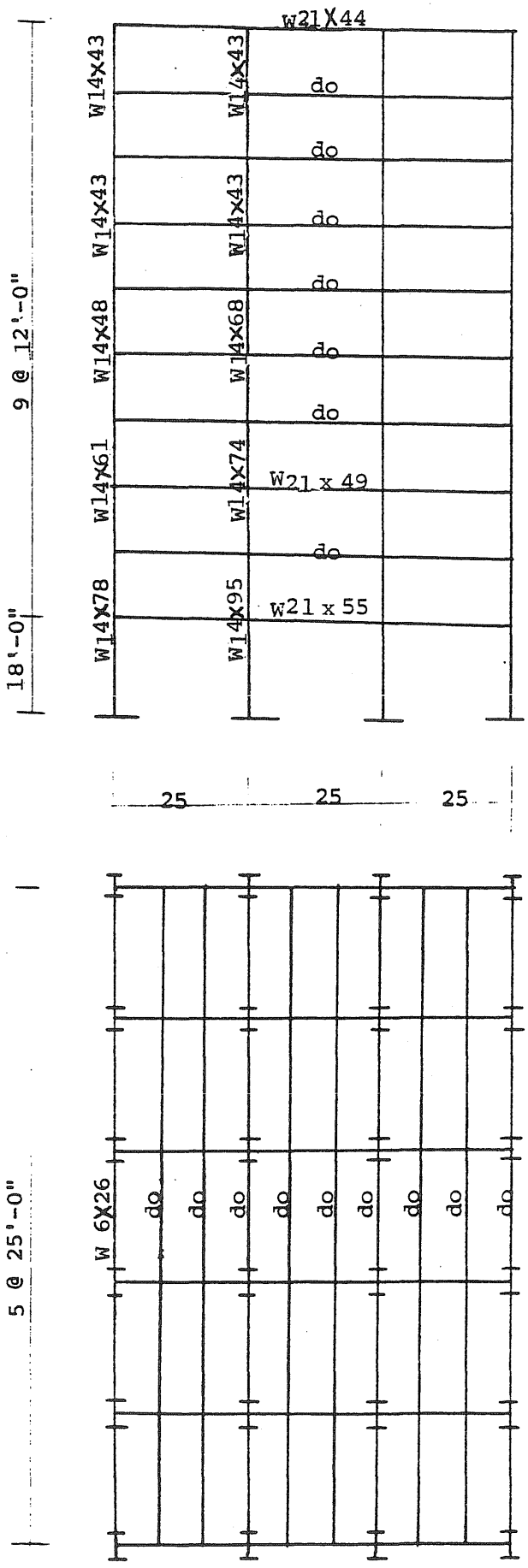

Fig. 6.1 Plan and Elevation of Ten-Story Steel Building Frame

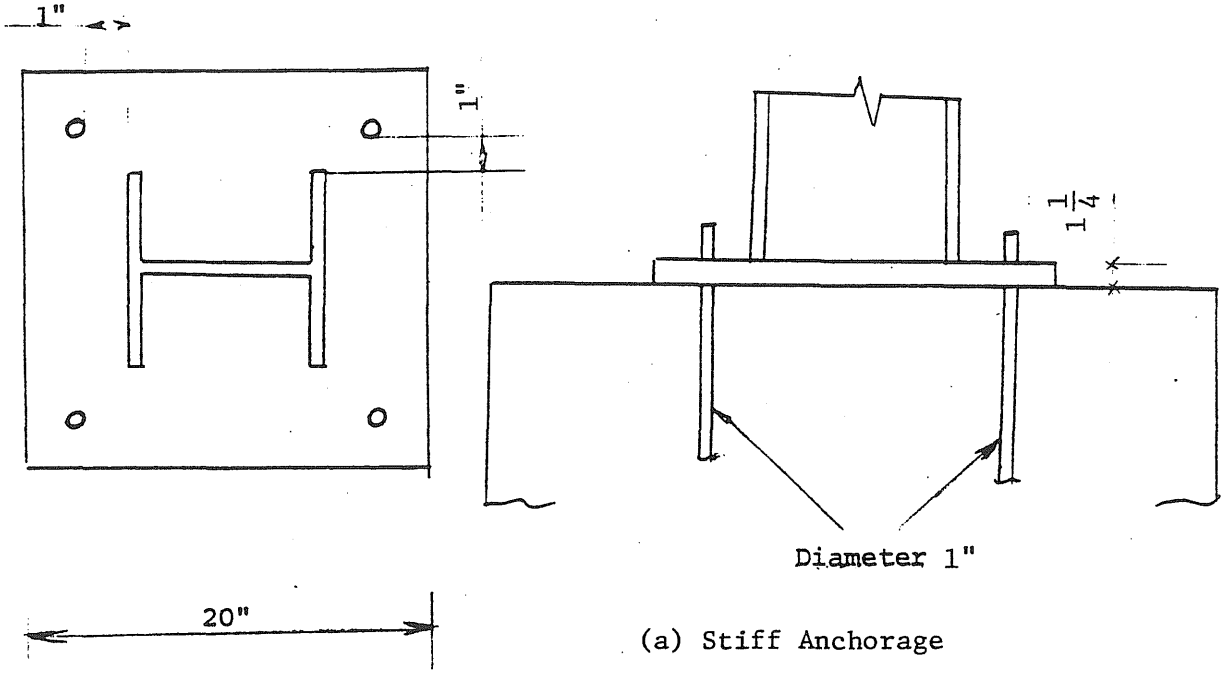

(a) Stiff Anchorage

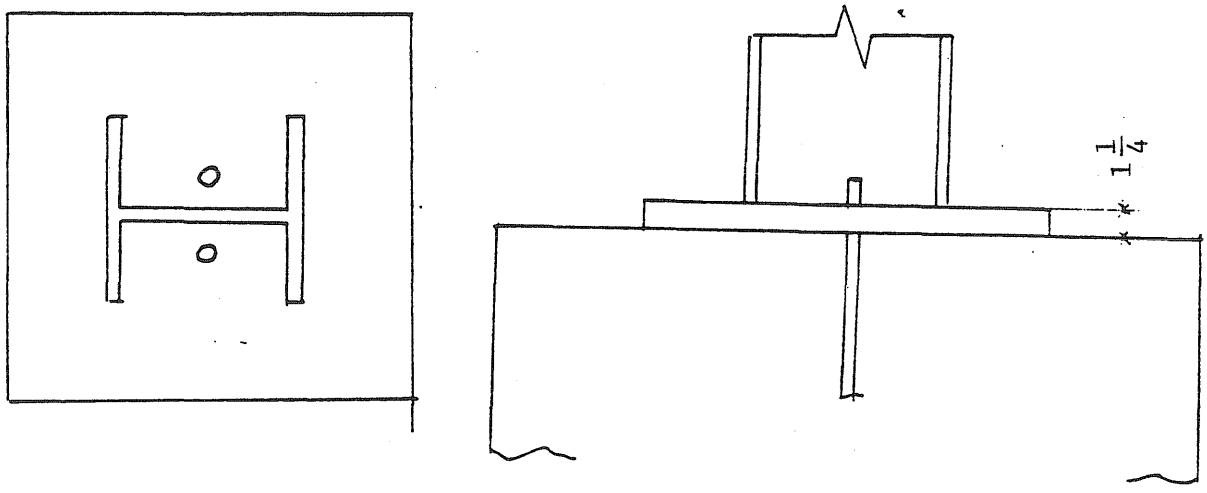

(b) Flexible Anchorage

Fig. 6.2 Dimensions of Column Anchorages of Ten-Story Building Frame

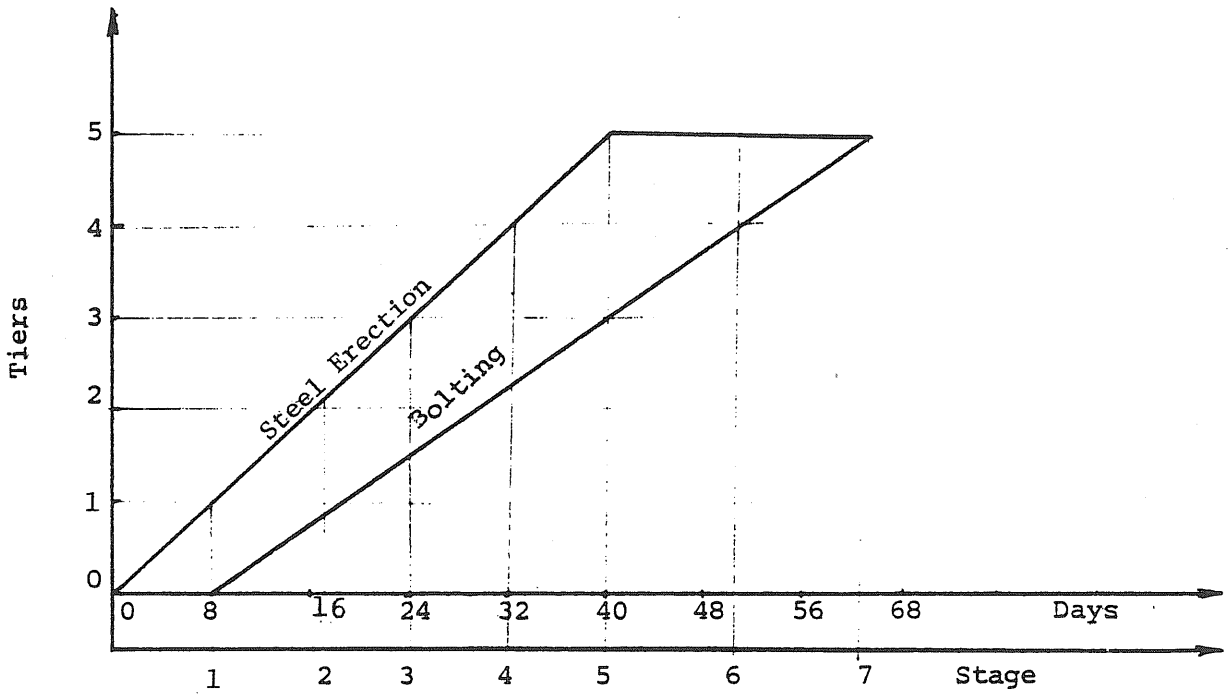

Fig. 6.3 Construction Schedule Assumed in Analysis

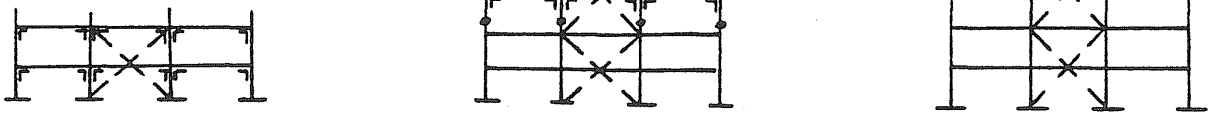

Stage 1 Stage 2 Stage 3

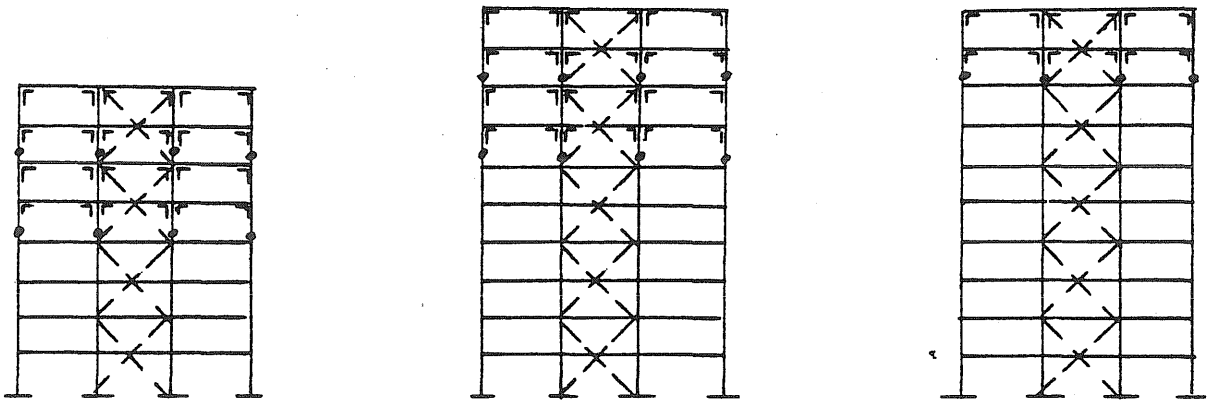

Stage 4 Stage 5 Stage 6

Legend:

Permanent Beam-Column Connections

Temporary Beam-Column Connections

Temporary Column Splices

Temporary Bracings

Note: all tiers are two-story high

Fig. 6.4 Stages Selected for Reliability Analysis (X-X Direction)

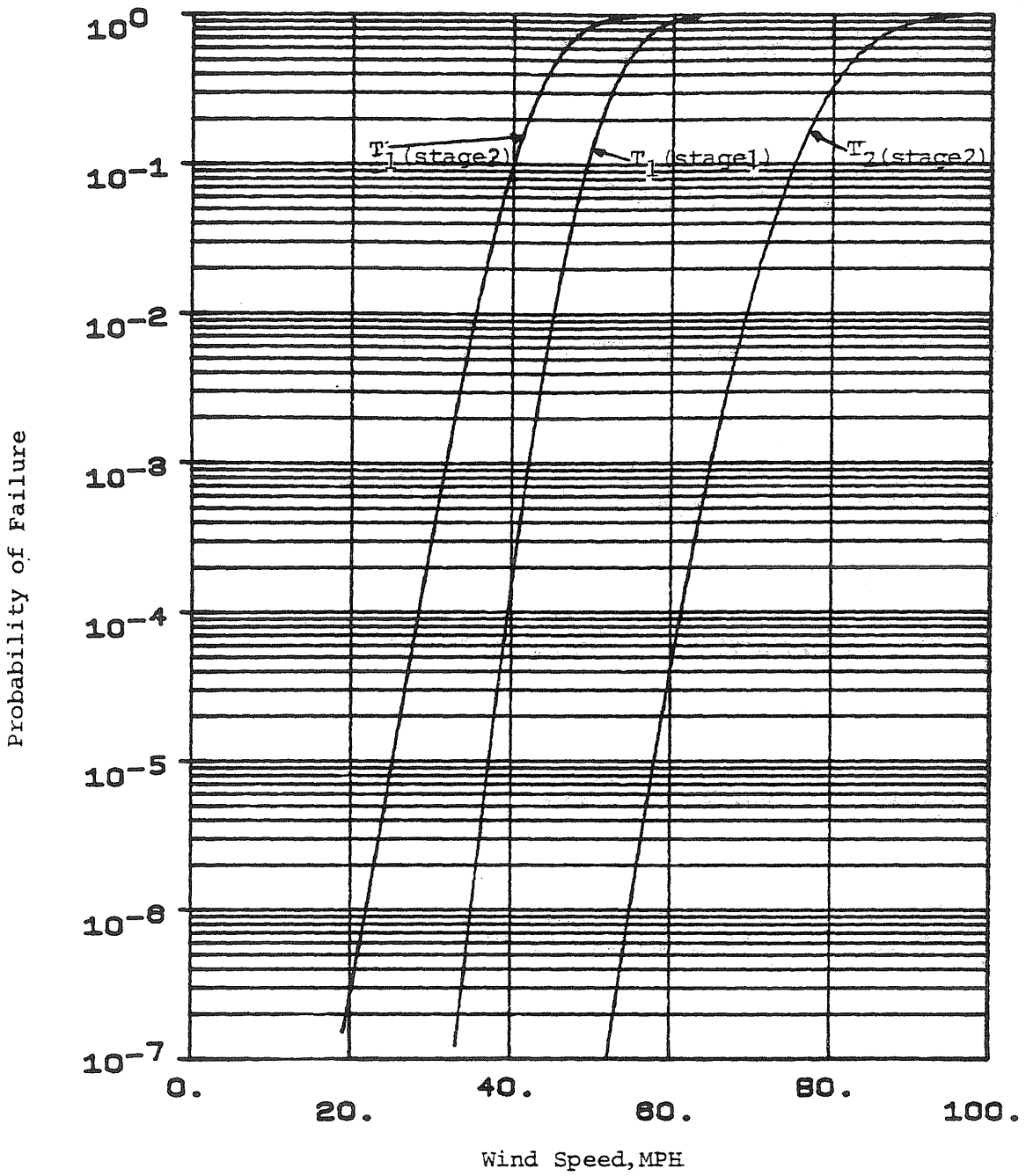

T_i=Failure of upper i tiers by yielding of connections

Fig. 6.5 Conditional Failure Probabilities, Stages 1 and 2 (X-X Direction)

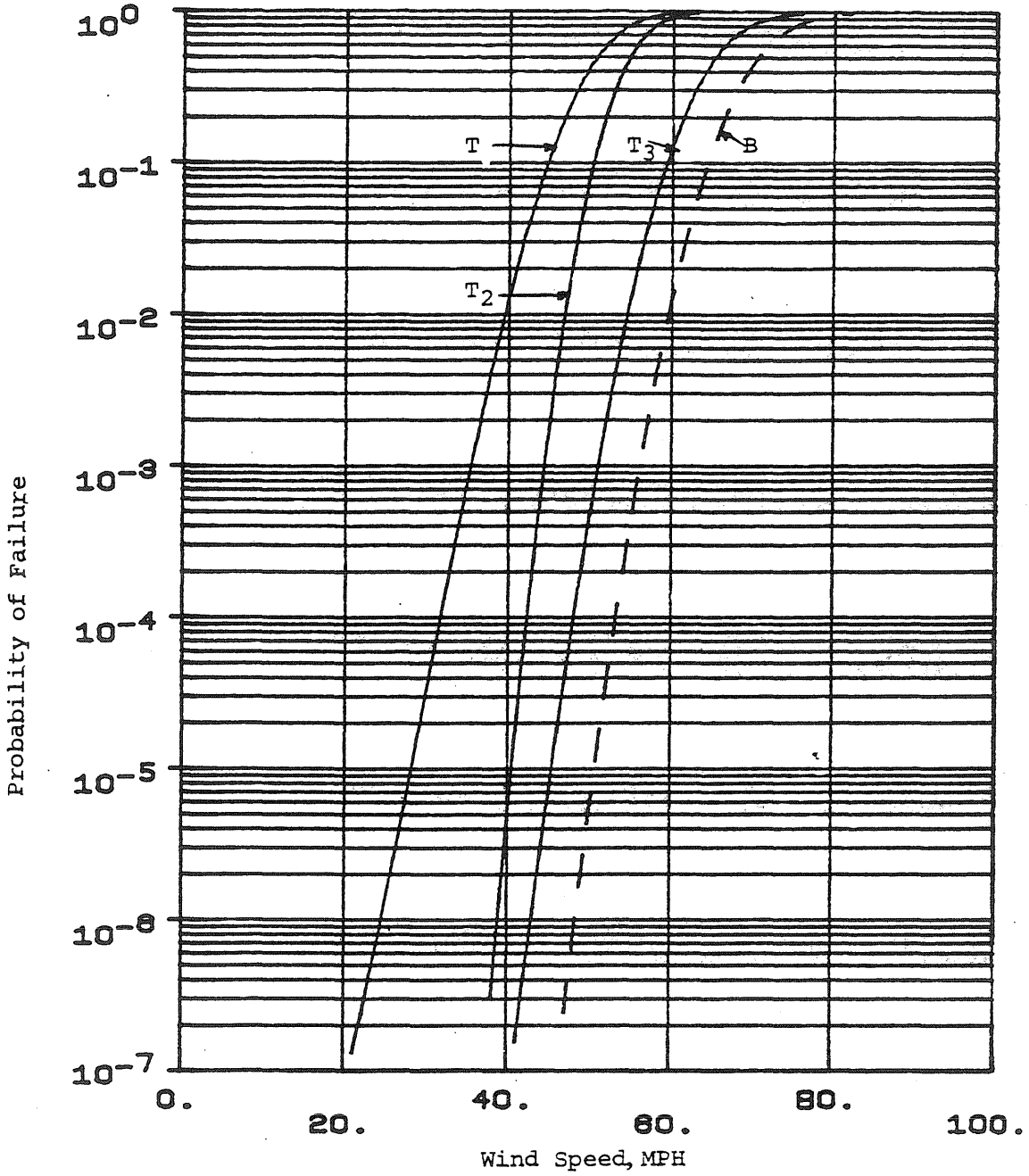

T_i = Failure of upper i tiers by yielding of connections

B = Beam Failure (Lateral Buckling) in First Floor

Fig. 6.6 Conditional Failure Probabilities, Stage 3 (X-X Direction)

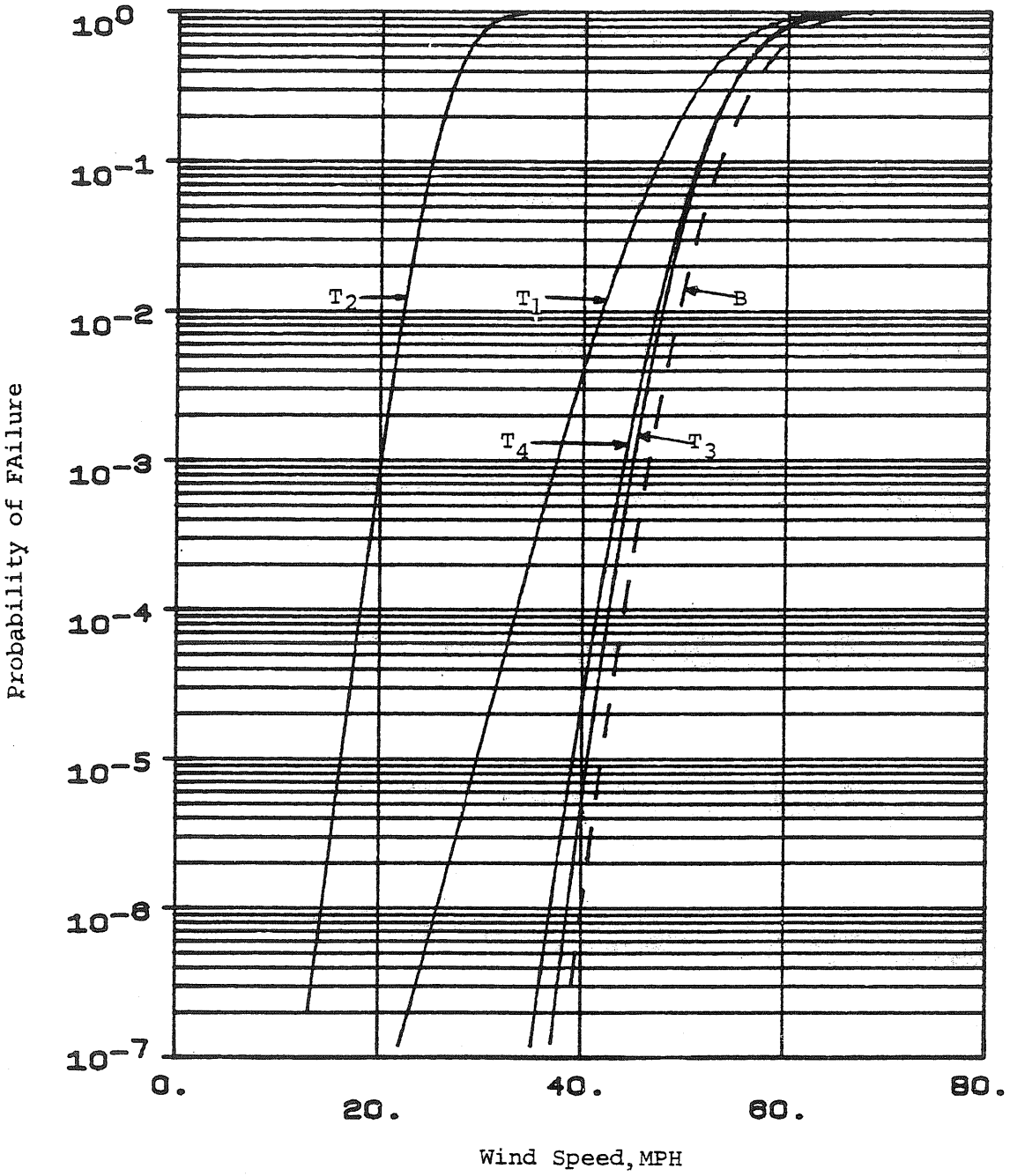

T_i = Failure of upper i tiers by yielding of connections

B = Beam Failure (Lateral Buckling) in First Floor

Fig. 6.7 Conditional Failure Probabilities; Stage 4 (X-X Direction)

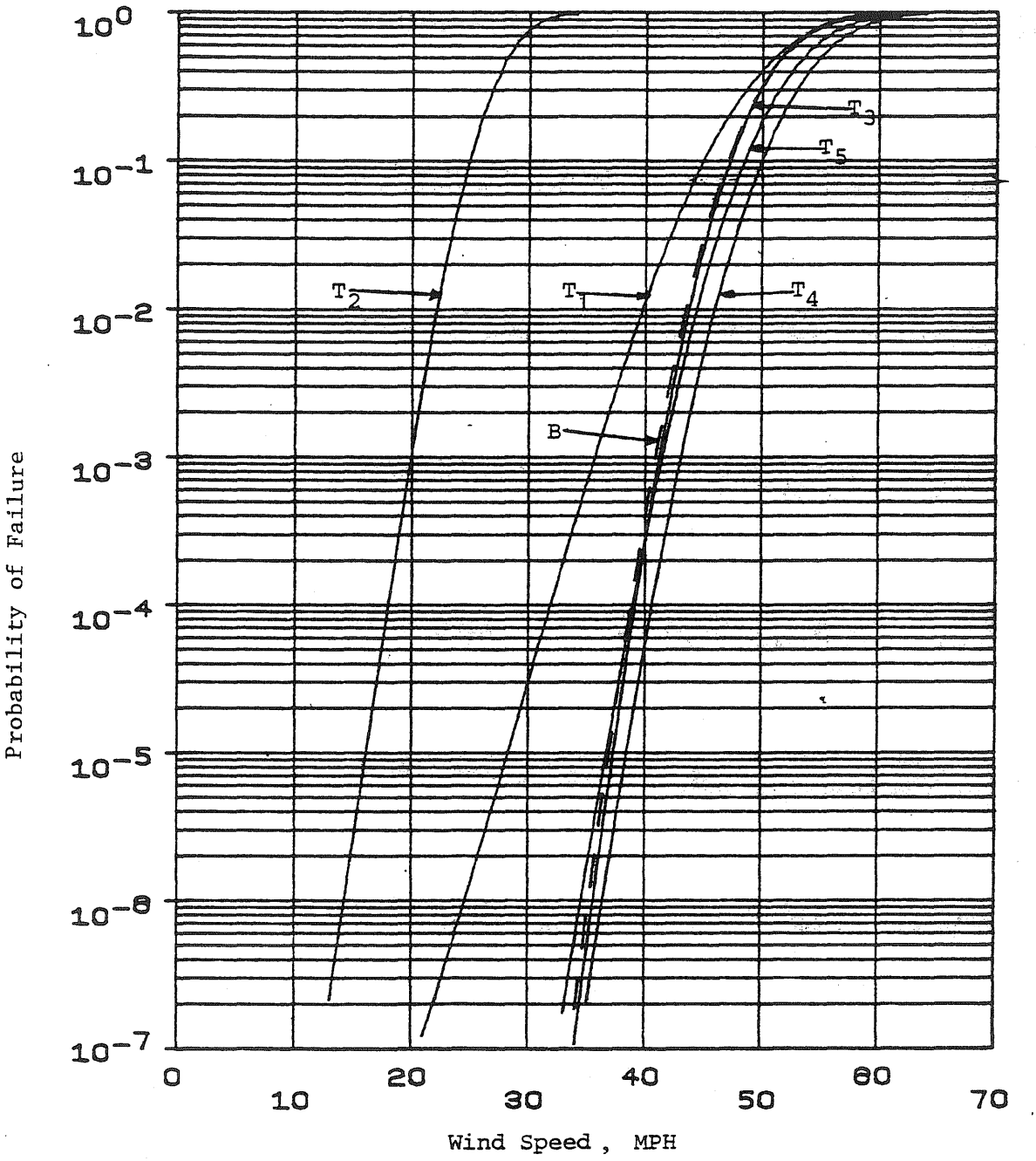

T_i = Failure of upper i tiers by yielding of connections

B = Beam failure (Lateral Buckling) in first floor

Fig. 6.8 Conditional Failure Probabilities; Stage 5 (X-X Direction)

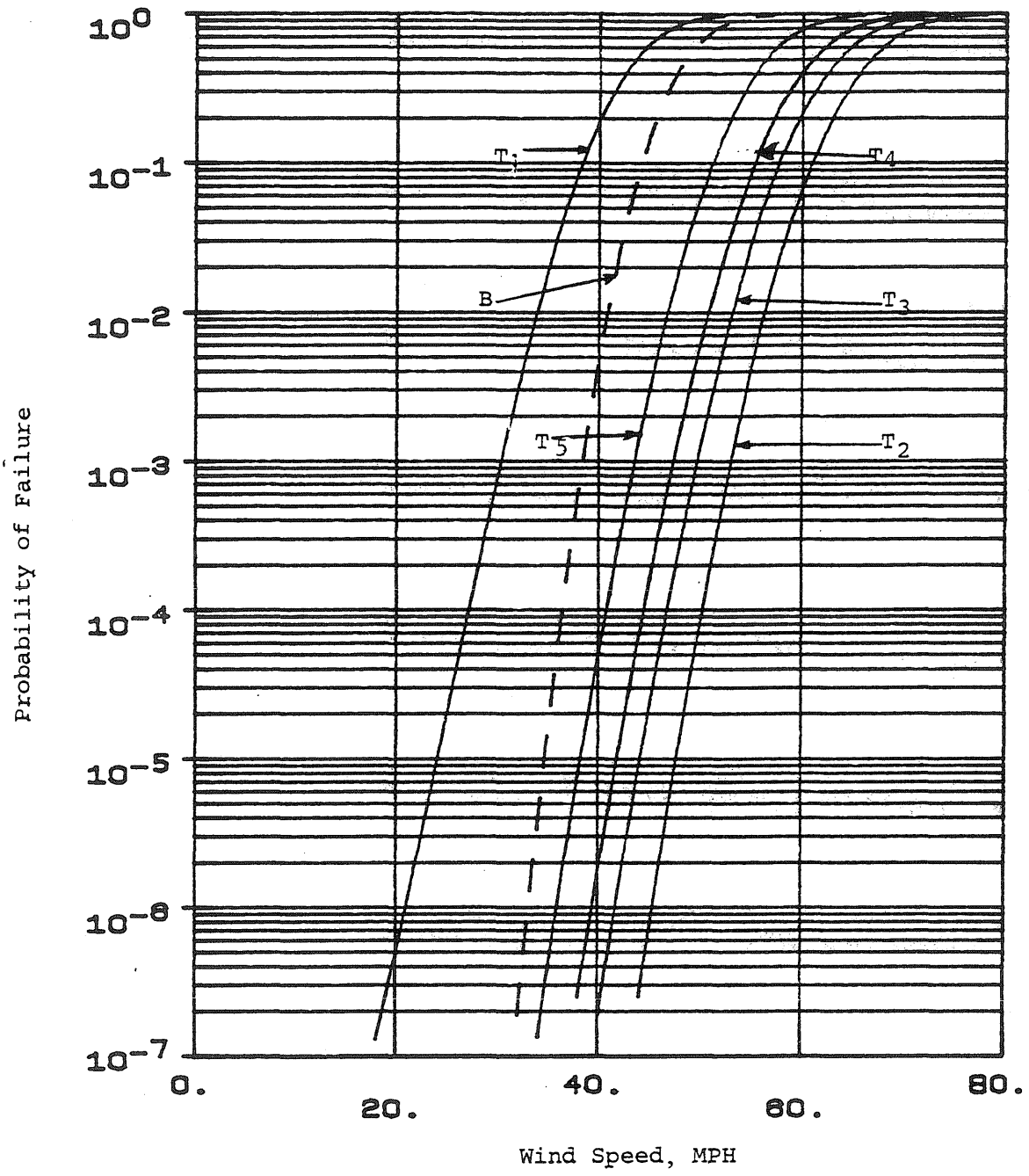

T_i = Failure of upper i tiers by yielding of connections

B = Beam failure (Lateral Buckling) in first floor

Fig. 6.9 Conditional Failure Probabilities; Stage 6 (X-X Direction)

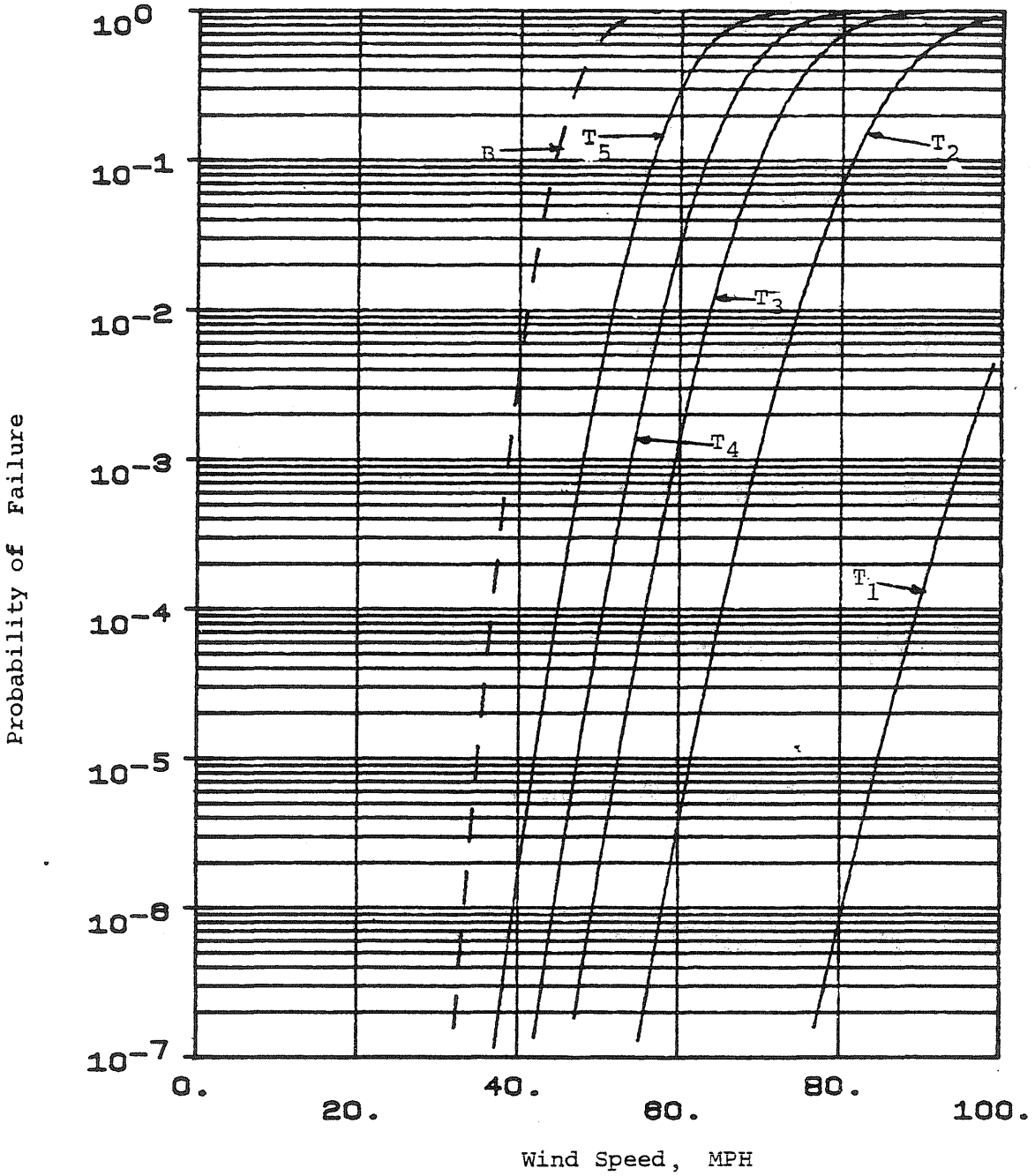

T_i = Failure of upper i tiers by yielding of connections

B = Beam Failure (Lateral Buckling) in first floor

Fig. 6.10 Conditional Failure Probabilities; Stage 7 (X-X Direction)

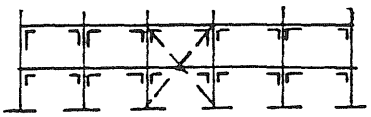

Stage 1

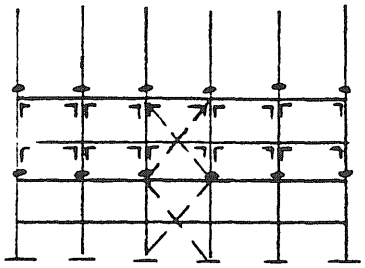

Stage 2

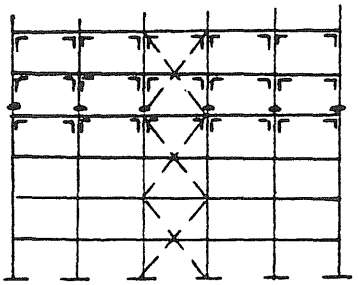

Stage 3

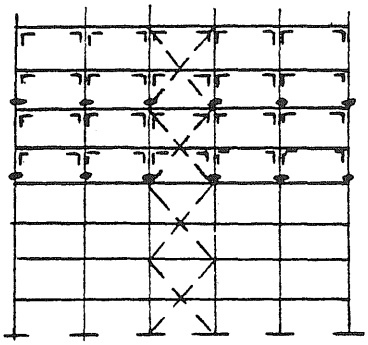

Stage 4

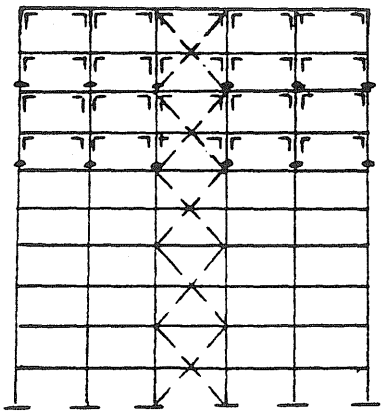

Stage 5

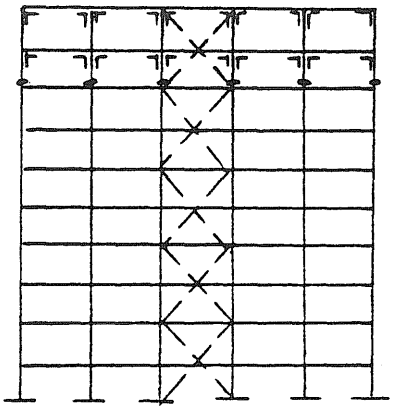

Stage 6

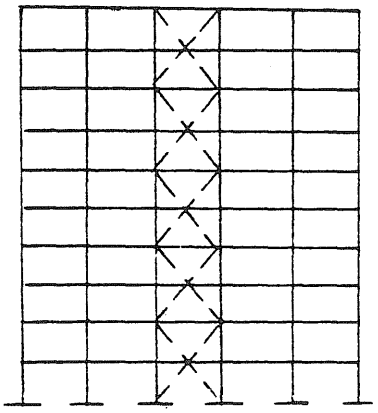

Stage 7

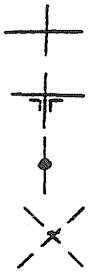

Legend:

Permanent Beam-Column Connections

Temporary Beam-Column Connections

Temporary Column Splice

Temporary Bracing

Note: All tiers are two-stories high

Fig. 6.11 Stages Selected for Reliability Analysis (Y-Y Direction)

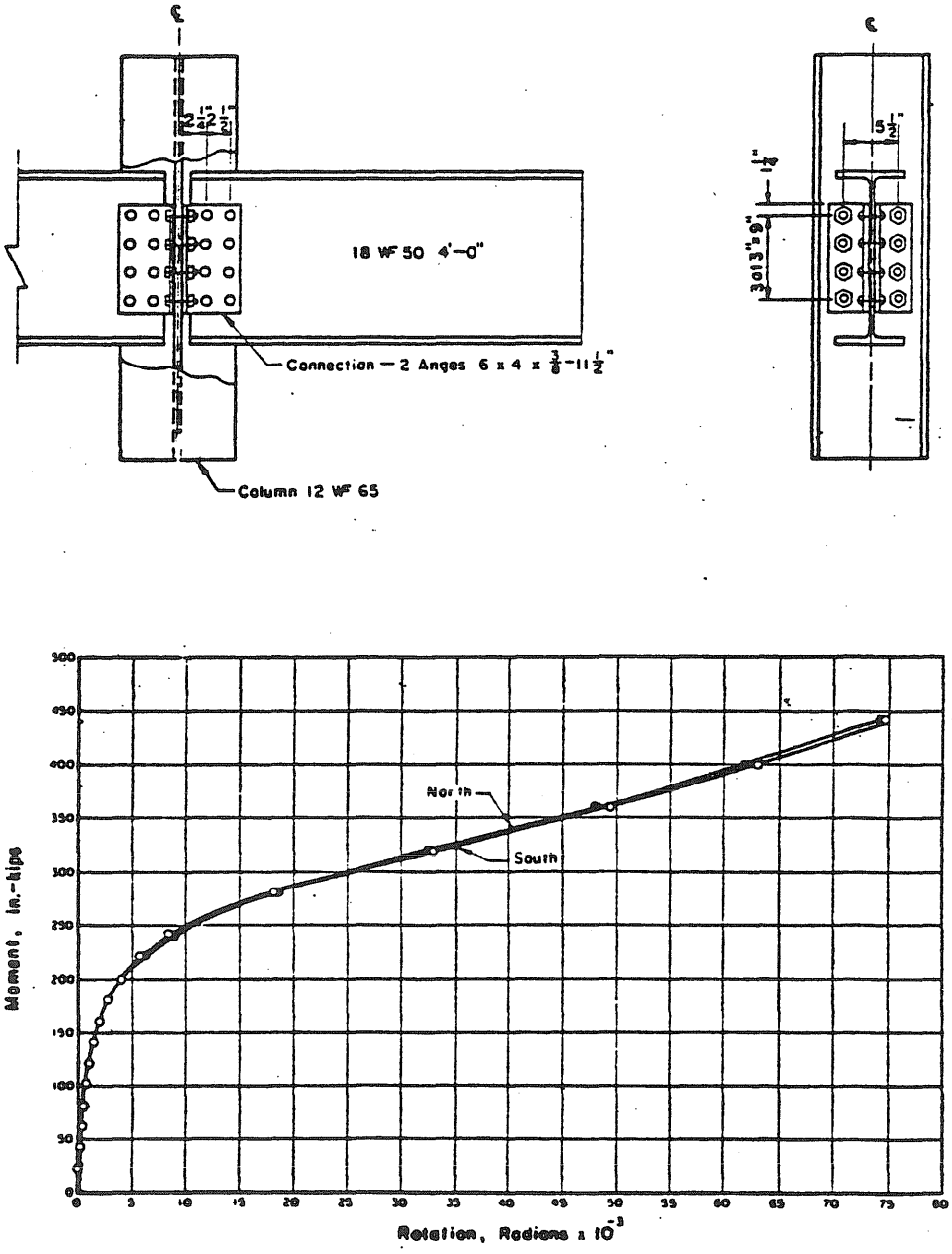

Fig. 6.12 Moment-Rotation Curve of Completed Flexible Connections in Y-Y Direction (Lewitt, 1969)

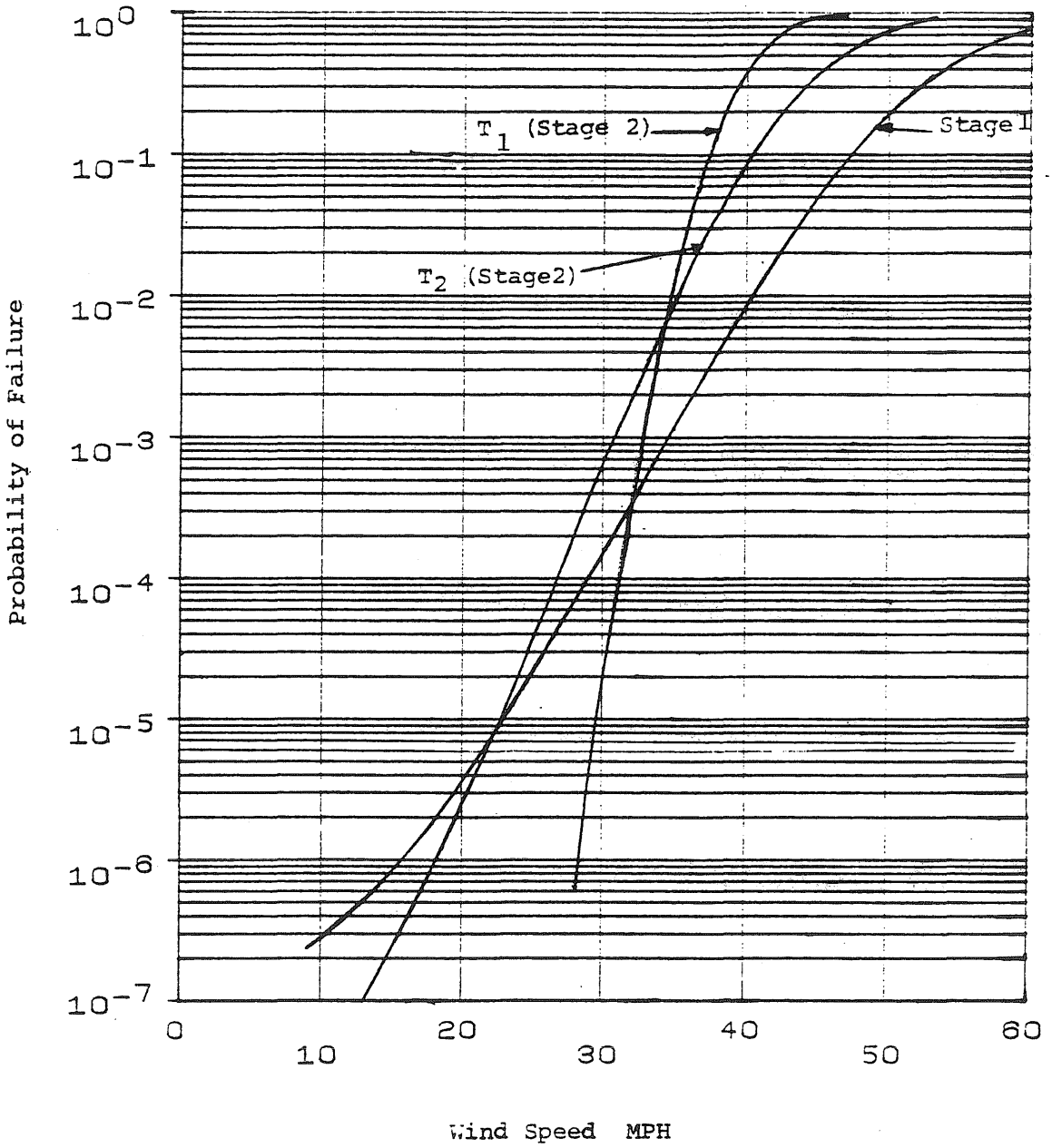

T_i = Failure of upper i tiers by yielding of connections

Fig. 6.13 Conditional Failure Probabilities; Stages 1 and 2 (Y-Y Direction)

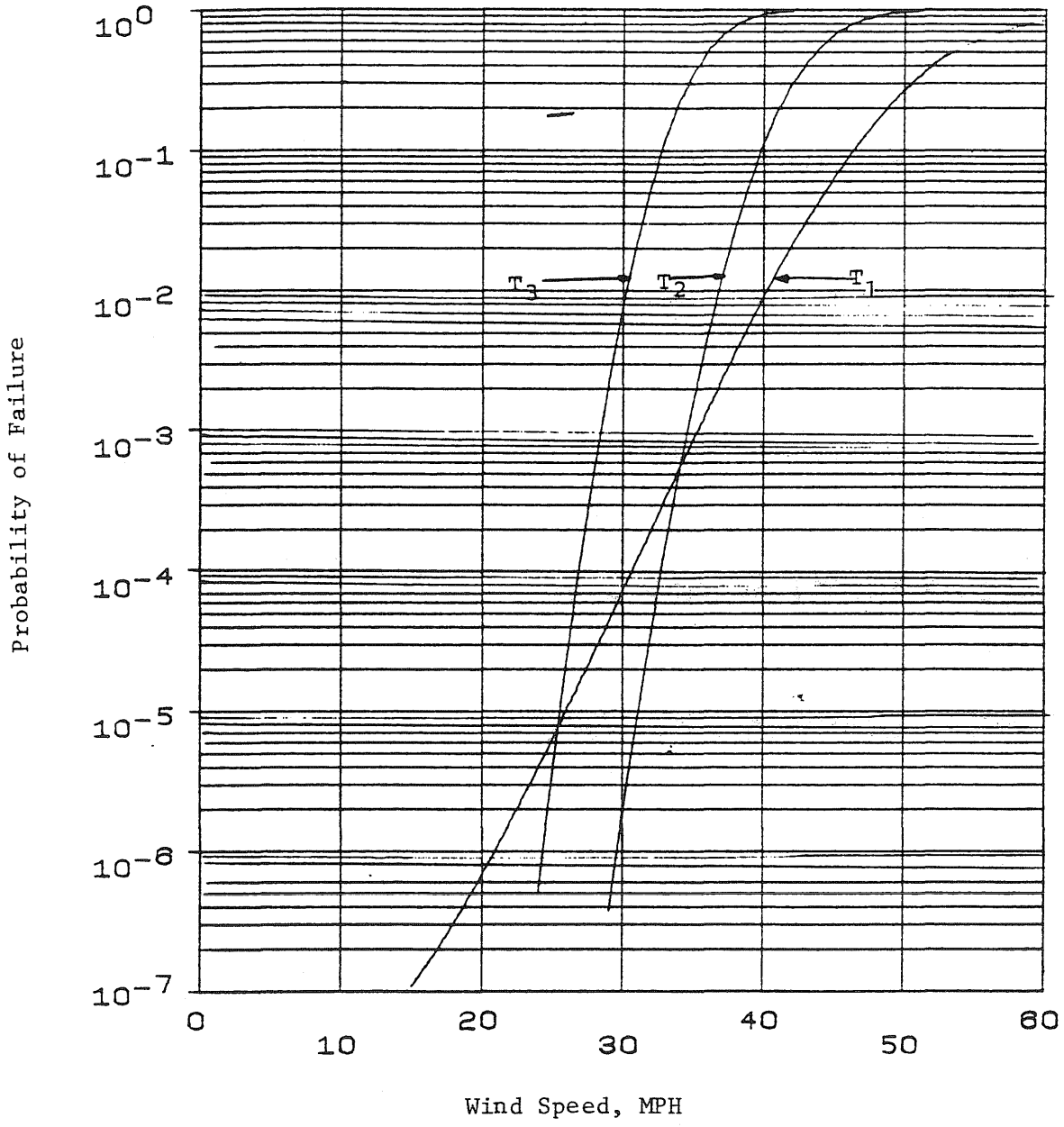

T_i Failure of upper i tiers by yielding of connections

Fig. 6.14 Conditional Failure Probabilities; Stage 3 (Y-Y Direction)

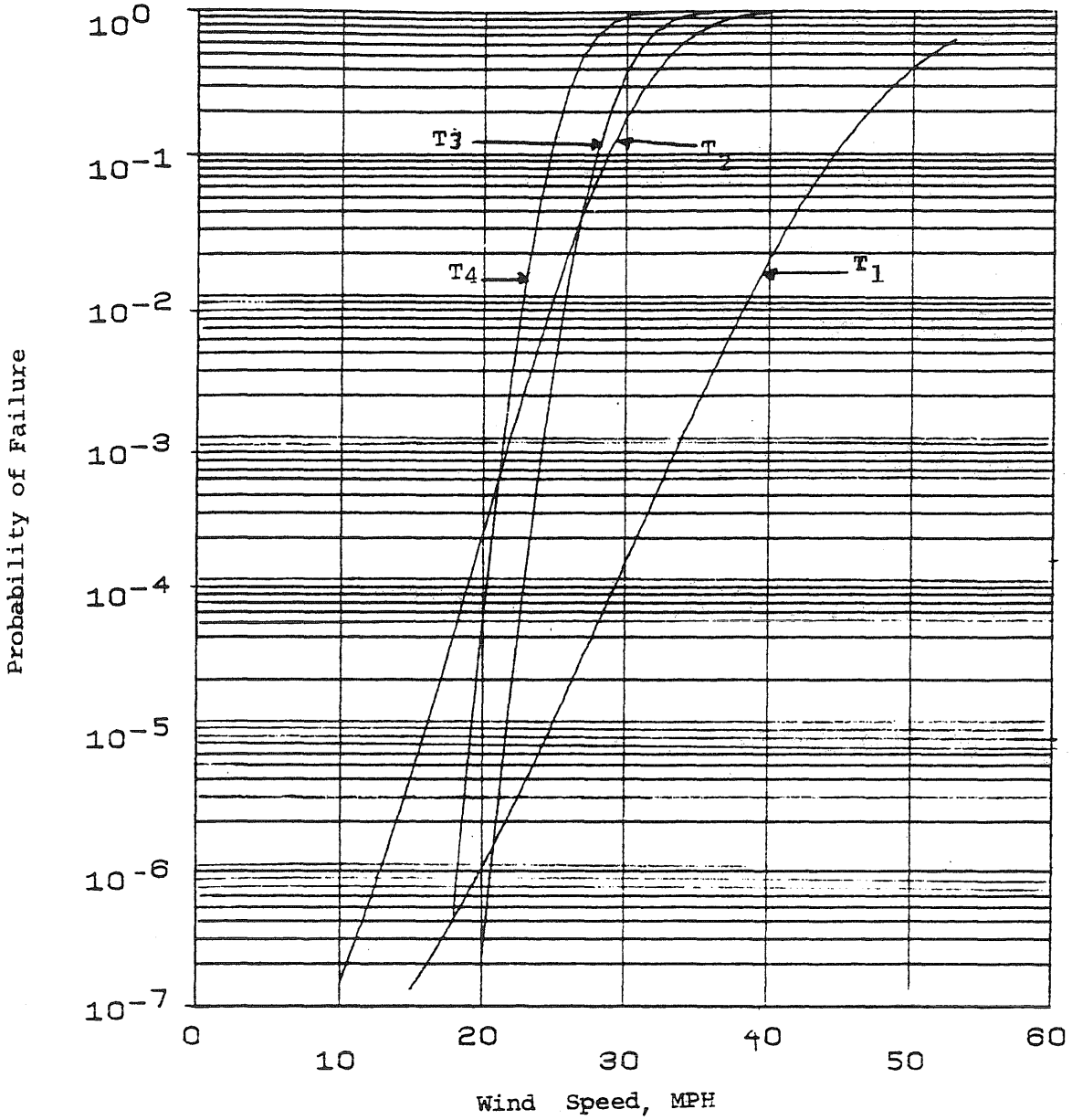

T_i = Failure of upper i tiers by yielding of connections

Fig. 6.15 Conditional Failure Probabilities; Stage 4 (Y-Y Direction)

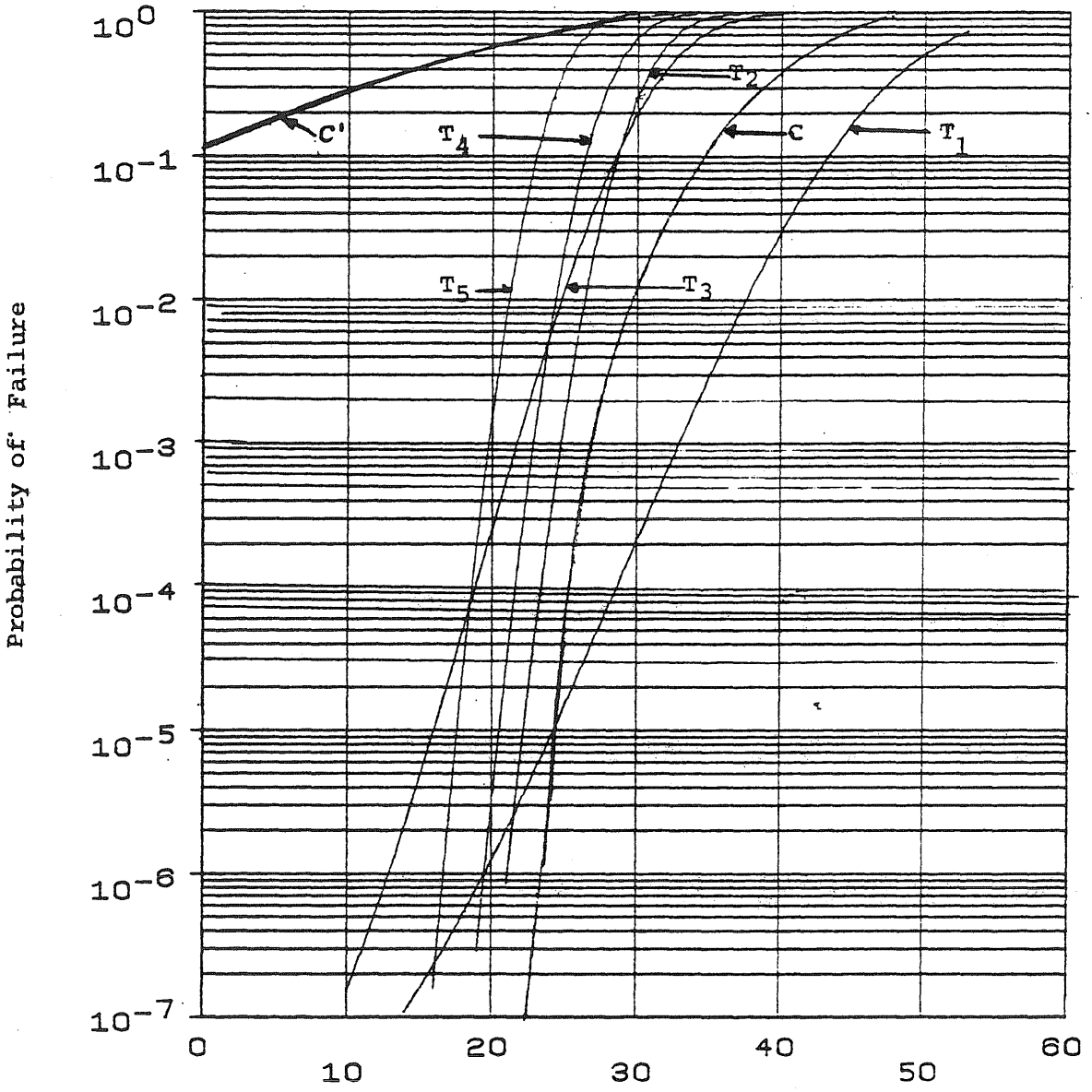

T_i = Failure of upper i tiers by yielding of connections

c = Failure of columns (instability) with stiff anchorages (see Fig. 6.2a)

C' = Failure of columns (instability) with flexible anchorages (see Fig. 6.2b)

Fig. 6.16 Conditional Failure Probabilities; Stage 5 (Y-Y Direction)

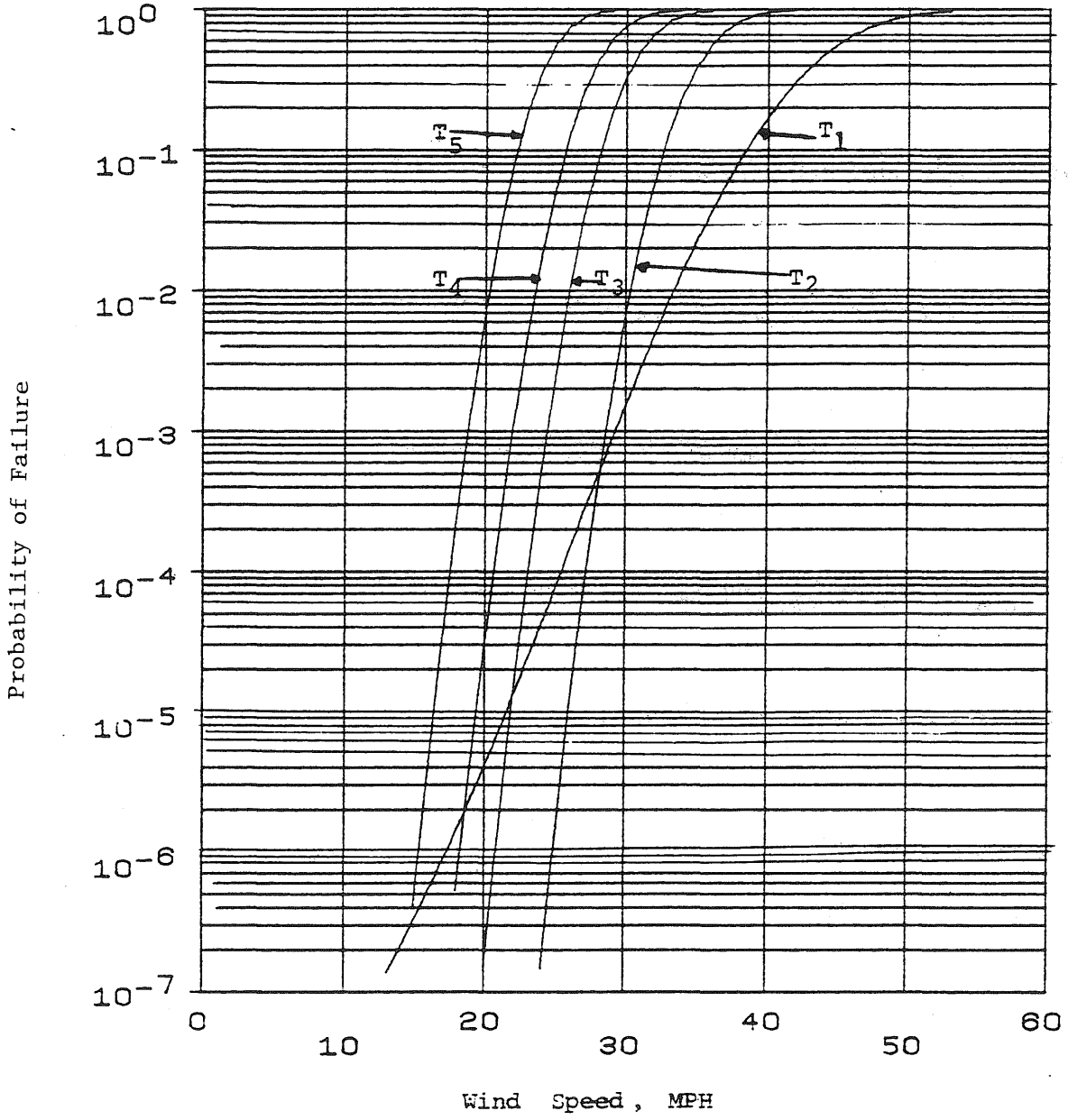

T_i = Failure of upper i tiers by yielding of connections

Fig. 6.17 Conditional Failure Probabilities; Stage 6 (Y-Y Direction)

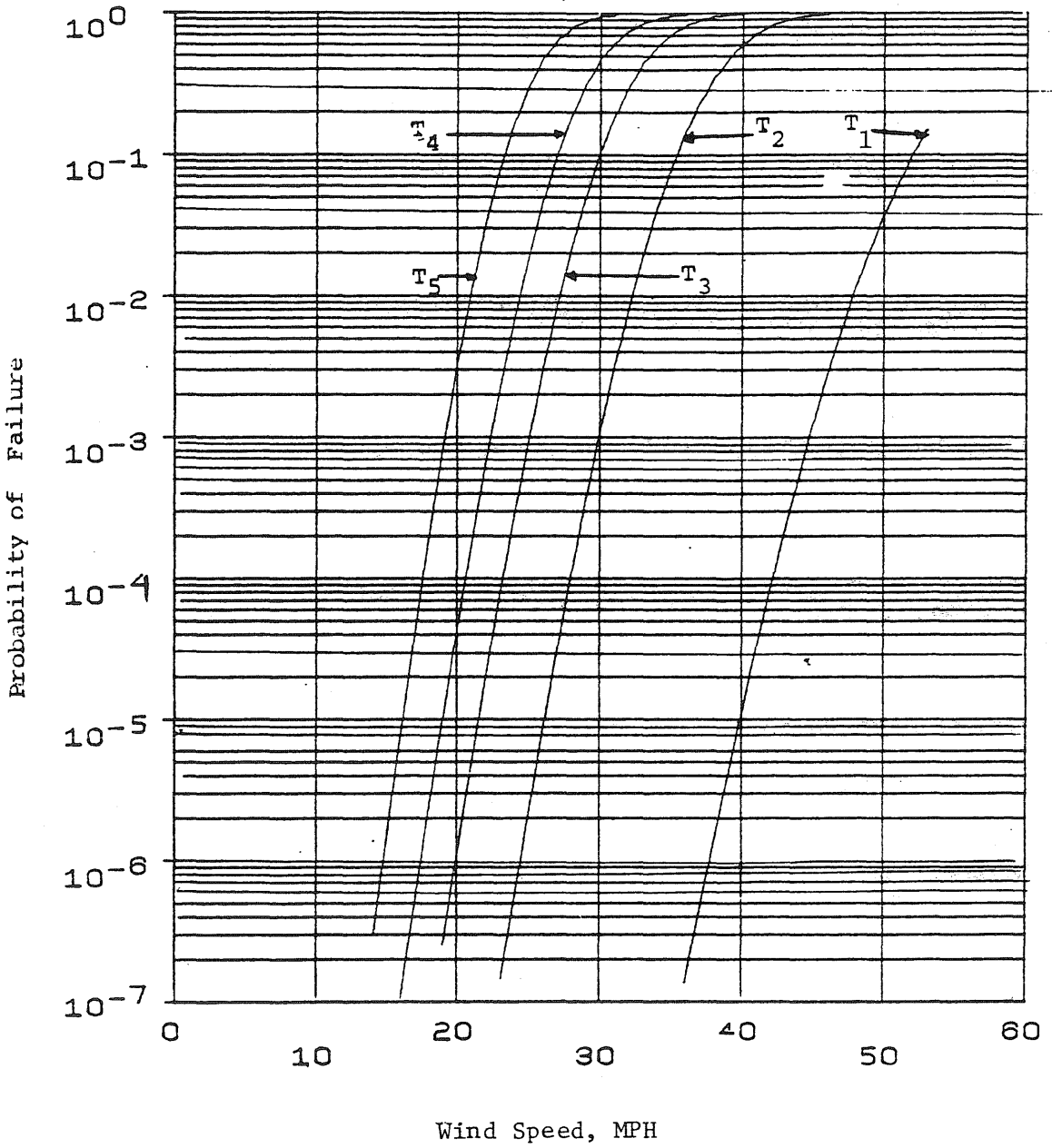

T_i = Failure of upper i tiers by yielding of connections

Fig. 6.18 Conditional Failure Probabilities; Stage 7 (Y-Y Direction)

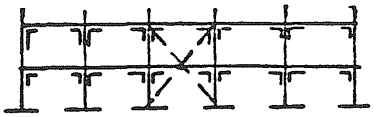

Stage 1

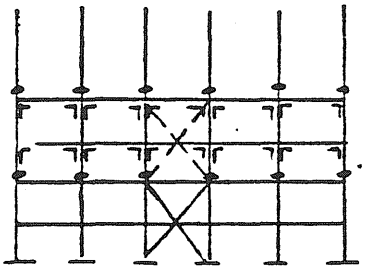

Stage 2

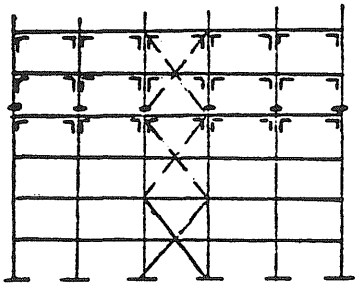

Stage 3

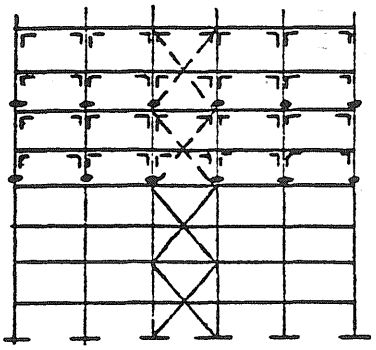

Stage 4

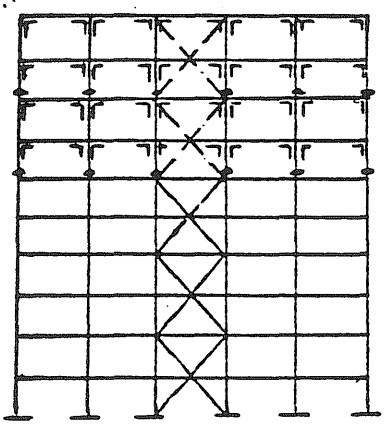

Stage 5

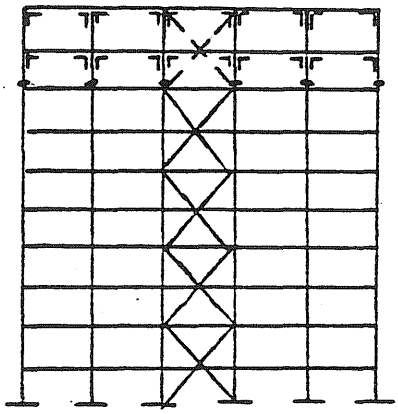

Stage 6

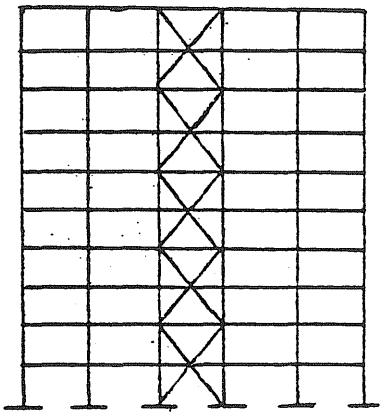

Stage 7

Legend:

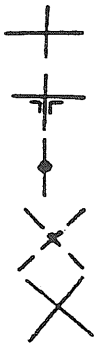

Permanent Beam-Column Connections

Temporary Beam-Column Connections

Temporary Column Splices

Temporary Bracings

Permanent X-Bracings

Note: All tiers are two-story high

Fig. 6.19 Stages Selected for Reliability Analysis (Y-Y Direction)

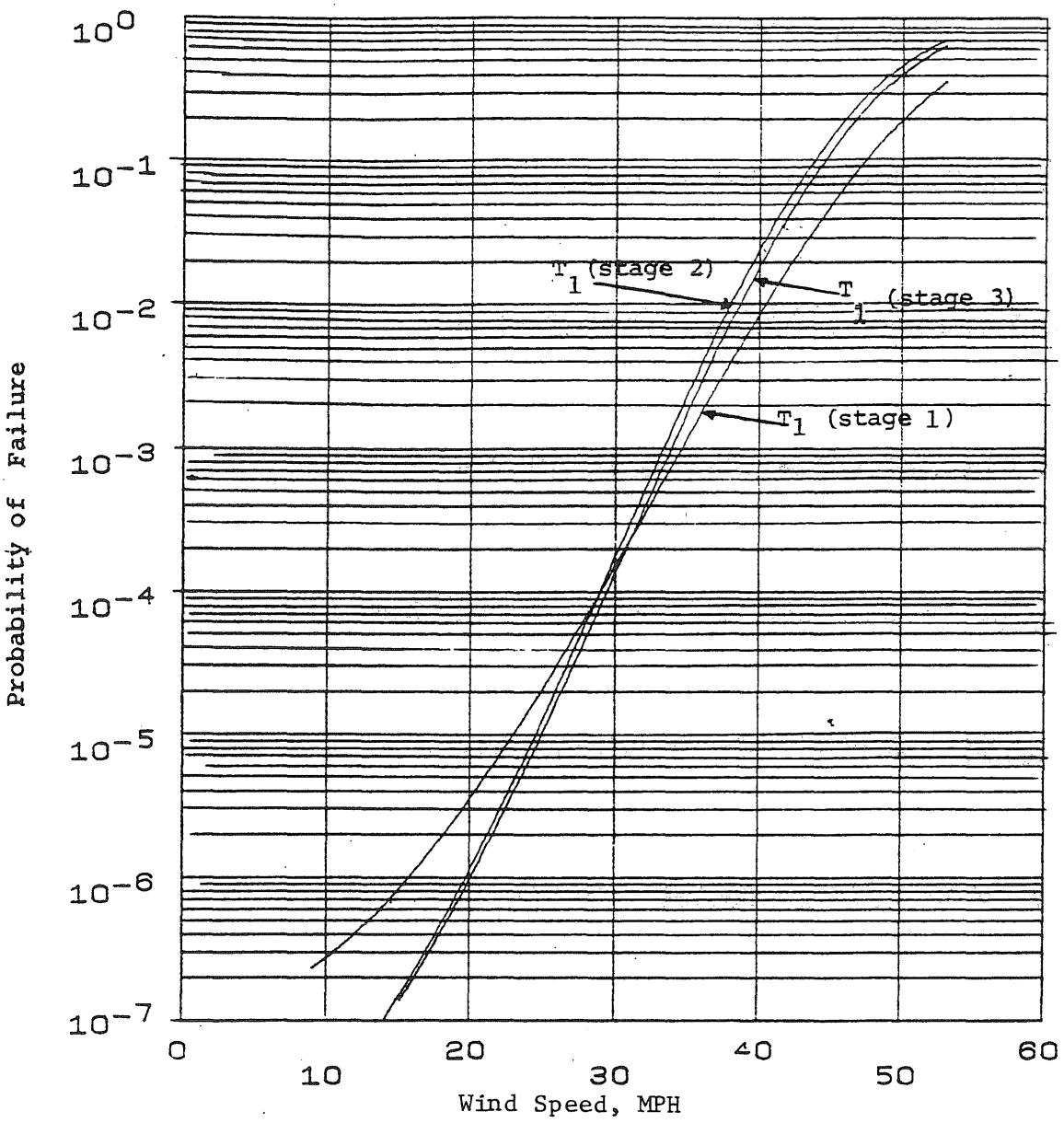

T_i = Failure of upper tiers by yielding of connections

Fig. 6.20 Conditional Failure Probabilities; Stages 1, 2 and 3 (Y-Y Direction X-Bracing)

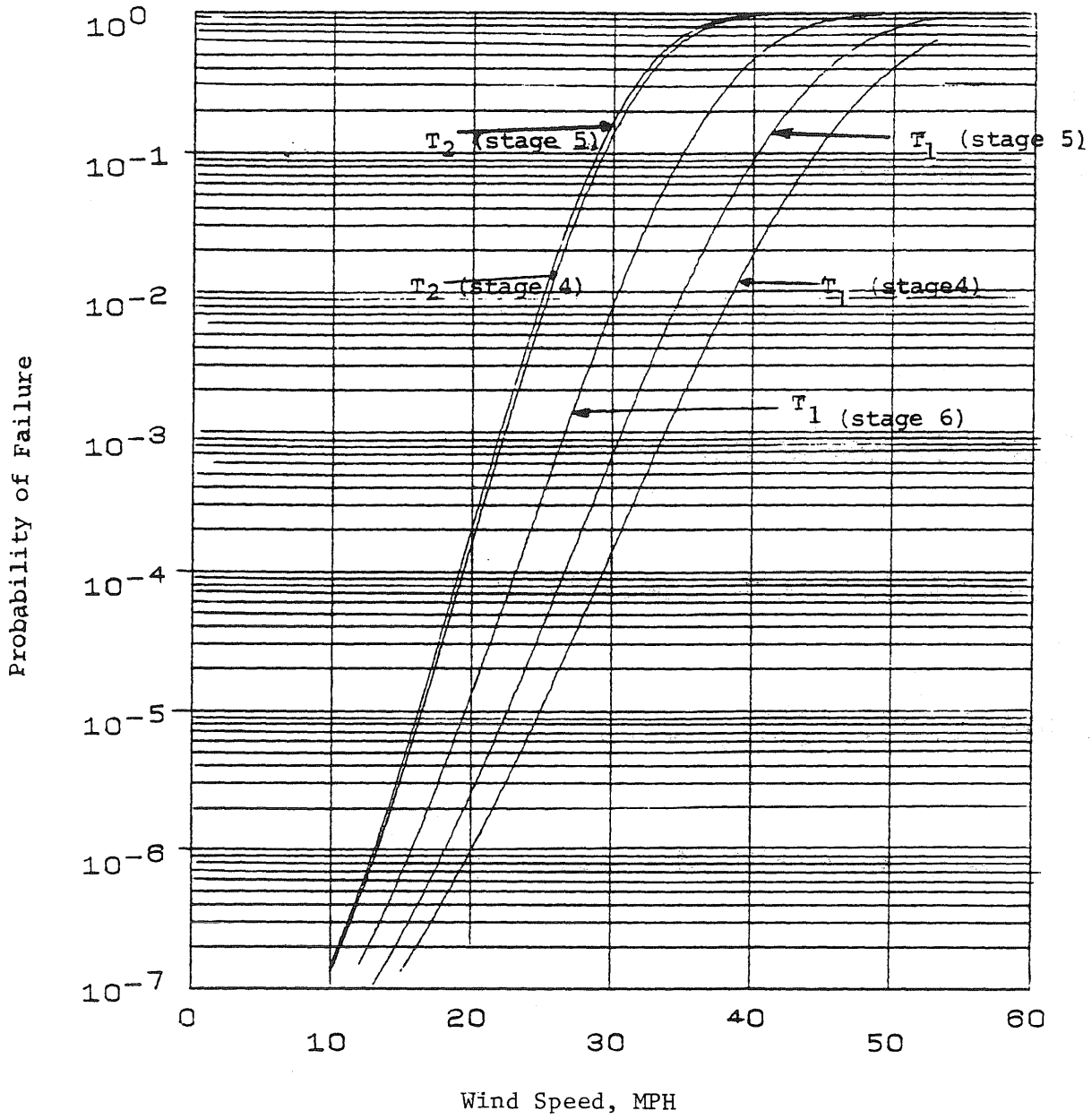

T_i = Failure of upper i tiers by yielding of connections

Fig. 6.21 Conditional Failure Probabilities; Stages 4,5, and 6 (Y-Y Direction X-Bracing)

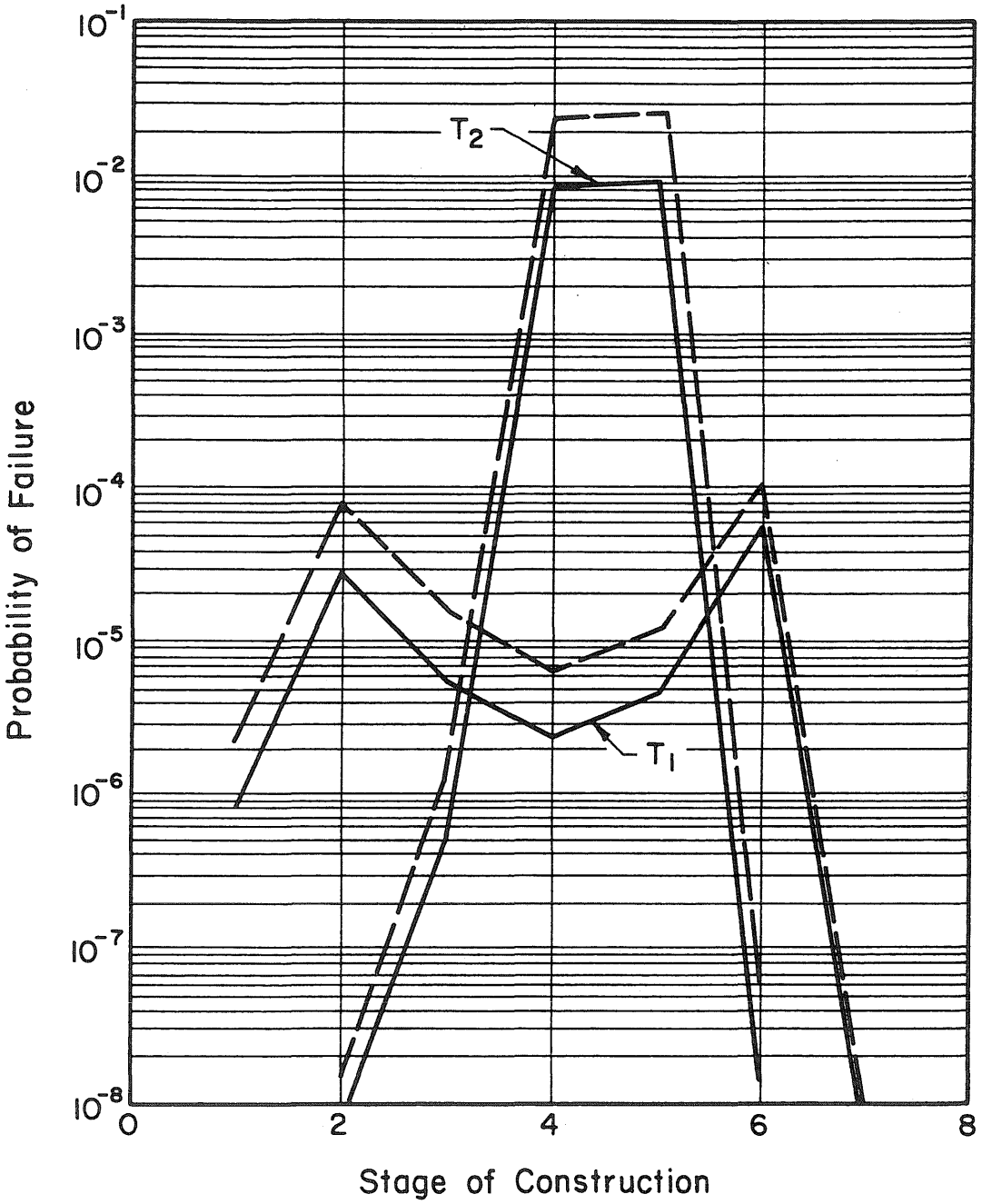

T_i = failure of upper i tiers by yielding of connections
3-day Duration
10-day Duration

Fig. 6.22 Probability of Failure During Different Stages of Construction (x-x Direction)

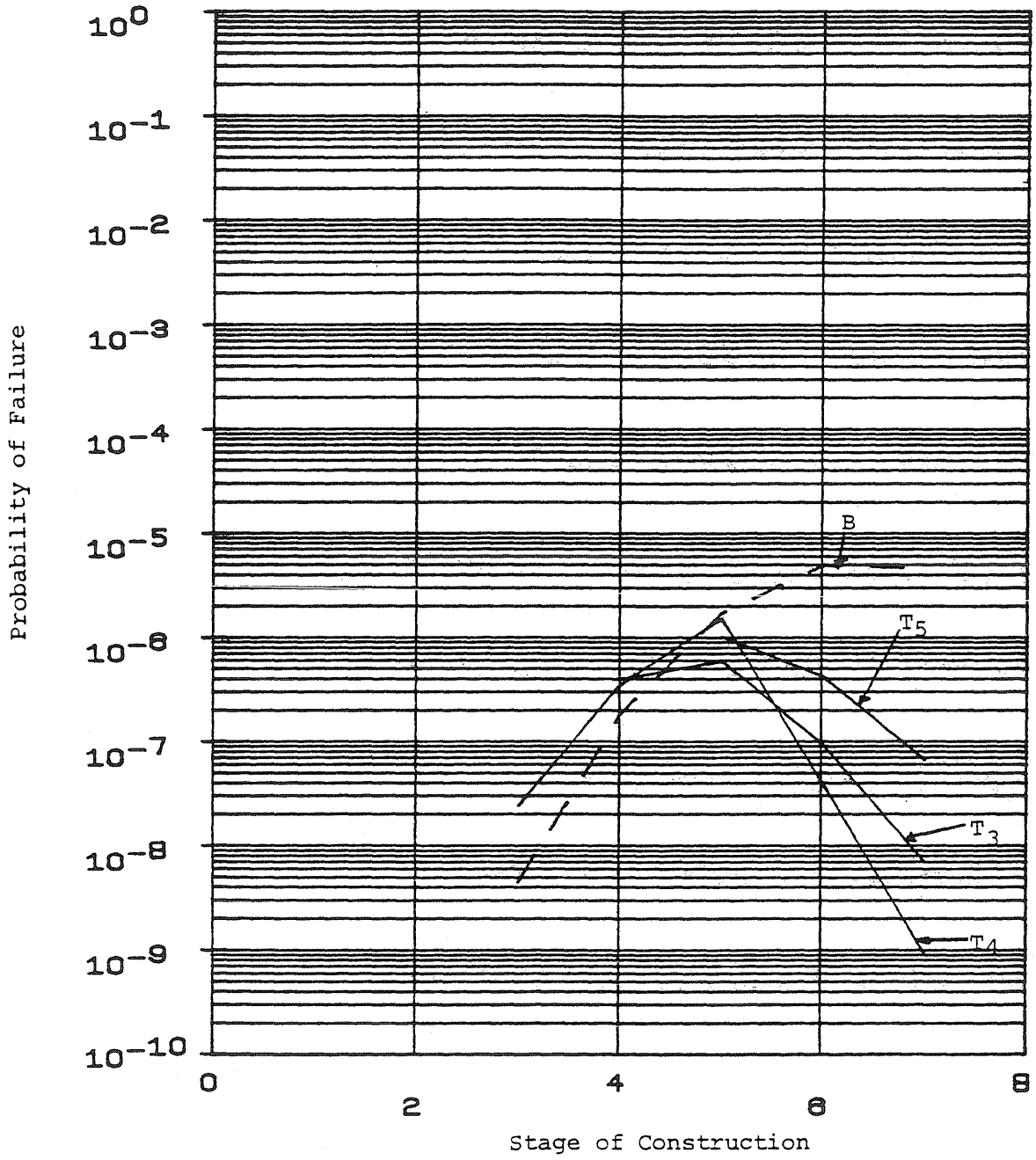

T_i = Failure of upper i tiers by yielding of connections

B = Failure of Beam (Lateral Buckling) in First Floor

Fig. 6.23 Probability of Failure During Different Stages of Construction (X-X Direction)

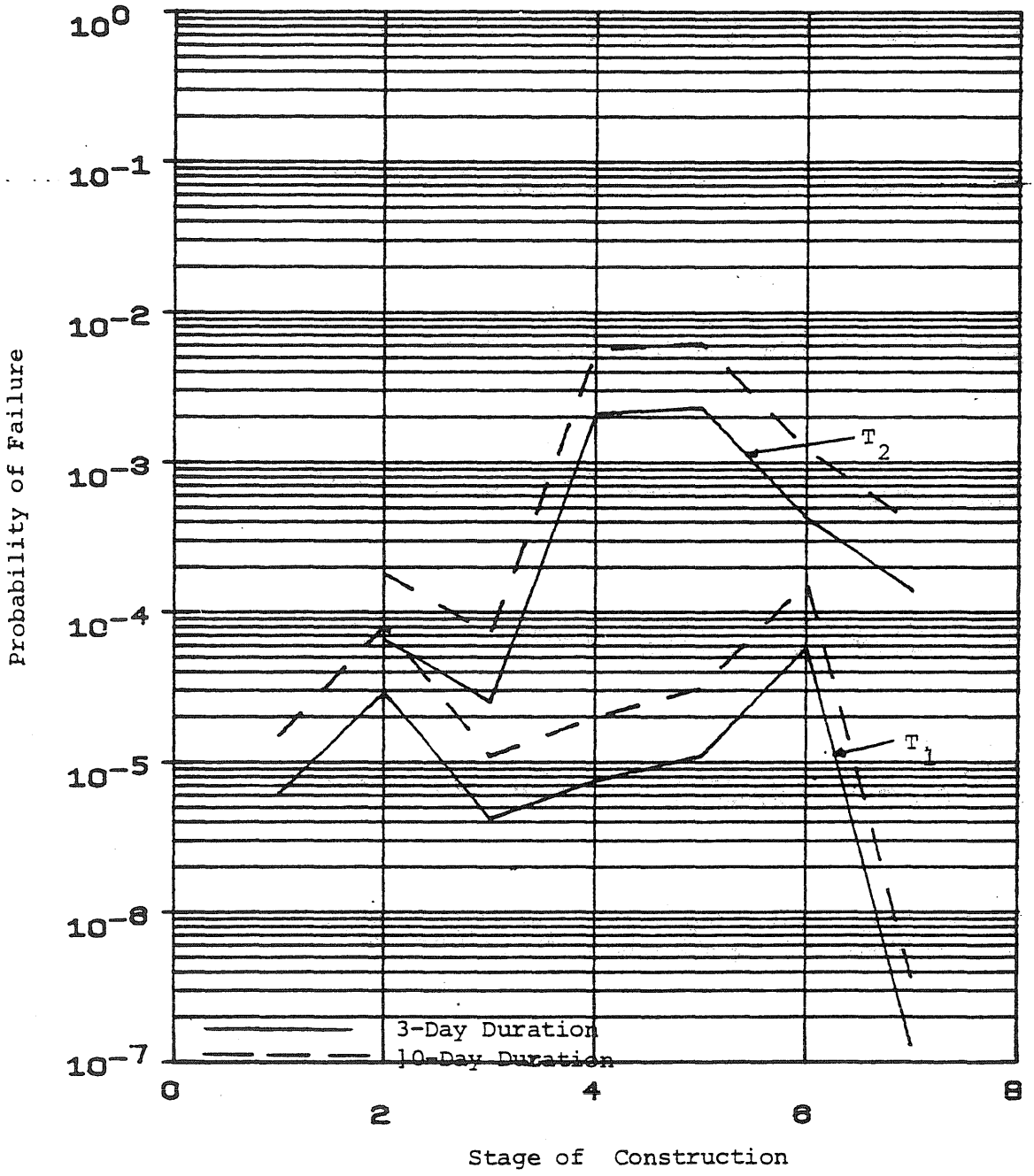

T_i = Failure of upper i tiers by yielding of connections

Fig. 6.24 Probability of Failure During Different Stages of Construction (Y-Y Direction)

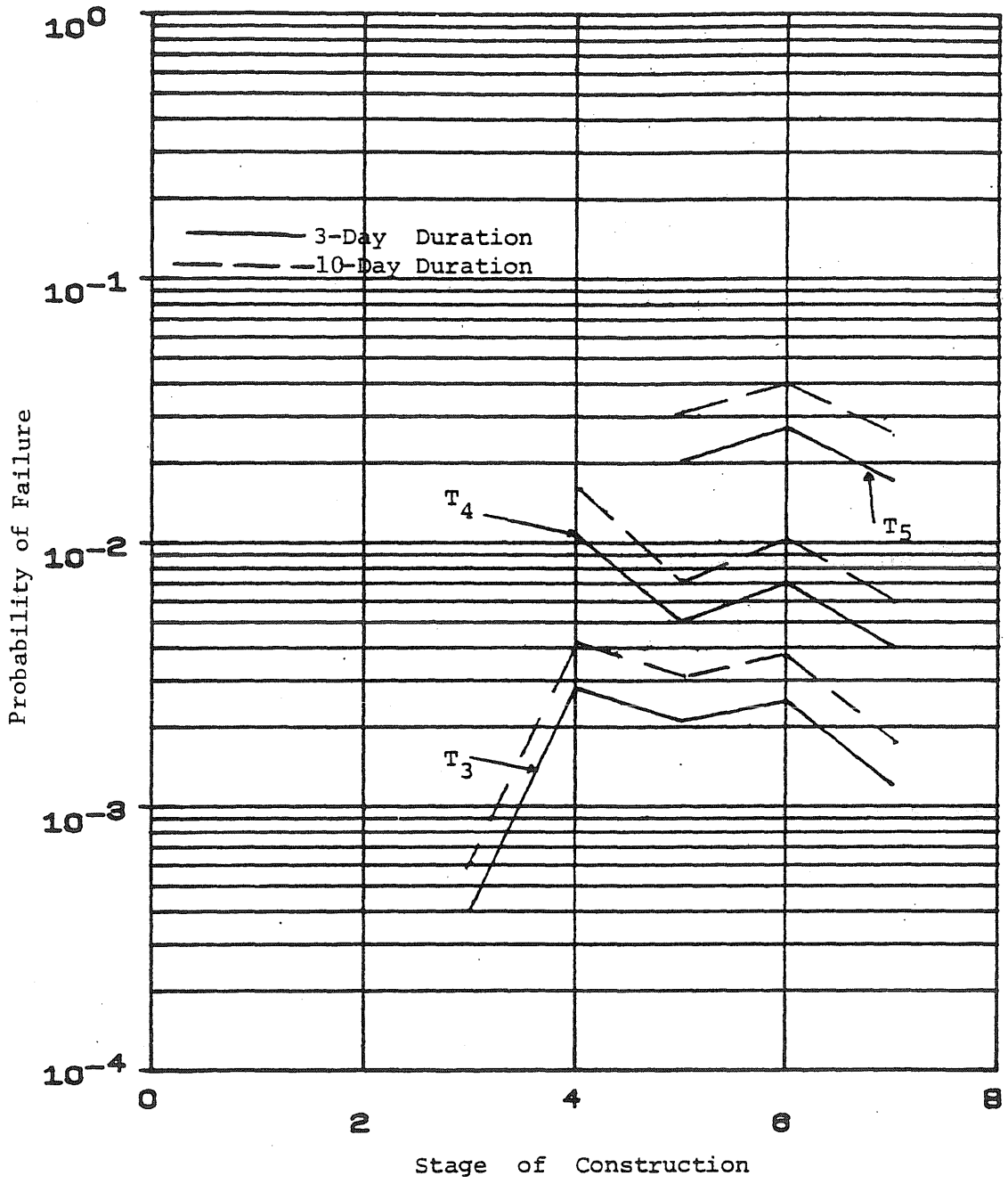

T_i = Failure of upper i tiers by yielding of connections

Fig. 6.25 Probability of Failure During Different Stages of Construction (Y-Y Direction)

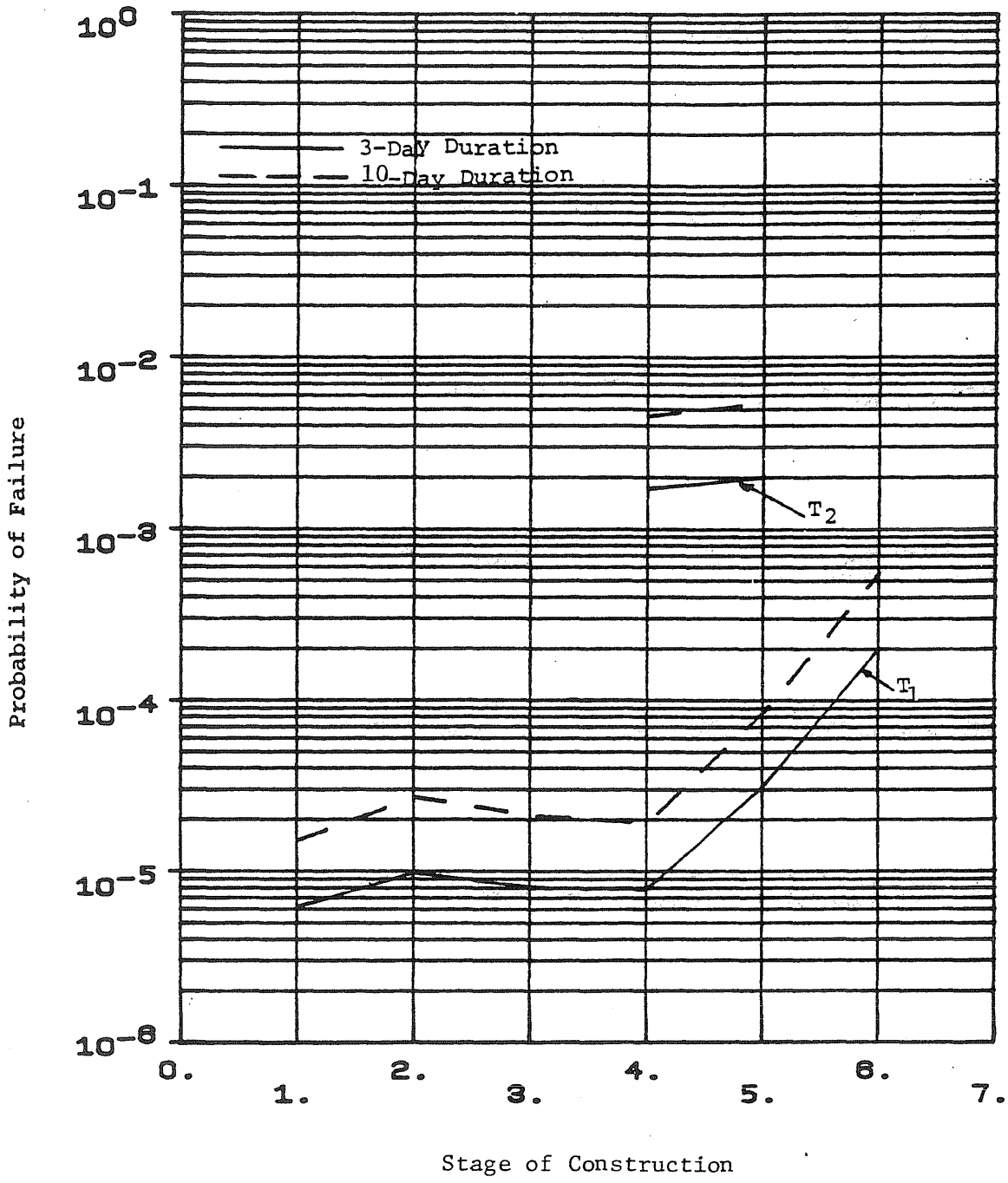

T_i = Failure of upper i tiers by yielding of connections

Fig. 6.26 Probability of Failure During Different Stages of Construction (Y-Y Direction X-Bracings)

APPENDIX A

Partial Derivatives of the Stiffness Matrix

The stiffness matrix of a structure is composed of the stiffness matrices of its members. Therefore, the partial derivative of the structure's stiffness may also be obtained from partial detivatives of the members' stiffness matrices.

The partial derivative of the stiffness matrix of a beam with two identical temporary connections at the ends (Eq. 4.1 with $r_J = r_k = r$), with respect to the connection stiffness, R_B, would be as follows;

$$\left[\frac{\partial S_M}{\partial R_B}\right] = \frac{EI}{R_B\, r^{*2}} \begin{bmatrix} \frac{4e_1}{\ell_1} & & & \\ \frac{6e_2}{\ell^2} & \frac{12e_2}{\ell^3} & & \\ \frac{2e_3}{\ell} & \frac{6e_2}{\ell^2} & \frac{4e_1}{\ell} & \\ -\frac{6}{\ell^2} & \frac{12e_2}{\ell^3} & -\frac{6e_2}{\ell^2} & \frac{12e_2}{\ell^3} \end{bmatrix} \qquad \text{(A.1)}$$

where:

$$e_1 = 36r^3 + 24r^2 + 5r$$
$$e_2 = 6r(2r + 1)^2$$
$$e_3 = 24r^2 + 8r$$

The derivative of the column stiffness matrix with respect to R_B is 0. The above matrices comprise the partial derivative of the sitffness matrix of the structure with respect to R_B.

The derivative of the stiffness matrix of a temporarily connected beam with respect to the beam stiffness, EI_B, would would be;

$$\left[\frac{\partial S_{MB}}{\partial EI_B}\right] = \frac{1}{r^2}\begin{bmatrix} \frac{4e_4}{\ell} & & & \\ \frac{6e_5}{\ell^2} & \frac{12e_5}{\ell^3} & & \\ \frac{2e_6}{\ell} & \frac{6e_5}{\ell^2} & \frac{4e_4}{\ell} & \\ \frac{-6e_5}{\ell^2} & \frac{-12e_5}{\ell^3} & \frac{6e_5}{\ell^2} & \frac{12e_5}{\ell^3} \end{bmatrix}$$

where: $e_4 = 12r^2 + 6r + 1$

$e_5 = (2r+1)^2$

$e_6 = -12r+1$

The derivative of the stiffness of a column with respect to the member stiffness would be; $\left[\frac{\partial S_{Mc}}{\partial EI_c}\right] = \frac{1}{EI_c}\left[S_{MC}\right]$

$\left[\frac{\partial K_s}{\partial EI}\right]$ may be obtained from the above matrices.

APPENDIX B

Partial Derivatives of the Maximum Wind Load Effect

The mean value of the maximum dynamic wind load effect a member is given by:

$$\bar{S}_{D_m} = \left(\sqrt{2\ell n\ \bar{\nu}_s t} + \frac{0.577}{\sqrt{2\ell n \bar{\nu}_s t}} \right) \bar{\sigma}_{SD} \qquad (B.1)$$

where $\bar{\nu}_s = \frac{1}{2\pi} \frac{\dot{\bar{\sigma}}_{S_D}}{\bar{\sigma}_{S_D}}$. S_{D_M} is a function of the fundamental natural frequency, n_o , damping ratio, β , and wind environment parameters, α, k_d, and C_d , as defined in Chapter 4. The derivative of Eq. B.1 with respect to the above variables is as follows (Rojiani, 1978),

$$\frac{\partial S_{D_m}}{\partial x_i} = \frac{1}{2} \left[\frac{1}{\bar{\sigma}^2_{S_D}} \left(\bar{S}_{D_m} - \frac{\dot{\bar{\sigma}}^2_{S_D}}{\bar{S}_{D_m}} \right) \frac{\partial \sigma^2_{S_D}}{\partial x_i^2} + \frac{1}{S_{D_m}} \frac{\partial \sigma^2_{\dot{S}_D}}{\partial x_i^2} \right] \qquad (B.2)$$

where: $$\sigma^2_{SD} = \frac{f^{*2}_{\omega}}{(2\pi n_o)^4 M^{*2}} \int_0^{\infty} c^2(n)\ S_v(n) |H(n)|^2 dn \qquad (B.3)$$

$$\sigma^2_{\dot{S}D} = \frac{f^{*2}_{\omega}}{(2\pi n_o)^4 M^{*2}} \int_0^{\infty} (2\pi n)^2 c^2(n) S_v(n) |H(n)|^2 dn \qquad (B.4)$$

The above integrals may be simplified as follows;

$$\sigma_{SD} = \frac{f_\omega^*}{(2\pi n_o)^2 M^*} \left[\frac{\pi n_o c^2(n_o) S_v(n_o)}{4\beta} + \int_o^\infty c^2(n) S_v(n) dn \right]^{1/2} \tag{B.5}$$

$$\sigma_{\dot{S}D} = \frac{f_\omega^*}{(2\pi n_o)^2 M^*} \left[c^2(n_o) S_v(n_o) \frac{\pi n_o}{4\beta} \right]^{1/2} \tag{B.6}$$

The power spectrum of the along-wind fluctuatinos $S_v(n)$ for a given wind velocity is given by;

$$S_v(n) = \frac{4K_d v^2 x^2}{n(1+x^2)^{4/3}} \quad ; \quad x = \frac{4000n}{v} \tag{B.7}$$

$$\frac{\partial \sigma_{SD}}{\partial \rho} = \frac{\sigma_{SD}}{\rho}$$

$$\frac{\partial \sigma_{\dot{S}D}}{\partial \rho} = \frac{\sigma_{\dot{S}D}}{\rho}$$

$$\frac{\partial \sigma_{SD}}{\partial \alpha} = \sigma_{SD} \frac{\sum_{i=1}^{n} \left(\frac{z_i}{30}\right)^\alpha \ell n\left(\frac{z_i}{30}\right)}{\sum_{i=1}^{n} \left(\frac{z_i}{30}\right)^\alpha}$$

$$\frac{\partial \sigma_{\dot{S}D}}{\partial \alpha} = \sigma_{\dot{S}D} \frac{\sum_{i=1}^{n} \left(\frac{z_i}{30}\right)^\alpha \ell n\left(\frac{z_i}{30}\right)}{\sum_{i=1}^{n} \left(\frac{z_i}{30}\right)^\alpha}$$

$$\frac{\partial \sigma_{SD}}{\partial K_d} = \frac{\sigma_{SD}}{K_d}$$

$$\frac{\partial \sigma_{\dot{S}D}}{\partial K_d} = \frac{\sigma_{\dot{S}D}}{K_d}$$

$$\frac{\partial \sigma_{SD}}{\partial \beta} = - \frac{f_\omega^{*2}\ \pi n_o c^2(n_o) S_v(n_o)}{8(2\pi n_o)^4\ \beta^2 M^{*2}.\delta_{SD}}$$

$$\frac{\partial \sigma_{\dot{S}D}}{\partial \beta} = - \frac{f_w^{*2}\pi\ S_v(n_o) c^2(n_o) n_o}{8(2\pi n_o)^4\ \beta^2 M^{*2} \delta_{\dot{S}D}}$$

$$\frac{\partial \sigma_{SD}}{\partial n_o} = - \frac{4 f_\omega^{*2}}{(2\pi n_o)^4 . n_o . M^{*2}} \int_o^\infty C^2(n) S_v(n) |H(n)|^2 dn +$$

$$+ \frac{f_\omega^{*2}}{(2\pi n_o)^4 M^{*2}} \int_o^\infty C^2(n) S_v(n) \frac{\partial}{\partial n_o} |H(n)|^2 dn$$

$$\frac{\partial \sigma_{\dot{S}D}}{\partial n_o} = - \frac{4 f_\omega^{*2}}{(2\pi n_o)^4 n_o M^{*2}} \int_o^\infty C^2(n) S_v(n) |H(n)|^2 dn +$$

$$+ \frac{f_\omega^{*2}}{(2\pi n_o)^4 M^{*2}} \int_o^\infty (2\pi n)^2 C^2(n) S_v(n) \frac{\partial}{\partial n_o} |H(n)|^2 dn$$

APPENDIX C

Statistics of Column Stability Relations

By second order approximation, the c.o.v. of z_s may be evaluated through Eq. 5.1 , yielding the following:

$$\delta^2_{z_1} = D_1^2\,\delta^2_{fa} + D_2^2\,\delta^2_{Fy} + D_3^2\,\delta^2_{F_y} + D_4^2\,\delta^2_{\lambda} + D_5^2\,\delta^2_{E} + \delta^2_{N_S}$$

Where D_i are defined as follows;

$$D_1 = \frac{\bar{N}_s}{z_s}\left[\frac{\bar{f}_a}{\bar{F}_a} - \frac{B.f_b}{\sum_i f_{ai} + \sum F'_{ei}}\right]$$

$$D_2 = \frac{\bar{N}_s}{\bar{z}_s}\,\bar{B}$$

$$D_3 = -\frac{\bar{N}_s}{\bar{z}}\left[\frac{\bar{f}_a(2\bar{F}_a-\bar{F}_y)}{\bar{F}_a^2} + \bar{B}\right]$$

$$D_4 = -\frac{\bar{N}_s}{\bar{z}}\left[\frac{\bar{f}_a\,\bar{F}_y^2\,\bar{\lambda}^2}{2\pi^2\bar{E}\,\bar{F}_a^2} + \frac{2\bar{B}\sum_i \bar{f}_{ai}}{\sum_i \bar{F}_{ai} + \sum_i \bar{f}_{ec}}\right]$$

$$D_5 = \frac{\bar{N}_s}{\bar{z}}\quad\frac{\bar{f}_a\,\bar{F}_y^2\,\bar{\lambda}^2}{4\pi^2\,E\,F_a^2} + \frac{B\sum \bar{f}_{ai}}{\sum \bar{f}_{ai} + \sum \bar{F}'_{ec}}$$

and;
$$\bar{B} = \frac{C_m \bar{f}_b}{\bar{F}_b(1 + \sum \bar{f}_{ai}/\sum F'_{ei})}$$

the covariance of z_s and z_p is,

$$Cov(z_s,z_p) = c_1^2 \ var(f_b) + c_2^2 \ var(F_y)$$

Where c_1 and c_2 are;

$$c_1 = \frac{\bar{N}_s}{\bar{f}_b} \ \bar{B}$$

$$c_2 = \bar{N}_s \ \frac{\bar{f}_a \ (2\bar{F}_a - \bar{F}_y)}{\bar{F}_a^2 \ \bar{F}_y} + \frac{\bar{B}}{\bar{F}_y}$$

the C.O.V. of the effective length coefficient, K , is given by the following relation;

$$\delta_K^2 = c_1' \ \delta_{r1}^2 + c_2' \ \delta_{r2}^2$$

where,

$$c_1' = \frac{r_1(\pi/K + r_2 \tan \pi/K)}{c}$$

$$c_2' = \frac{r_2(\pi/K + r_1 \tan \pi/K)}{c}$$

and, $$c = \frac{\pi}{K} \tan^2 \frac{\pi}{K} (r_1 r_2 - \frac{\pi^2}{K^2}) - \frac{2\pi^2}{K^2} \tan \frac{\pi}{K} +$$

$$+ \frac{\pi}{K}(r_1 + r_2 + r_1 r_2 - \frac{\pi^2}{K^2})$$

APPENDIX D

Rotational Restraint of a Column at a Joint

The equivalent rotational restraint of beams and columns at a joint may be evaluated on the assumption that all columns in a frame buckle simultaneously.

Consider a joint in a frame as shown in Fig. D.1. The axial compression in the beams is negligible; therefore, the slope-deflection equations for the moments on the beams at joint i become;

$$M_{b1}=K_{b1} \cdot \theta + K_{b1} \cdot COF_1 \cdot \theta \qquad (D.1)$$

$$B_{b2} = K_{b2} \cdot \theta + K_{b2} \cdot COF_2 \cdot \theta \qquad (D.2)$$

where K_{b1} and COF_1 are the stiffness and carry-over factor for beam 1, respectively.

The stiffness can carry-over factor of a beam with elastic restraints is given by (Gere, 1963);

$$K_{b12} = \frac{4EI_b}{\ell_b} \cdot \frac{1 + 3J_1}{1+4(J_1+3J_1J_2+J_2)} \qquad (D.3)$$

$$COF_{12} = \frac{1}{2(1+3J_2)} \qquad (D.4)$$

where, $J_i = \frac{EI_b}{\ell_b R_i}$ is the joint factor of end i of the beam. Substituting the beam stiffness and COFs in Eqs. D1 and D2, and assuming identical end restraints for the beam, Eqs. D1 and D2 become;

$$M_{b1} = \frac{6EI_{b1}}{\ell_{b1}} \quad \frac{1}{1+6J_1}\theta \tag{D.5}$$

and, $$M_{b2} = \frac{6EI_{b2}}{\ell_{b2}} \quad \frac{1}{1+6J_i}\theta \tag{D.6}$$

The total beam moment at joint i would be;

$$M_{bt} = \sum_{i=1}^{2} \frac{6EI_{bi}}{\ell_{bi}} \quad \left(\frac{1}{1+6J_i}\right)\theta \tag{D.7}$$

Assuming that the restraining moments exerted by the beams at a joint, when the columns begin to buckle, are distributed to the columns at that joint in proportion to the columns' stiffnesses, $\frac{EI_c}{\ell_c}$, the moment in clumn 1 at joint i would be;

$$M_{c_1} = \frac{EIc1}{\ell_{c1}} M_{ct} / \sum_{i=1}^{2} \frac{EI_{c1}}{\ell_{c1}} \tag{D.8}$$

where M_{ct} is the sum of the moments at joint i on the columns. Since $M_{ct} = -M_{bt}$, from Eqs. D7 and D8;

$$M_{c1} = -\frac{6EI_{c1}}{\ell_{c1}} \left[\sum_{i=1}^{2} \frac{EI_{bi}}{\ell_{bi}} \left(\frac{1}{1+6J_i}\right)\theta\right] / \sum_{i=1}^{2} \frac{EI_{ci}}{\ell_{ci}} \tag{D.9}$$

$$R_E = \frac{-M_{c1}}{\theta} = \frac{6EI_{c1}}{\ell_{c1}} \left[\sum_{i=1}^{2} \frac{EI_{bi}}{\ell_{bi}} \quad \frac{1}{1+6J_i}\right] / \sum_{i=1}^{2} \frac{EI_{ci}}{\ell_{ci}} \tag{D.10}$$

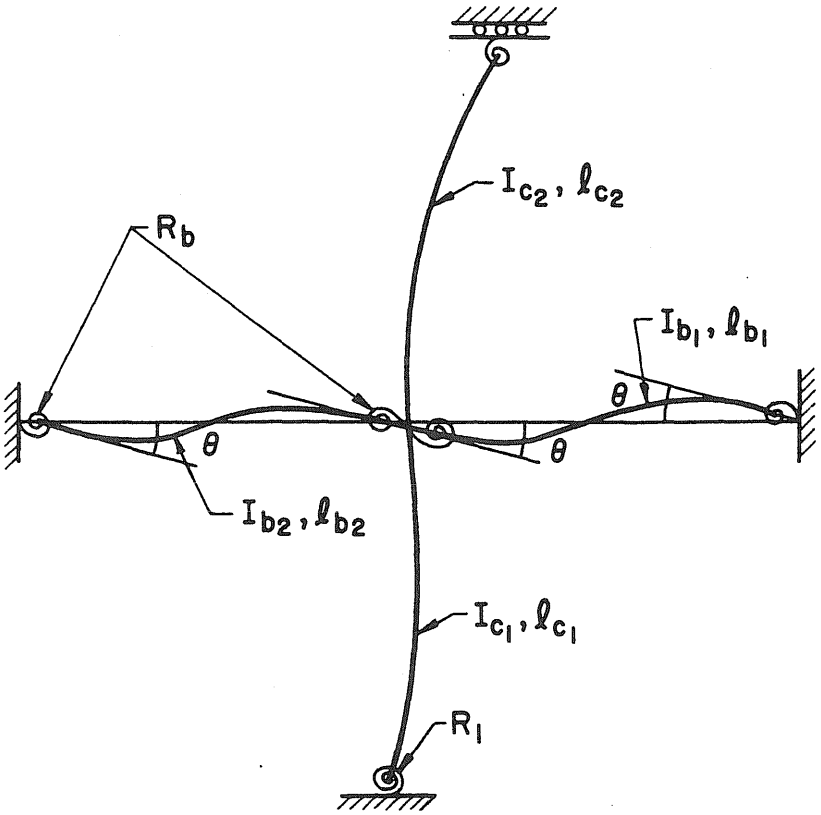

Fig. D.1 Model Used for Calculation of the Effective Length Factor of a Column

APPENDIX E

Statistics of Column Anchorage Strength

The strength of a column anchorage is the minimum of the two random variables M_{R_1} and M_{R_2} as defined in Chapter 5, with corresponding PDF's;

$$f_{M_{R_1}}(r_1) = \frac{1}{\sqrt{2\pi}\,\zeta_1 r_1} \exp\left[-\frac{1}{2}\left(\frac{\ell n r_1 - \lambda_1}{\zeta_1}\right)^2\right] \tag{E.1}$$

$$f_{11_{R_2}}(r_2) = \frac{1}{\sqrt{2\pi}\,\zeta_2 r_2} \exp\left[-\frac{1}{2}\left(\frac{\ell n r_2 - \lambda_2}{\zeta_2}\right)^2\right] \tag{E.2}$$

In order to obtain the cumulative distribution function of M_{R_i}, $F_{M_{R_i}}(r)$, it is necessary to integrate the joint probability density function of M_{R_1} and M_{R_2} over the region where the minimum of M_{R_1} and M_{R_2} are less than r.

$$\begin{aligned} F_{M_{R_i}}(r) &= P(M_{R_i} \leq r) = P[\text{Min.}(M_{R_1}, M_{R_2}) \leq r] \\ &= 1 - \int_r^\infty \int_r^\infty f_{M_{R_1}}(r_1)\cdot f_{M_{R_2}}(r_2)\, dr_1 dr_2 \\ &= F_{M_{R_1}}(r) + F_{M_{R_2}}(r) - F_{M_{R_1}}(r)\cdot F_{M_{R_2}}(r) \end{aligned} \tag{E.3}$$

The probability density function of M_{R_i}, therefore, is

$$\begin{aligned} f_{M_{R_i}}(r) = {} & f_{M_{R_1}}(r) + f_{M_{R_2}}(r) - f_{M_{R_1}}(r) F_{M_{R_2}}(r) - \\ & F_{M_{R_1}}(r) f_{M_{R_2}}(r) \end{aligned} \tag{E.4}$$

$$E(M_{R_i}) = \int_o^\infty r\cdot f_{M_{R_i}}(r)\, dr \tag{E.5}$$

$$E(M_{R_i}^2) = \int_o^\infty r^2\cdot f_{M_{R_i}}(r)\, dr \tag{E.6}$$

Substituting Eq. E.1 and E.2 into E.5 and E.6 and integrating,

$$E(M_{R_i}) = E(MR_1) * \Phi\left[\frac{\lambda_2-\lambda_1-\zeta_1^2}{\sqrt{\zeta_2^2+2\zeta_1^2}}\right] + E(M_{R_2}) * \Phi\left[\frac{\lambda_1-\lambda_2-\zeta_2^2}{\sqrt{\zeta_1^2+2\zeta_2^2}}\right] \qquad (E.7)$$

$$E(M_{R_i}^2) = E(M_{R_1}^2) * \Phi\left[\frac{\lambda_2-\lambda_1-2\zeta_1^2}{\sqrt{\zeta_2^2+2\zeta_1^2}}\right] + E(M_{R_2}^2) * \Phi\left[\frac{\lambda_1-\lambda_2-2\zeta_2^2}{\sqrt{\zeta_1^2+2\zeta_2^2}}\right] \qquad (E.8)$$

where, $\Phi(x)$ is the cumulative distribution function of the standard normal distribution.